Journal of Wind Engineering & Industrial Aerodynamics 251 (2024) 105777

Contents lists available at ScienceDirect

Journal of Wind Engineering & Industrial Aerodynamics

journal homepage: www.elsevier.com/locate/jweia

On the cybersecurity of smart structures under wind

Miguel Cid Montoya [a,*], Carlos E. Rubio-Medrano [b], Ahsan Kareem [c]

[a] Aero-Structural Optimization (ASTRO) Laboratory, Department of Engineering, Texas A&M University-Corpus Christi, Corpus Christi, TX 78412, USA
[b] Cybersecurity Research & Innovation Laboratory (CSRIL), Department of Computer Science, Texas A&M University-Corpus Christi, Corpus Christi, TX 78412, USA
[c] NatHaz Modeling Laboratory, Department of Civil and Environmental Engineering and Earth Sciences, University of Notre Dame, Notre Dame, IN, 46556, USA

ARTICLE INFO

Keywords:
Cybersecurity
Smart structures
Active structural control
Wind-induced responses
Operational technology
Cyber-physical systems
Cyber-secure aero-structural design

ABSTRACT

Controlling wind-induced responses is a challenging and fundamental step in the design of wind-sensitive critical infrastructures (CI). While passive design modifications and passive control devices are effective alternatives to a certain extent, further actions are required to fulfill design specifications under some demanding circumstances. Active countermeasures, such as active dampers, active aerodynamic devices, and operational control systems, stand out as a smart alternative that allows extra control over wind-induced responses of tall buildings, long-span bridges, wind turbines, and solar trackers. To make this possible, CI are equipped with operational technology (OT) and cyber–physical systems (CPS). However, as with any other OT/CPS, these systems can be threatened by cyberattacks. Changing their intended use could result in severe structural damage or even the eventual collapse of the structure. This study analyzes the potential consequences of cyberattacks against wind-sensitive structures equipped with OT/CPS based on case studies reported in the structural control literature. Several cyberattacks, scenarios, and possible defenses, including cyber-secure aero-structural design methods, are discussed. Furthermore, we conceptually introduce and analyze a new cyberattack, the "Wind-Leveraged False Data Injection" (WindFDI), that can be specifically developed by taking advantage of the positive feedback between wind loads and the misuse of active control systems.

1. Introduction

"*The hacker didn't succeed through sophistication. Rather he poked at obvious places, trying to enter through unlocked doors. Persistence, not wizardry, let him through.*" As described by Clifford Stoll in The Cuckoo's Egg (Stoll, 1989), the absence of security in some systems poses the highest risk in modern system development. In the light of this emerging challenge, national security agencies worldwide are committed to identifying and managing all potential threats and hazards that can impact the performance and integrity of critical infrastructure (CI). For example, the Cybersecurity and Infrastructure Security Agency (CISA) of the United States Department of Homeland Security has identified a number of threats, ranging from climatology events, such as extreme temperatures, drought, and wildfires, to cyber incidents, such as denial-of-service attacks, malware, and phishing (CISA, 2020). However, in a context where the number and format of cyberattacks on CI are growing at an incredible rhythm (Landers, 2024), engineers and researchers of any field are responsible for identifying potential security gaps and developing efficient countermeasures to limit the attacker's capacity of weaponing our infrastructure against us.

The accelerated growth of urban areas in the last decades has led to an unprecedented increase in the construction of long-span bridges, tall buildings (Lago et al. (2018), Council on Tall Buildings and Urban Habitat, CTBUH (2023a)), and other wind-sensitive structures, such as wind turbines and solar trackers. Passive countermeasures have been implemented to control wind-induced responses by improving the structure's aerodynamic performance or adjusting its mechanical properties, seeking to minimize wind-induced responses. However, more demanding design scenarios require more advanced mechanisms to mitigate wind-induced loads effectively. This includes (1) increasing slenderness due to the continuous growth of the main spans of long-span bridges and the height of tall buildings and wind turbine towers, (2) more complex architectural designs, and (3) more demanding extreme wind events. In this context, active countermeasures stand out as an effective alternative to mitigating wind-induced responses. Active countermeasures have mainly two advantages when compared to passive methods: (1) higher effectiveness in mitigating the undesired aeroelastic responses, which permits increasing the main span of bridges and height of buildings to limits not always achievable

* Corresponding author.
E-mail addresses: miguel.cidmontoya@tamucc.edu (M. Cid Montoya), carlos.rubiomedrano@tamucc.edu (C.E. Rubio-Medrano), kareem@nd.edu (A. Kareem).

https://doi.org/10.1016/j.jweia.2024.105777
Received 1 December 2023; Received in revised form 20 April 2024; Accepted 20 May 2024
Available online 8 June 2024

Fig. 1. An example of critical infrastructure (CI) equipped with operational technology (OT) and cyber–physical systems (CPS). (a) General view from the Dardanelles of the 1918 Çanakkale Bridge, Türkiye, opened in March 2022; and (b) View of the Çanakkale Bridge Control Center.

using only passive countermeasures, and (2) smaller size of devices, particularly in the case of inertial modifiers (e.g., active mass dampers (AMD) are typically smaller than tuned mass dampers (TMD)). On the other hand, their main drawbacks include (1) a typically higher implementation and maintenance cost, (2) an inherent challenge in terms of safety in case of failure due to multiple reasons, such as power outage or mechanical issues, and (3) their potential misuse, both unintentional and intentional. This last point is the goal of the present study, leveraged by the recent wave of cyberattacks targeting CI related to multiple engineering fields (Anguiano, 2022; McFadden, 2023).

In the wake of the advances of structural active control (Spencer and Nagarajaiah, 2003; Korkmaz, 2011; Preumont and Seto, 2008), wind-sensitive structures are progressively adding operational technology (OT) to improve their performance and operation, and increasing their level of complexity. Fig. 1 shows the Control Center of the 1918 Çanakkale Bridge (Güzel, 2023), Türkiye, a clear example of the widespread and increasing use of OT in CI, moving to the generalized use of "smart structures". Furthermore, OT is not limited to operation, and its use is extended to structural health monitoring (SHM) systems (Kijewski-Correa et al., 2013; Meng et al., 2018; Petersen et al., 2021) and cyber–physical systems (CPS) to control active countermeasure devices that modify the mechanical and aerodynamic properties, such as AMD (Yamazaki et al., 1992; Kareem et al., 1999; Zhou et al., 2022) or shape and flow modifiers (Sangalli and Braun, 2020; Hou et al., 2023). The development and implementation of these active systems are expected to keep growing given the increasing demands of modern designs and the expected intensity increase of wind events (Knutson et al., 2010; Snaiki and Wu, 2020; Orcesi et al., 2022). However, the existence of CPS that controls the resistance properties of civil, architectural, and energy harvesting structures poses a security problem that must be addressed. As highlighted in Naskar (2022): "Anything that says 'smart' in front of its name, is a potential magnet for trojans." This justifies the recent interest by states and gubernatorial agencies in developing cyberdefenses for any kind of structure that cyberattacks can threaten (Pattison-Gordon, 2022; Landers, 2023).

Nowadays, cyberattacks are threatening every aspect of life in modern societies, including education (Bank of America, 2023), research (McFadden, 2023), energy (Anguiano, 2022), industry (Pattison-Gordon, 2022), health systems (Lee, 2023; Okunyté, 2023) and warfare (Reavenlord, 2022). These attacks can cause very high damage in unexpected ways. For example, a recent attack on the National Science Foundation (NSF)-funded telescopes in Chile and Hawaii in August 2023 ceased the operation of many telescopes, causing important troubles for space observation since many essential windows of opportunity were missed. On the other hand, the high economic impact that these attacks can cause is very clear when the target is related to energy suppliers (Anguiano, 2022). Consequently, some recent efforts have been made to improve the safety of CI against cyberattacks, such as for hydraulic infrastructure (Pattison-Gordon, 2022). At the research level, the effects of cyberattacks on structures equipped with active mitigation systems have been recently studied in Zambrano et al. (2021), where two cyberattacks were analyzed: (1) Denial of Service (DoS); and (2) False Data Injection (FDI). This study showed the potential of cyberattacks on civil engineering structures and buildings. However, it was not considered the potential damage increase by leveraging the effects of the natural hazard that the active control system is intended to mitigate. In the case of earthquakes, active systems can threaten an infrastructure's integrity by (1) denying its service and (2) acting in an undesired way, which can be very harmful to the structures. However, wind-sensitive structures equipped with active systems involving OT/CPS can be especially vulnerable to cyberattacks since malicious actions can be leveraged by wind loads. In fact, wind-related phenomena are the only natural hazards that happen at a sufficiently low return period to be considered a specific component of a cyberattack. Hence, low return period winds, such as daily or monthly events, can be effectively used to increase the damage created by the misuse of active structural control systems, which may even lead to positive feedback, enabling structural instability. This "external help" has the potential to be a game-changer in the magnitude of the damage induced by the cyberattack, potentially leading to the eventual collapse of the structure. The wind engineering community is responsible for investigating this outstanding threat to CPS that controls the active countermeasures of architectural, civil, and energy-harvesting wind-sensitive structures. The complexity of the attacks on wind-sensitive structures and the potential damage that they can create demand specific investigations to avoid these attacks from the early stages of the structural design process. This study seeks to identify the "unlocked doors" in OT/CPS security, the potential damage of wind-leveraged cyberattacks, and develop effective defenses so we can produce "almost-unhakeable" structures.

We start by providing a general background on the cybersecurity of cyber–physical systems and describing previous cyberattacks to existing CI equipped with OT/CPS in Section 2. Section 3 reports a literature review of wind-sensitive structures equipped with OT/CPS that may be the target of cyberattacks, including long-span bridges, tall buildings, wind turbines, and solar trackers. We describe the transition from passive to active countermeasures to mitigate wind-induced loads and how these structures can be targets of existing and new cyberattacks. The goal of this section is to provide a comprehensive overview of the current state-of-the-art as a compulsory first step to identify potential cybersecurity vulnerabilities. Then, Section 4 deeps into the details of eventual attacks on wind-sensitive smart structures, focusing on the kind of actuators, the available knowledge about the target, and the kind of cyberattacks depending on the actuation used to damage the structure. Section 5 quantitatively analyze the potential effectiveness of the attacks envisioned in Section 4 by analyzing several demonstration examples based on previous studies addressing structural control problems. Finally, Section 6 addresses the issue of developing effective cyberdefenses, ranging from software and hardware to the design of

Table 1
List of abbreviations and their corresponding full terms.

Abbreviation	Full term
AGS	Active Gyroscope Stabilizer
AVS	Active Variable Stiffness
AMD	Active Mass Damper
ATMD	Active Tuned Mass Dampers
APT	Advanced Persistent Threat
CAV	Connected Automated Vehicles
CCATMD	Cable Connected Active Tuned Mass Damper
CFD	Computational Fluid Dynamics
CI	Critical Infrastructures
CISA	Cybersecurity and Infrastructure Security Agency
CPS	Cyber-Physical Systems
CTBUH	Council on Tall Buildings and Urban Habitat
DL	Deep Learning
DNN	Deep Neural Network
DoS	Denial of Service
ER	Electro-Rheological
FDI	False Data Injection
FEM	Finite Element Models
HMD	Hybrid Mass Damper
ICS	Industrial Control Systems
HMI	Human Machine Interface
LQR	Linear Quadratic Regulator
MAMD	Multiple Active Mass Dampers
MDOF	Multi-Degree-of-Freedom
MTD	Moving Target Defense
MTMD	Multi-Tuned Mass Dampers
MR	Magneto-Rheological
NSF	National Science Foundation
OPC	Open Platform Communications
OT	Operational Technology
PAFC	Ping-An Finance Center
PLC	Programmable Logic Controllers
PV	Photovoltaic
RL	Reinforcement Learning
RTU	Remote Terminal Units
SAT	Single-axis trackers
SATLD	Semi-Active Tuned Liquid Dampers
SATLCD	Semi-Active Tuned Liquid Column Dampers
SATMD	Semi-Active Tuned Mass Dampers
SAVS	Semi-Active Variable Stiffness
SIS	Safety Instrumented System
SCADA	Supervisory Control and Data Acquisition
SHM	Structural Health Monitoring
TLCD	Tuned Liquid Column Damper
TLD	Tuned Liquid Damper
TMD	Tuned Mass Damper
TRD	Twin Rotor Damper
VIV	Vortex-Induced Vibrations
WindFDI	Wind-Leveraged False Data Injection
WT	Wind Tunnel

the actuators to reduce the impact of an eventual cyberattack. Section 7 reports the conclusions of this study, future work, and design recommendations to move towards cyber-secure wind-sensitive smart structures. A list of abbreviations and their corresponding full terms used along the paper is reported in Table 1.

2. Cyber-physical systems and vulnerability to cyberattacks

Operational technology (OT) can be defined as the combination of hardware and software systems aimed to detect and/or cause a change in physical systems through the direct network-based monitoring and/or control of dedicated equipment, assets, processes, and events. As shown in Fig. 2, the term OT usually describes environments containing CPS, e.g., Connected Automated Vehicles (CAV), Industrial Control Systems (ICS), e.g., Supervisory Control and Data Acquisition (SCADA) systems, and may be, in turn, composed of dedicated devices such as Remote Terminal Units (RTU) and Programmable Logic Controllers (PLC).

Industrial Control Systems (ICS) are a sub-field of OT/CPS controlling mission-critical infrastructures such as the power grid, water plants, etc., and are an important asset to the economies of towns, states, and countries. In recent years, ICS have been transferring to electronic systems due to the vast opportunities available through the implementation and use of digital technology, such as increased reliability, flexibility, resilience, and efficiency (Goff et al., 2014). A typical ICS environment, graphically shown in Fig. 3, includes the following:

- **Actuator**. A hardware component that moves or operates a device in the physical world. Examples of actuators include valves, motors, or piezoelectric actuators.
- **Sensor**. A device that generates an electrical analog or digital signal that represents a physical property of a process. Examples include temperature or magnetic field sensors.
- **Controller**. A computing device that acts as a bridge connecting the *cyber* and the *physical* worlds. A controller may either take the form of a general-purpose computer or may also be implemented by means of a PLC (Bolton, 2015), a small, rugged, domain-purpose computer that has programmable memory to store functions such as timers and logic gates, which allow them to control actuators and physical machines, such as water pumps or centrifuges, and receive and compile data from sensors. PLCs can be, in turn, controlled by an Engineering Station, a general-purpose computer that is used to write the control logic or ladder logic code that is typically executed by a PLC. It is usually connected to the PLC so that the compiled control logic program can be uploaded.
- **Human Machine Interface (HMI)**. The hardware or software used to interact with devices such as a PLC, e.g., a physical control panel with buttons and lights or a software display. Fig. 1 shows an example of an HMI designed to control a bridge.

2.1. Attacks to Cyber-Physical Systems (CPS)

While the benefits of these changes are unparalleled, cyberattacks targeting CPS have increased in number and sophistication in recent years, which may lead to serious consequences such as physical damage to critical infrastructure. Famous recent attacks on CPS include the Kyivoblenergo and the Prykarpattyaoblenergo attacks (2015) (Whitehead et al., 2017) and the Ukrenergo transmission station attack (2016) (Dragos, Inc., 2017b), all of them in Ukraine. Moreover, there have been recent concerns that foreign actors may be already launching a series of attacks on CPS infrastructures in the United States and Europe (The New York Times, 2018). As a response, and to ensure CPS are built on a trustworthy and secure foundation, the "Securing Energy Infrastructure Act" (S.174, 2019) highlights the need for urgent actions on CPS security (U.S. Congress - A.S. King, 2019).

2.1.1. Attacks to Programmable Logic Controllers (PLCs)

Stuxnet. Stuxnet was the first-ever documented malware specifically developed to target PLCs, as it showed a high level of sophistication, a deep understanding of industrial processes, and the use of four *zero-day* exploits (Falliere et al., 2011). After compromising a general-purpose computer that was equipped with software for programming PLCs, as featured in Fig. 3, Stuxnet uploaded its malicious control program to the target Siemens 315 and 417 PLC models and made them damage centrifuges while reporting to operators that everything was normal (Langner, 2011).

Triton. Also known as TRISIS and HatMan (CISA ICS-CERT, 2019; Dragos, Inc., 2017b), Triton was identified in 2017 after a petrochemical facility in Saudi Arabia was shut down. After compromising an engineering workstation, Triton was able to launch a dropper (trilog.exe) to deliver backdoor files to a Safety Instrumented System (SIS) PLC. The first backdoor file was a zero-day exploit that allowed the attackers to

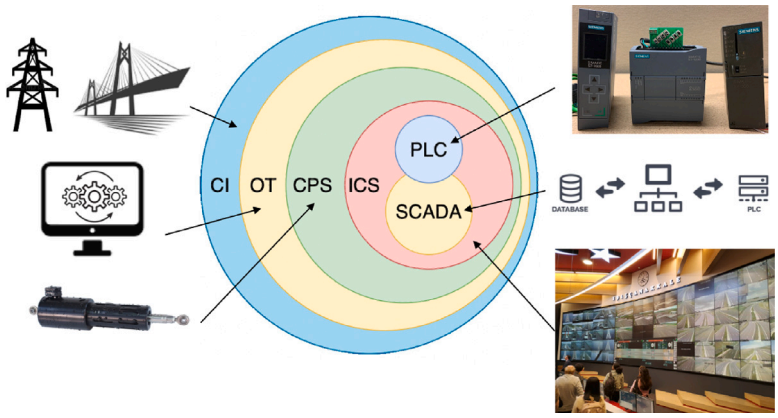

Fig. 2. A conceptual overview of critical infrastructure (CI), operational technology (OT), cyber–physical systems (CPS), industrial control systems (ICS), supervisory control and data acquisition (SCADA) systems and programmable logic controllers (PLC).

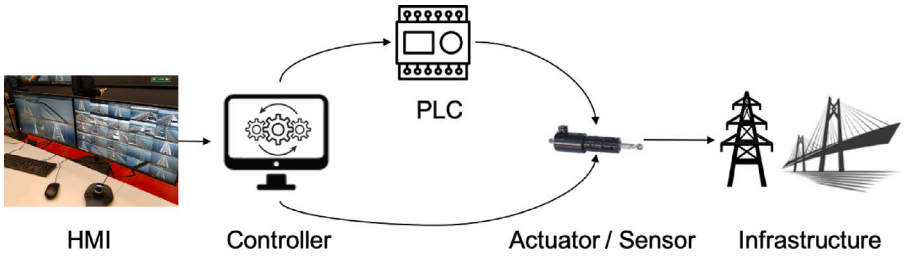

Fig. 3. A conceptual overview of the components of an ICS environment.

inject the second file into the PLC's memory. With a program in the memory of the PLC, the attackers could have control of the device. The attackers were unable to take full control of the system because an error in the PLC caused a system shutdown.

Pipedream Toolkit. Pipedream (also known as Incontroller) is a modular framework that includes multiple exploits that target different PLCs. Once the attackers compromise a computer in the control network, Pipedream can be used to scan and compromise Scheider Electric PLCs, OMROM Sysmac NEX PLCs, and Open Platform Communications (OPC) Unified Architecture servers. Pipedream is believed to have been developed by a nation-state and was classified as an Advanced Persistent Threat (APT) by the United States Department of Energy (CISA, 2022).

2.1.2. Attacks to Industrial Control Systems (ICS)

Dragonfly. Also known as Havex malware (Symantec Inc., 2014), Dragonfly was a large scale cyberespionage campaign that targeted ICS software in the energy sector in the United States and Europe. In order to infect its targets, three different attack vectors were used. First, a spam campaign that used spear phishing targeted senior employees in energy companies. Second, Watering Hole attacks (Symantec Inc., 2014) that compromised legitimate energy sector websites were deployed to redirect the target to another compromised website that hosted the Lightsout exploit, which ultimately dropped the Oldrea or Karagany malwares (Dragos, Inc., 2017a) in the target's host. The third and final attack vector used was a dedicated *trojanized* software (legitimate software that is turned into malware), which was leveraged by the attackers to successfully compromise various legitimate ICS software packages, ultimately inserting their own malicious code. Once a host was infected, the Havex malware would leverage legitimate functionality available through the OPC protocol to draw a map of the industrial devices present in the ICS network, which would be highly valuable when designing future attacks.

Crashoverride. Also known as Industroyer (Slowik, 2018), CRASHOVERRIDE is a sophisticated malware designed to disrupt ICS networks used in electrical substations, as it shows an in-depth knowledge of ICS protocols used in the electrical industry, which would only be possible with access to specialized industrial equipment. CRASHOVERRIDE dealt physical damage by opening circuit breakers and keeping them open even if the grid operators tried to close them back to restore the system. It is believed to have been the cause of the power outage in Ukraine in December of 2016 (Hemsley et al., 2018).

3. Wind-sensitive CI equipped with OT/CPS

Critical Infrastructure is defined in the United States according to the Patriot Act of 2001 as "systems and assets, whether physical or virtual, so vital to the United States that the incapacity or destruction of such systems and assets would have a debilitating impact on security, national economic security, national public health or safety, or any combination of those matters" (CISA, 2020). In particular, several infrastructure sectors are identified, including transportation systems, energy, financial services, and markets. Several wind-sensitive civil and architectural structures, such as long-span bridges, tall buildings, wind turbines, wind farms, and solar panel arrays, fall into this description, which makes their rigorous study a top priority. The goal of this section is to provide a comprehensive review of the state-of-the-art of active control systems that permits the identification of security vulnerabilities in already existing and envisioned at the research level wind-sensitive CI equipped with OT/CPS. The following subsections review the most up-to-date OT/CPS used in wind-sensitive CI and the risks to their integrity and functionality.

3.1. Long-span bridges

Long-span bridges are very flexible structures that are sensitive to the action of wind. The rapid growth of coastal cities has increased the demand for their construction with even longer span lengths and lighter weights. The most recent example is the completion of the 1915 Çanakkale Bridge in 2022 with a world record-braking main span of

2023 m (Arıoğlu, 2021; Güzel, 2023). The subsequent reduction in damping and natural frequencies increases their susceptibility to wind loads. Besides the well-known cases of bridge collapses in the past, such as the Tacoma Narrows Bridge (Ammann et al., 1941), there are multiple examples of recent vulnerabilities, even under winds that are far from being considered extreme. This includes the vertical oscillations recorded in December 2022 in the Verrazzano-Narrows Bridge deck, US, the vortex-induced vibrations (VIV) of the Humen Bridge, China, in May 2020 (Ge et al., 2022), and the vertical oscillations of the Alconétar Arc Bridge, Spain, during its construction (Astiz, 1999). These undesired responses will be more present as we keep increasing the main span of new bridge projects (Ge et al., 2011), such as the Zhangjinggao Yangtze River Bridge in China, spanning 2300 m (Wei, 2023), and the Shiziyang Bridge in China, with a main span of 2180 m (Zhao et al., 2023), or the well-known Messina Bridge (Diana et al., 2004).

Deck shape tailoring is one of the most successful and cost-effective approaches to mitigate wind-induced effects (Larsen and Wall, 2012; Argentini et al., 2019). However, long-span bridges are slender and flexible structures subject to several wind-induced responses (Larsen and Larose, 2015), which may require complex and sometimes contradictory deck shape modifications to address all aeroelastic phenomena. This was investigated in Cid Montoya et al. (2021b), where a twin-box deck was optimized considering flutter and buffeting responses simultaneously. VIV is another wind-induced response that can drive the wind-resistant design of single- and multi-box decks. Adding and/or tailoring existing appendages, such as guide vanes and stabilizers, can be used to control the flow and avoid undesired flow features, such as the formation of vortices that may lead to VIV. Real application examples are described in Larsen and Poulin (2005), including the guide vanes installed in the Osteroy Suspension Bridge, Norway, the StoreBaelt Suspension Bridge, Denmark, and the Stonecutters Cable-Stayed Bridge, China. More recent studies (Bai et al., 2021b) focus on finding the best configuration for these devices by studying the influence of their shape and position. On the other hand, passive inertial modifications can improve the aeroelastic responses of bridge decks (Gu et al., 2002). TMDs were successfully used in mitigating the VIV in the approaching spans of the StoreBaelt Bridge (Larsen and Poulin, 2005). Current research further explores new configurations to increase the effect of TMD in bridge decks (Xu et al., 2022) and design methods to optimize their effectiveness (Gu and Xiang, 1992; Bui and Tran, 2022). Furthermore, the combination of multiple actions may be required in some situations, as was the case of the Humen Bridge (Ge et al., 2022).

However, passive measures can improve aerodynamic response up to a certain limit (Cid Montoya et al., 2022), where the effectiveness of the passive aerodynamic control is depleted, and alternative modifications are required. For this reason, several active systems have been developed to improve the aeroelastic performance of long-span bridges. Some of them have only been explored within the research realm (Gao et al., 2019), and some others have been successfully implemented in real bridges, such as in the Xihoumen Bridge (Yang et al., 2022). A summary of the main passive and active systems developed for long-span bridges is reported in Table 2. Several works reviewed some applications for long-span bridges (Gao et al., 2021). The most relevant active systems used to improve the aeroelastic responses of bridges are discussed below.

3.1.1. Aerodynamic control in bridges: Active appendages

Adding passive aerodynamic appendages to bridge decks is an effective approach to modify the wind loading and improve the bridge stability (Raggett, 1987). Given its aerodynamic benefits, this concept was considered in the design of the Messina Strait Bridge (Brown, 1996). However, the effectiveness of these appendages can be improved by adding mechanical actuators and active control. This was developed in the 1990s by several authors (Ostenfeld and Larsen, 1992, 1997; Wilde and Fujino, 1998; Cobo del Arco and Aparicio, 1999), achieving great results. The aerodynamic and aeroelastic benefits of active appendages have been highlighted by multiple authors, and it is currently an active research topic (Huynh and Thoft-Christensen, 2001; Bera and Chandiramani, 2019; Truong and Phan, 2021; Sangalli and Braun, 2020). For instance, Cobo del Arco and Aparicio (1999) highlighted that "considering the control of the windward winglet and the leeward winglet fixed to the deck, the analyses show that it is possible to stabilize a bridge of any desired length against flutter". Hence, it is expected to have an important role in developing the new super-long-span bridges of the future. Active appendages installed on bridge decks can be classified into two main groups: (1) separate control surfaces or winglets; and (2) combined control surfaces or flaps. Fig. 4 shows multiple configurations envisioned for these two kinds of appendages.

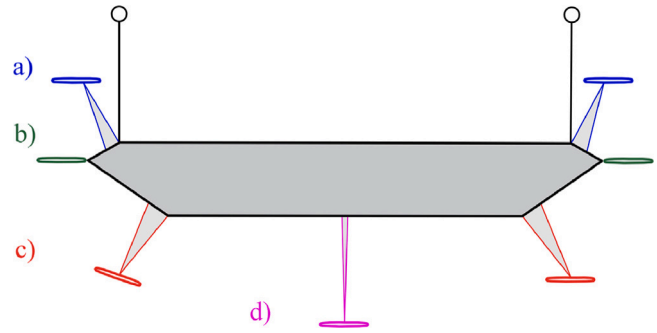

Fig. 4. Representative active appendages systems studied for the active control of bridge decks. (a) Upper winglets (e.g., Li et al. (2015), Sangalli and Braun (2020)); (b) Flaps (e.g., Kwon and Chang (2000), Li et al. (2022)) ; (c) Bottom winglets (e.g. Cobo del Arco and Aparicio (1999), Huynh and Thoft-Christensen (2001) and Nissen et al. (2004)); (d) Central winglet located below the deck (e.g. Preidikman and Mook (1997)).

Winglets are plates or airfoils installed on one or two sides of the bridge decks at a given separation to handle undesired aerodynamic features of bluff deck cross-sections. They can be installed adopting multiple configurations as described in Cobo del Arco and Aparicio (1999). Their location can impact their installation and maintenance in terms of operability and associated costs. The effective control of the wiglets to improve the wind-induced responses of bridges relies on the accurate modeling of the response of the bridge equipped with winglets under the action of wind. Following Wilde and Fujino (1998) and Cobo del Arco and Aparicio (1999), assuming that (1) the flow around the winglet is not disturbed by the presence of the deck and therefore can be obtained using the Theodorsen's functions (Theodorsen, 1949), and (2) the flow around the deck is not distributed by the presence of the winglets, then the total load on the winglet-deck system can be obtained by superimposing the contribution of the winglet to the load on the deck. Hence, the deck flutter derivatives can be modified by adding the contribution of the winglet. Following the formulations derived in Wilde and Fujino (1998) and Cobo del Arco and Aparicio (1999), the flutter derivatives of the deck-winglet system can be written as a function of the winglet position, movement amplitude, and rotation phase, which enables the effective control of the bridge aeroelastic response by changing the winglet rotation phase. More advanced analysis considering the shape of winglets requires wind tunnel (WT) tests or computational fluid dynamics (CFD) simulations to consider the shape contribution of the winglets. This approach is used in current research studies (Li et al., 2017; Sangalli and Braun, 2020).

On the other hand, combined control surfaces, commonly known as flaps or active fairings, are installed on the windward and/or leeward edge of the deck, as shown in Fig. 4(b), which permits utilizing the interference effect to control the aeroelastic responses (Hansen and Thoft-Christensen, 2001; Zhuo et al., 2020). The theoretical framework for flutter control using active flaps was first developed in aeronautical

Table 2
Summary of means to suppress wind-induced responses of bridges with application examples.

Means	Type	Method	Application
Passive	Structural	Stiffness and mass design	Heuristic-based modifications (Astiz, 1996; Arıoğlu, 2021) Structural optimization (Nieto et al., 2009; Kusano et al., 2015)
		Inertial modification device	Deck dampers (Gu et al., 2002; Ge et al., 2022) Tower dampers (Ogawa et al., 1997; Casciati and Giuliano, 2009)
	Aerodynamic	Deck cross-section design	WT-based aerodynamic design (Brown, 1980; Larsen and Wall, 2012; Argentini et al., 2022; Cid Montoya et al., 2023) CFD-based aerodynamic design (Nieto et al., 2010; Cid Montoya et al., 2018b; Xu et al., 2020) Aero-structural design optimization (Cid Montoya et al., 2020, 2022) Passive attachments (Larsen and Poulin, 2005; Starossek et al., 2018; Bai et al., 2021b) Passively controlled winglets (Omenzetter et al., 2000; Phan, 2018) Wind barriers (Buljac et al., 2017; Hu et al., 2019; Bai et al., 2020; Ge et al., 2022) Self-issuing jets (Karniadakis and Triantafyllou, 1992; Chen et al., 2015, 2019; Yang and Li, 2021)
Active	Structural	Inertial control device	Active mass dampers (AMD) in decks (Battista and Pfeil, 2000; Gu et al., 2002; Körlin and Starossek, 2007; Chang, 2020) Semi-active tuned mass dampers (SATMD) in decks (Gu et al., 2002) Active mass dampers (AMD) in towers (Kagaya et al., 2011) Active gyroscope stabilizer (AGS) (Giaccu and Caracoglia, 2021, 2023)
	Aerodynamic	Shape control device	Active winglets (Raggett, 1987; Kobayashi and Nagaoka, 1992; Brown, 1996; Cobo del Arco and Aparicio, 1999; Sangalli and Braun, 2020) Active flaps (Kwon and Chang, 2000; Wilde et al., 2001; Boberg et al., 2015; Zhao et al., 2016; Li et al., 2022; Wang et al., 2023) Active wind barriers (Yang et al., 2022)
		Flow control device	Suction and jets (Zhang et al., 2016; Tao et al., 2017; Gao et al., 2019) Rotors for flow separation control in decks (Kubo et al., 1999) Rotors for flow separation control in towers (Kubo, 2004)
	Combined	Shape and inertial control	Winglets and rotating mass dampers (Bera and Chandiramani, 2020)

engineering (Theodorsen, 1949; Edwards et al., 1978). These formulations were later extended to be applied for bridge deck-flap systems (Omenzetter et al., 2000, 2002; Kwon and Chang, 2000). However, since there is flow interaction between the flaps and the deck, analytical methods are insufficient to properly model complex flow separations around the bridge-flap system and to consider the impact of flaps and deck cross-section shape on the results to assess the flutter derivatives of the system properly. Hence, wind tunnel tests or CFD simulations are required to properly model active flaps' performance and control strategies (Zhuo et al., 2022). Alternatively, active control can be carried out by using reinforcement learning (RL) (Adam and Smith, 2008; Fan et al., 2020; Han et al., 2022). This approach was adopted for the active flutter control of long-span bridges in Wu et al. (2023) by implementing a nonlinear model-free controller based on a deep neural network (DNN).

Moreover, fundamental research on bluff body aerodynamics provides ideas for developing potential effective countermeasures for real applications in bridge engineering. An interesting approach to controlling the flow's boundary layer around bluff bodies consists of implementing moving surfaces (Modi et al., 1991; Kubo et al., 1992). Its application to bridge deck aerodynamics was proposed by Kubo et al. (1999), where a shallow rectangular cylinder is added to the leading edge of the bridge deck to control the boundary layer by changing the flow separation. This approach was also proposed for improving the aerodynamics of bridge towers (Kubo, 2004). This methodology was also investigated for mitigating VIV of bluff bodies (Silva-Ortega and Roque da Silva Assi, 2017). Recent contributions suggest the use of suction (Ke et al., 2014; Zhang et al., 2016; Tao et al., 2017) and blowing systems (Gao et al., 2019) to control the flow structure and improve the aerodynamic properties of bridge decks, which increases the variety of possibilities to control the flow and wind-induced loads actively.

3.1.2. Aerodynamic control in bridges: Active wind barriers

Wind barriers are able to improve the traffic conditions (Coleman and Baker, 1992; Kwon et al., 2011; Kozmar et al., 2012) at the cost of worsening the deck cross-section aerodynamic characteristics (Buljac et al., 2017; Su et al., 2017; Yang et al., 2020). Research efforts have been recently carried out to reduce their influence on the aerodynamic performance of the deck (Bai et al., 2020). Also, small-scale components can be advantageously tailored to mitigate VIV (Hu et al., 2019; Ge et al., 2022). A smart alternative is the development of active wind barriers that change their configuration depending on the wind conditions. As shown in Fig. 5, this concept was recently applied in the Xihoumen Bridge by installing an adjustable wind barrier that is automatically controlled by an LSA2000 control platform and computer remote control technology (Yang et al., 2022). This reference reports a force coefficient for the twin-box deck cross-section without barriers of $C_D = 1.16$. This value increases up to $C_D = 1.79$ when installing the barrier in the upright configuration. This 54% increase in the force coefficient highlights the negative effect of the wind barriers on the bridge deck aerodynamics. However, by taking advantage of the adjustable wind barrier, the force coefficient drops to $C_D = 1.28$, which is close to the value obtained for the original configuration, remarking the benefits of using cyber–physical systems to adapt to structure for different wind scenarios. However, the potential effects of a cyberattack on this CPS can be intuitively anticipated.

3.1.3. Inertial control in bridges

Moving from passive tuned mass dampers to more efficient semi-active and active mass dampers to mitigate bridge deck wind-induced displacements allows us to reduce the size of these active devices. An example of AMD's better performance is reported in Gu et al. (2002), where the performance of a TMD and a semi-active mass damper were studied in the Yichang bridge, a suspension bridge with a main span of 960 m. Another example showing the superior performance of AMD was reported in Battista and Pfeil (2000), where an AMD was used to mitigate the VIV of the Rio-Niterói Bridge in Rio de Janeiro, Brazil. Furthermore, the promising performance of these inertial active devices increased the research efforts on the topic. Körlin and Starossek (2007) conducted wind tunnel tests of a deck sectional

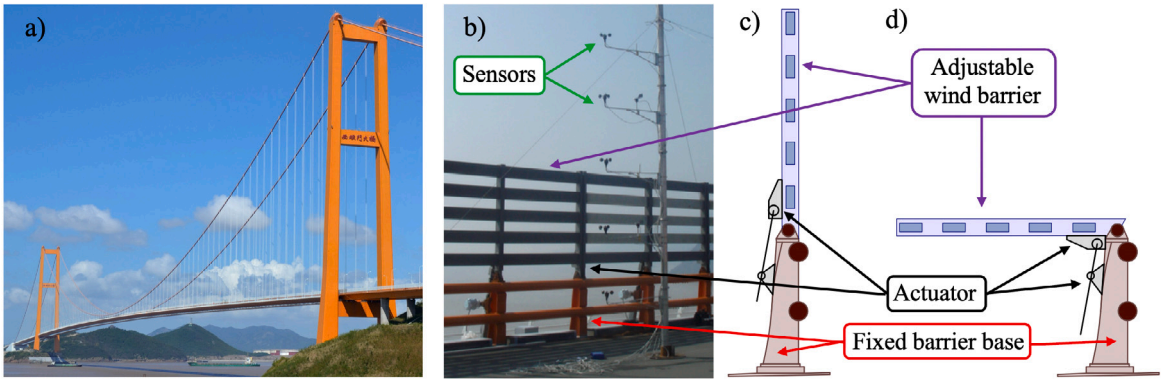

Fig. 5. Illustration of the adjustable wind barrier installed in the Xihoumen Bridge. (a) General view of the Xihoumen Bridge, Zhejiang, China. Reproduced from Ref. Wikimedia Commons (Glabb) (2012) with the author credit "Glabb" and permission of the Creative Commons Attribution-Share Alike 3.0 Unported license, ©2012; (b) Detail of the adjustable wind barrier, reproduced from Ref. Yang et al. (2022) with permission from Elsevier, ©2022; (c) Upright configuration of the barrier; and (d) barrier lying down. Sketches based on Yang et al. (2022).

model equipped with servo motors controlling the rotational motion of control masses. This system increased the measured critical wind speed of the sectional model by about 16.5%. Chang (2020) reported an experimental study of a reduced-scale bridge model where an AMD successfully mitigated the excitation induced by external loads. On the other hand, Giaccu and Caracoglia (2021) proposed using gyroscopes for mitigating the flutter of long-span bridges. These devices have been used in several engineering fields (Kan et al., 1992; Ghommema et al., 2010), including for seismic vibration isolation (Carta et al., 2017). This device modifies the mass moment of inertia by rotating a lumped mass at a given angular velocity. As reported in Giaccu and Caracoglia (2023), some ranges of angular velocities drastically improve the bridge flutter performance. However, the critical flutter velocity can worsen at some angular velocity values compared with the original bridge, which represents a relevant safety vulnerability.

Another important issue is the wind-induced vibrations of bridge towers, both in service (Siringoringo and Fujino, 2012) and during construction. It is important to control the responses during the different construction phases (Kagaya et al., 2011), as their dynamic characteristics can largely change from the initial construction stages to the free-standing tower (Diana et al., 2013) before reaching the final configuration when the cable supporting system provides a remarkable contribution to the longitudinal stiffness of the towers. In all these cases, inertial control systems are an effective countermeasure to mitigate these undesired wind-induced responses. Moving from passive TMD, including impact mass dampers (Ogawa et al., 1997) and multi-tuned mass dampers (MTMD) (Casciati and Giuliano, 2009), to active mass dampers permits a better control of the wind-induced responses. An interesting and recent example is the case of the Çanakkale Bridge Tower (TESolution, 2020; Güzel, 2023), where AMD systems were installed in the tower to control its responses as the construction progresses (see Fig. 6). This system can control the tower's first and second bending modes and the torsional mode.

3.2. Tall buildings

The accelerated growth of urban areas in the last decades has led to an unprecedented increase in the construction of tall buildings. According to the CTBUH skyscraper center database (Lago et al., 2018; CTBUH, 2023a), 79% of the buildings above 250 m have been built in the last decade (2010–2020), and this trend is expected to continue in the future. Furthermore, the number and height of mega-tall skyscraper projects under development and construction are rapidly growing. The best example is the Jeddah Tower (CTBUH, 2023b), previously known as the Kingdom Tower, which is currently under construction in Jeddah, Saudi Arabia, and will reach a World record-breaking height of 1008.2 m, currently held by the Burj Khalifa (Abdelrazaq, 2012), with 829.8 m.

Increasing height leads to more slender, flexible, and low damping structures, which make them more susceptible to earthquakes and wind loads (Tamura et al., 2005; Irwin, 2008, 2009; Kwok, 2013; Kwon and Kareem, 2013). This has led to the adoption of dynamic modification systems as an effective alternative to control buildings performance and to improve human comfort (Kareem et al., 1999; Kwok et al., 2009; Rahimi et al., 2020; Jafari and Alipour, 2021b; Koutsoloukas et al., 2022). According to Lago et al. (2018), about 11% of tall buildings above 250 m worldwide are equipped with dynamic modification systems, and 97% of those have been equipped in the last three decades. This approach is particularly popular in the US, where 25% of tall buildings are damped. Currently, 12% of damped buildings worldwide over 250 m use AMD systems (Lago et al., 2018; CTBUH, 2023a), such as the Shanghai World Financial Center (Shi et al., 2012) and the Ping-An Finance Center (PAFC), China (Zhou et al., 2022; Zhou and Li, 2022), and this trend is expected to grow as architectural requirements increase.

The first approaches for designing TMDs started in the first half of the 20th century (Den Hartog, 1956) and were later extensively developed in the 1970s and 1980s (Ayorinde and Warburton, 1980; Clark, 1988; Kwok and Samali, 1995; Xu et al., 1992a). Dampers are not limited to lumped masses inside buildings. Alternative passive inertial modification devices are fluid-containing appendages (Kareem and Sun, 1987; Gao et al., 1997), such as water-containing tanks, which permit mitigating the wind-induced loads with not only the tank lump mass effect but also with the sloshing modes. Examples of tuned liquid dampers (TLD) are the air traffic towers of Haneda and Narita airports, Japan (Tamura et al., 1992). Later investigations led to the development of passive MTMD (Igusa and Xu, 1994; Kareem and Kline, 1995; Casciati and Giuliano, 2009), also known as distributed dampers. Moreover, dampers can be installed entirely inside the building or take advantage of adjacent buildings to use friction dampers (Malhotra et al., 2020).

As described for long-span bridges in Section 3.1, wind-induced response mitigation strategies evolved from passive aerodynamic countermeasures (e.g. cross-section modifications (Kwok et al., 1988; Tanaka et al., 2012; Gu et al., 2020)) and inertial systems (e.g. TMD in the Shanghai Tower (Xie et al., 2023)) to active systems (Karnopp, 1990). Active and semi-active control devices have the advantage that they do not introduce mechanical energy into the structural system under control. However, they modify the system properties to reduce the structural response (Hrovat et al., 1983; Housner et al., 1997). Comprehensive reviews of tall buildings and towers equipped with TMD systems can be found in Sun et al. (1995), Gutierrez Soto and Adeli (2013) and Jafari and Alipour (2021b). A summary of current

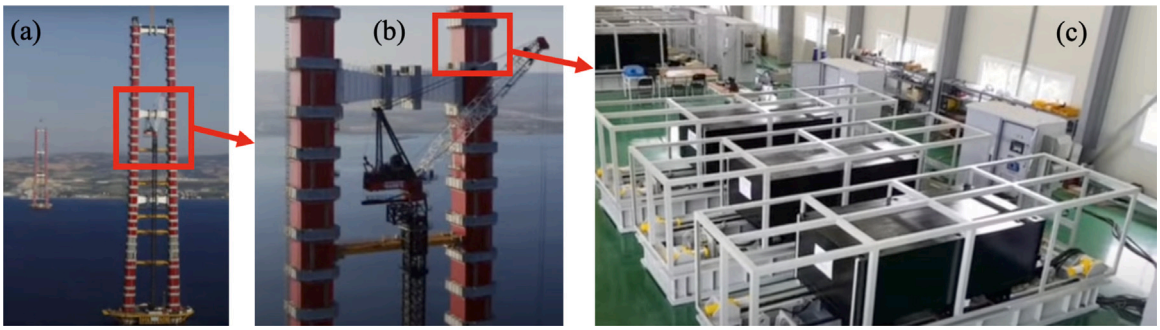

Fig. 6. AMD installed in the Çanakkale Bridge Tower, Türkiye. (a) General view of the towers during construction; (b) Detail of the location of the AMD; and (c) view of the AMD system. Reproduced from Ref. TESolution (2020) with permission from TESolution, ©2020.

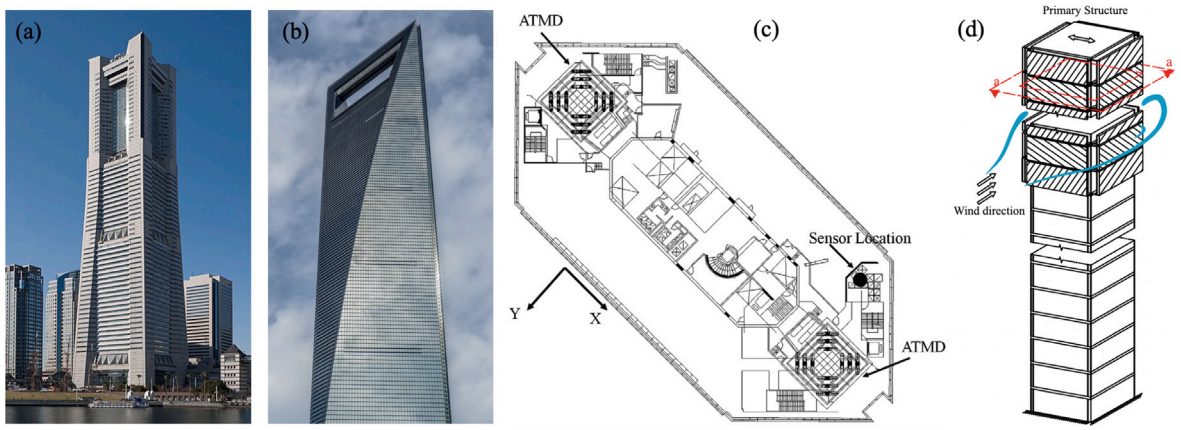

Fig. 7. Inertial active systems in tall buildings: (a) View of the Minato Mirai (MM) 21 Landmark Tower in Yokohama, Japan, equipped with tuned active dampers. Reproduced from Ref. Wikimedia Commons (Rs1421) (2011) with the author credit "Rs1421" and permission of the Creative Commons Attribution-Share Alike 3.0 Unported license, ©2011; (b) View of the Shanghai World Financial Center equipped with two ATMD. Reproduced from Ref. Wikimedia Commons (2015) with permission of the Creative Commons Attribution License CC0 1.0, ©2015; (c) Floor plan of the ninetieth floor of the Shanghai World Financial Center where the ATMD are installed. Reproduced from Ref. Shi et al. (2012) with permission from Elsevier, ©2022; and (d) Movable façade design used as an active damping system. Reproduced from Ref. Zhang et al. (2022) with permission of the Creative Commons Attribution License CC BY, ©2022.

technologies for mitigating wind-induced responses in tall buildings and towers is provided in Table 3. The most effective control scheme selection can be based on multiple criteria, such as performance and cost-effectiveness (Wang et al., 2015).

3.2.1. *Inertial control in tall buildings*

Active inertial control devices are tall buildings' most widespread active control methods. A few examples are shown in Fig. 7. While passive systems consist of suspending an additional mass to the main structure and tuning the natural frequency of the suspended mass to the dominant frequency of the main structure (Andersson et al., 2015), variable damping systems are a more sophisticated alternative that overcomes the sensitivity of detuning by controlling variable properties. AMDs achieve this goal by force control, i.e., by applying forces to the system to minimize the full structure response. These systems are very popular in Asia, and representative examples of tall buildings equipped with AMD are the Ping-An Finance Center, China (Zhou et al., 2022; Zhou and Li, 2022), the Shanghai World Financial Center, China, which has two parallel active tuned mass dampers (ATMD) in its ninetieth floor, as described in Shi et al. (2012) and shown in Fig. 7(b) and (c), and the 21 Landmark Tower in Yokohama, Japan (Yamazaki et al., 1992). Alternatively, semi-active tuned mass dampers and adaptive tuned mass dampers are based on controlling the damping and stiffness, respectively. A good example of a semi-active tuned mass damper (SATMD) is the real-time controlled semi-active damper installed in the Danube City Tower in Vienna, Austria (Weber et al., 2016). On the other hand, hybrid mass dampers (HMD) combine the previous devices by connecting them in series or parallel, which permits taking advantage of the benefits of each type. An HMD has been installed in the Canton Tower in Guangzhou (Tan et al., 2012; Guo et al., 2012a), China, by combining a passive TMD with a two-stage damping level and a compact AMD. Another example is the air traffic control tower at Incheon International Airport on Yongjong Island, Korea (Park et al., 2006).

Current research also explores advancing the passive MTMD concept (Igusa and Xu, 1994; Kareem and Kline, 1995; Casciati and Giuliano, 2009) by implementing the active control of each individual TMD, resulting in multiple active mass dampers to further improve the control of the structure (Yang et al., 2017; Talib et al., 2019). Moreover, active mass dampers are not limited to adding masses inside the buildings. Kareem (1995) proposed using movable façades working as damping systems to mitigate wind-induced loads. Moon (2009) extended the approach by using double-skin façades. A recent contribution by Zhang et al. (2022) conducted the optimization of a passive/semi-active vibration control system using the concept of moving façades that can be actively controlled and extending it by adopting parallel movable connections that work as distributed dampers.

An alternative approach to systems based on translational mass is using rotational masses. Gyroscopes (Yamada et al., 1997; He et al., 2017; Curadelli and Amani, 2022; Nagarajaiah et al., 2022) consist of rotating masses that generate a moment, which is a function of the angular velocity, that is useful for stabilizing the response of the structure. Depending on its orientation, it can be used to control the bending and torsional responses of the structure. Twin rotor dampers (TRD) (Bäumer and Starossek, 2016; Terrill and Starossek, 2022) consist of two masses rotating in the opposite direction with a constant angular velocity with

Table 3
Summary of means to suppress wind-induced responses of buildings with application examples.

Means	Type	Method	Application
Passive	Structural	Stiffness and mass design	Structural optimization: Spence and Kareem (2014) and Aldwaik and Adeli (2014)
		Inertial modification device	Tuned mass dampers (TMD): Ueda et al. (1992), Xu et al. (1992a) and Xie et al. (2023) Multiple tuned mass dampers (MTMD): Igusa and Xu (1994), Kareem and Kline (1995) and Casciati and Giuliano (2009) Tuned liquid damper (TLD): Kareem and Sun (1987), Xu et al. (1992), Reed et al. (1998), Marivani and Hamed (2009) and Vilceanu et al. (2023) Tuned liquid column damper (TLCD): Gao et al. (1997), Yalla and Kareem (2000) and Di Matteo et al. (2017) Movable façade damping system: Kareem (1995) and Moon (2009)
		Stiffness modification device	Passive negative stiffness: Nagarajaiah et al. (2022) Passive viscous dampers: Wang et al. (2015) Passive friction dampers: Malhotra et al. (2020)
	Aerodynamic	Cross-section shape design	WT-based corners modification: Kwok et al. (1988), Tamura et al. (2005), Irwin (2008), Tse et al. (2009), Tanaka et al. (2012), Kwok (2013) and Gu et al. (2020) CFD-based drag minimization: Kareem et al. (2013), Bernardini et al. (2015), Mooneghi and Kargarmoakhar (2016), Elshaer et al. (2017) and Ding and Kareem (2018) CFD-based performance constraints: Cid Montoya et al. (2021a) and Abdelwahab et al. (2023)
		3D shape design	Twinsting: Elshaer et al. (2016) and Kim et al. (2018) Openings: Miyashita et al. (1993), Kim et al. (2017), Elshaer and Bitsuamlak (2018) and Marsland et al. (2022) Tappering: Kim et al. (2017) and Chen et al. (2021)
		Façade design	Façade roughness and porosity: Belloli et al. (2014) and Skvorc and Kozmar (2023) Façade shape configuration: Pomaranzi et al. (2020) and Jafari and Alipour (2021a)
Active	Structural	Stiffness control device	Active variable stiffness (AVS): Dong et al. (2011) Semi-active magneto-rheological (MR) dampers: Spencer et al. (1997) and Baheti and Matsagar (2022) Semi-active electro-rheological (ER) dampers: Gavin (1998) Semi-active friction dampers: Xu et al. (2001) Active cable/tendon control: Yang and Samali (1983) and Reinhorn et al. (1987)
		Inertial control device	Active mass damper (AMD): Kareem et al. (1999), Yamazaki et al. (1992), Ricciardelli et al. (2003), Shi et al. (2012) and Zhou et al. (2022) Multiple active mass dampers (MAMD): Yang et al. (2017) and Talib et al. (2019) Semi-active tuned mass dampers (SATMD): Hrovat et al. (1983) and Ricciardelli et al. (2000) Semi-active variable stiffness tuned mass dampers (SAVS-TMD): Varadarajan and Nagarajaiah (2011) Semi-active tuned liquid dampers (SATLD): Abe et al. (1998) Semi-active tuned liquid column dampers (SATLCD): Yalla et al. (2001) and Balendra et al. (2001) Semi-active movable façade damping system: Zhang et al. (2022) Hybrid mass damper (HMD): Tan et al. (2012) and Demetriou and Nikitas (2016) Active gyroscope stabilizer (AGS): Yamada et al. (1997), He et al. (2017), Curadelli and Amani (2022) and Nagarajaiah et al. (2022) Twin rotor dampers (TRD): Bäumer and Starossek (2016) and Terrill and Starossek (2022)
	Aerodynamic	Façade shape control device	Active cross-section: Ding and Kareem (2020) and Hareendran et al. (2023) Active plates: Abdelaziz et al. (2021) Active porosity and roughness: Karanouh and Kerber (2015) and Hou et al. (2023)
		Flow control device	Rotor for corner flow control: Kubo et al. (1993, 1996) Suction and jets: Zheng and Zhang (2012) and Zheng et al. (2018)

the goal of creating a monofrequency harmonic force that can be used to control the structural response.

All these systems require the implementation of active control strategies through controllers so the structure can react to real-time structural responses captured by sensors in accordance with a pre-defined control policy (Spencer and Nagarajaiah, 2003; Datta, 2003; Lewis et al., 2012). This task has been traditionally carried out by model-based methods, which rely on accurately modeling structural dynamics for its effective control (Casciati et al., 2012). Examples of control algorithms include the linear quadratic regulator (LQR) (Yang, 1975), pole assignment (Abdel-Rohman and Leipholz, 1978), and sliding mode control (Song and Gu, 2007), among others. Alternatively, model-free control methods are more versatile, and they are not limited by nonlinear dynamics modeling inaccuracies (Khodabandehlou et al., 2018; Xie et al., 2020). Current research on inertial control of buildings explores the implementation of reinforcement learning algorithms for this task (Eshkevari et al., 2023; Zhang and Zhu, 2023; Gheni et al., 2024).

3.2.2. *Aerodynamic control in tall buildings*

As in the case of long-span bridges, tall building aerodynamics can be actively modified to control their aeroelastic performance, as shown in Fig. 8. Some contributions were very recently published (Ding and Kareem, 2020; Abdelaziz et al., 2021; Hareendran et al., 2023) with solutions in this direction. Ding and Kareem (2020) proposed

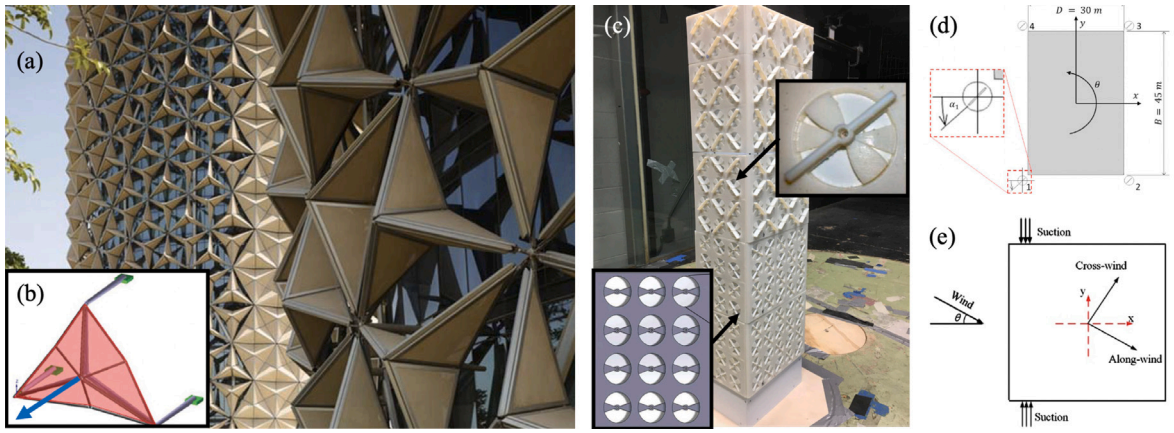

Fig. 8. Aerodynamic active systems in tall buildings: (a) Active façade of the Al-Bahr Towers, Abu Dhabi, UAE. Reproduced from Ref. Karanouh and Kerber (2015) with permission of the Creative Commons Attribution License CC BY 4.0, ©2015; (b) Detail of the origami-like façade unit showing the role of the actuator. Adapted from Ref. Karanouh and Kerber (2015) with permission of the Creative Commons Attribution License CC BY 4.0, ©2015; (c) View of the morphing façade system investigated through wind tunnel tests in Hou et al. (2023). Reproduced from Ref. Hou et al. (2023) with permission from Elsevier, ©2023; (d) Detail of the plates used to control the building aerodynamics in Abdelaziz et al. (2021). Reproduced from Ref. Abdelaziz et al. (2021) with permission from Elsevier, ©2021; and (e) Detail of the suction mechanism studied in Zheng et al. (2018). Reproduced from Ref. Zheng et al. (2018) with permission from Elsevier, ©2018.

the development of autonomously morphing structures by combining sensing systems, actuators, and computation so that the system assesses the most efficient aerodynamic cross-section configuration based on the information obtained by the sensing. The control strategies are based on employing RL agents to predict the optimal shape for the data collected from the distributed sensor network. The feasibility of combining CPS with control policies was recently studied by Whiteman et al. (2021), where a reduced-scale mechatronic aeroelastic model of a tall building was successfully tested in a boundary layer wind tunnel to conduct the tall building shape optimization by instantaneously introducing shape modifications on the building cross-section. An interesting alternative to actively control the aerodynamics of buildings without directly changing the cross-section is the addition of external appendages, as discussed for long-span bridges in Section 3.1.1. Abdelaziz et al. (2021) studied the performance of plates installed in tall building corners to improve the building aerodynamics, achieving reductions in the oscillation amplitudes of 94%.

On the other hand, small-scale shape modifications can impact the aerodynamics of the building by changing the porosity and roughness of the façade. This approach was studied in Hou et al. (2023) by developing a smart-morphing-façade attached to the original façade with a set of circular ducts equipped with a fixed base and a rotating part that enables active control. Furthermore, while still needing further development, origami-like structures (Filipov et al., 2015) are a suitable alternative to advance dynamic facade techniques (Del Grosso and Basso, 2010; Reis et al., 2015) that can impact the building aerodynamics, as shown in the early application of the Al-Bahr Towers, Abu Dhabi, UAE (Karanouh and Kerber, 2015). The mechanism controlling the origami-like façade in the Al-Bahr Towers is based on single mashrabiya dynamic units driven by a centrally positioned electric screw-jack linear actuator that controls the shape of the triangular origami members, as described in detail in Karanouh and Kerber (2015). As these structures rely on actuators to control the changes in the origami's shape, they can also be under the threat of malicious actions.

Another alternative approach to control tall building aerodynamics is to use flow controllers that impact the boundary layer and flow separation and reattachment without changing the actual shape of the building. The first proposal in this direction dates from the 1990s, when Kubo et al. (1993, 1996) developed a system based on a rotor installed in the building corner seeking to control the flow separation at the corner. Another approach is using suction to change the aerodynamics of tall buildings. Zheng and Zhang (2012) studied the effect on suction using CFD simulations and highlighted the impact of the so-called suction flow coefficients. Zheng et al. (2018) conducted wind tunnel tests on a reduced-scale aeroelastic model to verify the improvements achieved by the suction system in both the along-wind and across-wind responses at the cost of increasing the torsional response.

3.3. Wind turbines

The energy sector is considered one of the critical infrastructure sectors defined by the United States Department of Homeland Security (CISA, 2020). Among the multiple energy sources available, only a few require infrastructure that, due to their configuration and operation, can be considered sensitive to wind loads. Wind turbines are the energy harvesters with the highest sensitivity to wind, given the large size of contemporary blades and slender towers that are currently reaching heights up to 140 m.

According to the United States Energy Information Administration (USEIA, 2022), wind energy is the renewable energy source with the highest consumption share, reaching 10.3% of the share of total US energy consumption in 2022. The development and energy consumption share of wind energy is expected to grow, which is evident from the sector hiring tendencies (Keyser and Tegen, 2019). In Europe, according to WindEurope.org (2023), the share of wind energy in electricity demand was 31.5% on November 23, 2023. Furthermore, the European Wind Energy Association predicts that the European wind energy share will reach 50% by 2050 (European Wind Energy Association, 2019). It must be noted that most of the current share is provided by onshore wind farms with a share of 26.8%, while the current share of offshore wind turbines is 4.7%. However, the European Commission is pushing for the further development of offshore wind energy infrastructure (European Commission, 2023).

These trends have led in the last decades to the quick development of analysis methods (Bachynski et al., 2015; Bayati et al., 2016, 2017), design techniques (Rosenberg et al., 2014), and vibration control techniques (Njiri and Söffker, 2016; Xie and Aly, 2020). Similarly, the operation and active control of these structures, including at the local level (active dampers, active blades, etc.) and at the system level (wind farm control), has been remarkably advanced in the last two decades for both on-shore and off-shore farms. A summary of existing active control and operation methods is reported in Table 4, and further details are provided in the following subsections.

Table 4
Examples of active control and operation systems in wind turbines and wind farms with application examples.

Scale	Type	Method	Application
Turbine	Structural	Inertial control in tower and nacelles	Active mass dampers (AMD): Fitzgerald and Basu (2013), Fitzgerald et al. (2018) and Basaran et al. (2021) Twin rotor dampers (TRD): Bai et al. (2021a) Semi-active magneto-rheological (MR) dampers in nacelles: Martynowicz (2015) Semi-active TMD with cables in towers: Rezaee and Aly (2018) Active mass dampers in the nacelle of fixed offshore wind turbines: Brodersen et al. (2016) Semi-Active tuned liquid dampers in floating wind turbines: Coudurier et al. (2015) Hybrid mass dampers in nacelle of floating wind turbines: Hu and He (2017)
		Inertial control in blades	Active mass dampers in blades: Fitzgerald et al. (2013) Cable connected active tuned mass damper (CCATMD) in blades: Fitzgerald and Basu (2014)
		Stiffness control in blades	Active tendons: Staino and Basu (2015) Active strut controller for damping: Svendsen et al. (2011) and Krenk et al. (2012)
	Aerodynamic	Blade control	Collective blade control Burton et al. (2001) and Gambier and Nazaruddin (2018) Individual blade control for load reduction: Bossanyi (2003, 2005)
Farm	Control goals	Loads mitigation	Fatigue minimization: Zhao et al. (2021) Tower bending moment: Soleimanzadeh et al. (2012)
		Energy extraction Grid services and regulations Multiple goals	Power maximization: Marden et al. (2013) Targeting power demand: Hur and Leithead (2016) Maximum power and minimum load: Soleimanzadeh et al. (2012)
	Wake control	Wake steering Axial induction	Wake steering: Liew et al. (2015) Dynamic induction control (DIC): Muscari et al. (2022)

3.3.1. Active structural control in wind turbine towers and nacelles

The first category of vibration control methods are those based on actively controlling the structural or mechanical properties of the tower, nacelle, or the tower-nacelle system. Active inertial control devices are used to mitigate wind-induced vibrations in the same way as in tall buildings, as discussed in Section 3.2.1. A straightforward approach is using active mass dampers commonly located in the nacelle. Fitzgerald and Basu (2013) and Fitzgerald et al. (2018) proposed the use of ATMD to control the vibrations of a wind turbine tower. Basaran et al. (2021) investigated using active electromagnetic mass dampers in the nacelle to mitigate vibrations. Moreover, AMD in nacelles has also been used for fixed offshore wind turbines (Brodersen et al., 2016). An alternative approach to classical ATMD for tower vibration control is using TRD, as proposed by Bäumer and Starossek (2016) and Bäumer et al. (2018). Their implementation in wind turbine towers was recently investigated by Bai et al. (2021a).

On the other hand, floating towers are under the influence of waves, which further complicates the wave-wind-structure interaction problem. Coudurier et al. (2015) proposed a passive and semi-active control method for an offshore floating wind turbine using a tuned liquid column damper located in the tower base. Hu and He (2017) studied the performance of a hybrid mass damper in the nacelle to control wind- and wave-induced vibrations. A specific review of damping systems for floating wind turbines can be found in Tian et al. (2023).

3.3.2. Active structural blade control

Blade vibrations can occur in the same plane of rotation of the blades, which is known as in-plane vibration, and in the perpendicular direction of the rotation plane, commonly defined as out-of-plane vibration (Fitzgerald and Basu, 2014). The first developments on structural control of large and slender structures were developed in the aerospace engineering field several decades ago (Meirovitch, 1977; Balas, 1978; Goh and Caughey, 1985). Current control methods in modern wind turbine blades consist of inertial and stiffness control devices. Active inertial dampers are an effective technique to mitigate blade vibrations. For example, Fitzgerald et al. (2013) studied using active tuned mass dampers to control in-plane vibrations of wind turbine blades. An alternative version to ATMD installed inside the blades is the use of cable-connected active tuned mass dampers (CCATMD), as proposed by Fitzgerald and Basu (2014) and shown in Fig. 9(a). On the other hand, stiffness control methods can be used to mitigate blade vibrations. Svendsen et al. (2011) and Krenk et al. (2012) proposed using an axial extensible strut near the root of each blade to introduce a bending moment that controls the deflection of each blade. Later, Staino and Basu (2015) investigated the effectiveness of active tendons located inside the blade for controlling the blade vibrations. However, active inertial dampers are the most widespread technique for blade vibration control.

3.3.3. Active aerodynamic blade control

The most widespread wind turbine configuration consists of a three-blade turbine with horizontal axis variable speed and variable blade pitch because they allow for the optimization of power generation at variable wind velocities. These turbines can work in five operational modes depending on the wind velocity (Fragoso et al., 2017): (1) cut-in, (2) partial load, (3) transition, (4) full load, and (5) cut-out. During the partial load operation mode, the wind turbine seeks to maximize power production by optimizing the pitch angle (Kumar and Chatterjee, 2016). Later, during the full load operation mode, the turbine produces the maximum rated electric power, and the goal of the controller is to limit this power by changing the pitch angle to avoid overloading the wind turbine (Boukhezzar et al., 2007). After surpassing the high wind cut-out limit, the wind turbine is powered down to avoid excessive operating loads. This limit is typically about 20 or 30 m/s for large wind turbines (Simani, 2015). In order to change from one operational model to another and properly perform the turbine's control in each operation mode, the wind turbine blades are controlled, as shown in Fig. 9(b). Collective pitch control can be performed to either maximize the energy production or reduce the wind load, depending on the operational mode (Burton et al., 2001; Manwell et al., 2009; Pao and Johnson, 2009; Gambier and Nazaruddin, 2018). Alternatively, Bossanyi (2003, 2005) proposed individual blade control to improve load reduction.

Specific cybersecurity risks for these systems involve changing the intended use of the blades between different operational regions: (1) during the partial load operational mode, cyberattacks can target disruptions in the energy production; (2) during the full load operational mode, attackers can damage the wind turbine by increasing the load through malicious blade control; and (3) delaying the high wind cut-out

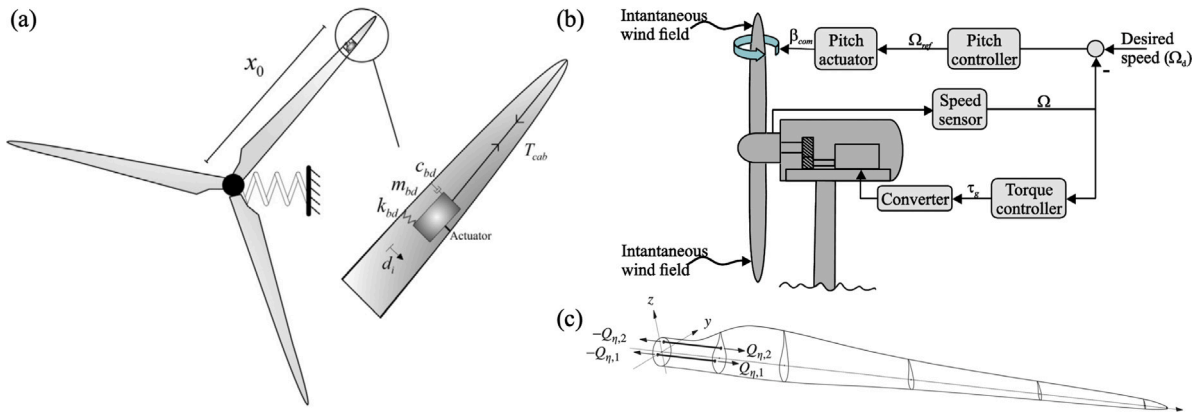

Fig. 9. Blade control in wind turbines: (a) Active control using cable connected active tuned mass dampers (CCATMD). Reproduced from Ref. Fitzgerald and Basu (2014) with permission from Elsevier, ©2014; (b) Wind turbine controls and standard loops, including blade pitch control and torque control. Reproduced from Ref. Njiri and Söffker (2016) with permission from Elsevier, ©2016; and (c) Blade structural control system consisting of an axial extensible strut located near the root of each blade. Reproduced from Ref. Svendsen et al. (2011) with permission from Elsevier, ©2011.

limit, i.e., surpassing the maximum wind velocity, which would cause relevant damage to the wind turbine.

3.3.4. Wind farms

Wind farm control is another field that can be under the threat of cyberattacks. While the farm control (system level) is physically executed on each wind turbine (local level), malicious actions on the farm control can lead to damage to each individual turbine. Modern wind turbines are controlled by the generator torque and the blade pitch controller (Goit and Mayers, 2015), which was discussed in the previous section. Hence, while this section does not provide more information about the physical actuation at the wind turbine level, it provides an overview of different potential malicious actions that can be carried out to change the intended goal of the system to (1) affect the energy production by the farm, and (2) damage one or multiple individual turbines of the farm.

Wind farm safety and efficiency are major concerns in both onshore and offshore wind farms (Barthelmie and Jensen, 2010), which are conditioned by the ambient conditions (Doekemeijer and van Wingerden, 2020; Hansen et al., 2011). Wind farm controllers (Spruce, 1993; Stock and Leithead, 2022) seek to achieve these goals, and they can be classified based on how these goals are formulated on the control algorithm or strategy (Knudsen et al., 2015) as (1) structural load mitigation (Zhao et al., 2021), (2) energy extraction maximization (Marden et al., 2013), and (3) grid services and power regulations and demand (Hur and Leithead, 2016). These goals can be managed in hybrid control strategies seeking a balance between goals demanding contradictory actuation policies by using multi-objective optimization frameworks seeking the maximization of a goal, such as the power generation, and the minimization of other goals, such as the structural load (Soleimanzadeh et al., 2012). Another classification can be made based on the actuator method for wake control: (1) based on axial induction (Muscari et al., 2022) and (2) based on wake steering (Liew et al., 2015). Further classifications can be made based on the control concept or model adopted (model-based, model-free, open-loop, closed-loop, etc.) and the kind of control of the structure (distributed, decentralized, and centralized). However, they do not have a major impact on the cybersecurity of the system.

3.4. Solar panels

Another source of energy relying on wind-sensitive infrastructure is solar photovoltaic (PV) panel trackers. Solar trackers consist of an array of PV panels, as shown in Fig. 10(a), oriented to maximize the sun energy captured (Aziz and Hassan, 2017; Racharla and Rajan, 2017). Single-axis trackers (SATs) are a popular alternative due to their higher power generation compared to fixed-tilt arrays. According to Enslin (1992), automatic tracking systems can increase the power generated by up to 25%. Examples of SATs can be found in Al-Mohamad (2004) and Mousazadeh et al. (2009). An advanced version seeking to track both the solar inclination and the azimuth angle variation is the two-axis solar tracker (Yao et al., 2014; Oh et al., 2015; Hoffmann et al., 2018), as shown in Fig. 10(d). Multiple other configurations are possible (Hao et al., 2022). A comprehensive review of sun-tracking methods can be found in Mousazadeh et al. (2009).

Active trackers are automatic systems composed of sensors, controllers, and actuators that move the panels following one of the following approaches (Hoffmann et al., 2018): (1) Trackers based on optical sensors and microprocessors; and (2) Trackers based on date and time controlled by a computer that calculates the solar position. An example of the first approach is described in Al-Mohamad (2004), where the PLC and the input-controller-output system are described in detail, as shown in Fig. 10(c). This system relies on a PLC, so it can be vulnerable to the cyberattacks described in Section 2.1.1.

The malicious control of solar trackers can be dangerous under some wind conditions, given that wind loads are drastically impacted by the panel's tilt angle (Kopp et al., 2012; Ma et al., 2023; Enshaei et al., 2023). Several studies have addressed the dependency of wind loads on the tilt angle for several wind directions (Aly and Bitsuamlak, 2013; Irtaza and Agarwal, 2018; Abiola-Ogedengbe et al., 2015; Strobel and Banks, 2014), as shown in Fig. 10(b). For this reason, solar energy companies conduct wind engineering studies to analyze the wind-resistant capacity of the arrays for the full range of tilt angles permitted by the array and analyze its performance for several aeroelastic phenomena (Young et al., 2020; Quintela et al., 2020; Martinez-Garcia et al., 2021; Valentin et al., 2022). Moreover, solar companies are currently developing approaches in collaboration with wind engineering consultants to deal with wind load mitigation more efficiently (Cherukupalli et al., 2022) and avoid catastrophic failures of solar arrays, as the one investigated by Valentin et al. (2022), which resulted in serious damage on the axis bar, PV modules, and supporting frames (see Fig. 11). In view of the contemporary wave of cyberattacks on CI and the potentially destructive effect of high wind events, it is fundamental to address eventual cybersecurity issues in solar trackers leveraged by the action of wind.

4. Potential attacks on CI equipped with OT/CPS

In this section, we analyze the effects of DoS and FDI focusing on wind-sensitive structures and expand the study to introduce Wind-leveraged False Data Injection (WindFDI), a new kind of cyberattack where a natural hazard, the wind, is leveraged to significantly increase

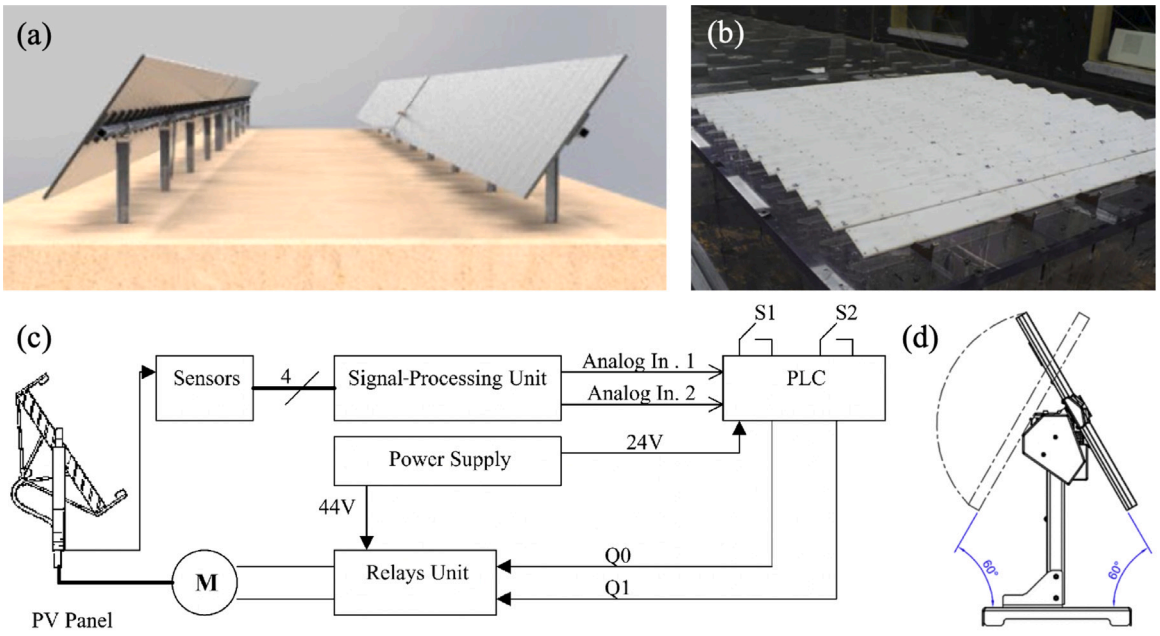

Fig. 10. Tilt angle control in PV panels: (a) Render of PV panels mounted on a single-axis tracker (Quintela et al., 2020); (b) Photo of the array layout of PV tunnels tested in the Boundary Layer Wind Tunnel Laboratory at Western University at different tilt angles. Reproduced from Ref. Kopp et al. (2012) with permission from Elsevier, ©2012; (c) Block diagram of the control system of a single-axis tracker controlled by a PLC. Reproduced from Ref. Al-Mohamad (2004) with permission from Elsevier, ©2004; and (d) Amplitude of movements of a two-axis solar tracker. Reproduced from Ref. Hoffmann et al. (2018) with permission from Elsevier, ©2018.

Fig. 11. Damage on a single-axis solar tracker due to wind-induced torsional load. Reproduced from Ref. Valentin et al. (2022) with permission from Elsevier, ©2022.

the affectations to physical structures. We start by describing a threat model, which details the assumptions, circumstances, scenarios, as well as the information needed to carry out a successful attack. Then, we use our threat model to describe three different cyberattacks against wind-sensitive structures.

4.1. Threat model

For the purposes of the attacks we will discuss later in this section, we assume that wind-sensitive structures are equipped with different kinds of CPS to control the wind-induced responses, as discussed in Section 3. Since this research effort aims to define criteria for designing and evaluating active control systems, we discuss the attack planning depending on the available information about the structural system and wind conditions. Also, in order to develop efficient cyberdefenses, the architecture behind all potential cyberattacks that the CPS installed on wind-sensitive structures can suffer must be investigated. Next, we classify the potential cyberattacks to wind-sensitive structures by using the following criteria: (1) kind of affectation based on the actuation or nature of the CPS; (2) attack scenarios depending on the available data to plan the attack; and (3) kind of cyberattack depending on the formulation of the actuation on the CPS.

4.1.1. Kind of affectations enabled by the CPS

A first classification can be made depending on the expected affectations to the CPS based on the kind of actuators involved, which will later condition the cyberattack planning and the development of appropriate cyberdefenses. With that in mind, the following classification is proposed:

- *Mechanical affectations* involve using any actuator able to modify the stiffness and inertial properties. This includes the ICS listed in Section 3, such as AMDs. These active systems are very generalized in the case of tall buildings and wind turbines, and AMDs are also getting more popular in long-span bridges.
- *Aerodynamic affectations* entail controlling an actuator capable of changing the aerodynamic properties of the structure, such as active façades, winglets, barriers, etc. Active systems are very common in wind-mill towers (Bossanyi, 2005; Kumar and Chatterjee, 2016) and solar panel arrays (Mousazadeh et al., 2009). Some applications can be found for long-span bridges, such as the automatic wind barriers of the Xihoumen Bridge (Yang et al., 2022), and multiple systems are currently being investigated (Gao et al., 2021). Applications in tall buildings are currently being

developed (Ding and Kareem, 2020; Chang, 2020; Hou et al., 2023).

4.1.2. Cyberattacks scenarios: The role of knowledge in the cyberattack plan and its impact on cyberdefenses

While the target and kind of actuation needed to perform a cyberattack to some CI described in Section 3 are more or less straightforward, planning an attack on wind-sensitive active structures is not obvious from both the perspectives of computer science and civil engineering experts, since these attacks must be adapted to the specific characteristics of each structural systems. In this context, knowledge about the structural system and insider information is crucial for the definition of the cyberattack, and, consequently, for developing efficient cyberdefenses. The importance of insider knowledge was highlighted after the Stuxnet cyberattack, as highlighted in Fildes (2010): "…with the forensics we now have it is evident and provable that Stuxnet is a directed sabotage attack involving heavy insider knowledge…". With that in mind, the data required for planning the attack properly include:

- Mechanical information of the structure, i.e., dimensions, natural frequencies, mode shapes, etc.
- Local wind data, including wind velocity, wind direction, return periods of moderate and extreme wind events, turbulence characteristics, non-synoptic features, effects of the surrounding terrain, build environment, and other obstacles, etc.
- Aerodynamic properties and aeroelastic performance enable the attack's design.
- Information about the CPS that permits the actuation of the target structure. This includes its effect on the structure's mechanical and aerodynamic properties, depending on the kind of actuation.

Hence, four kinds of attack scenarios are considered depending on the previous information available and how the required information about the target is acquired to execute the attack.

- *Informed cyberattack.* Informed attacks are characterized by the availability of all required information for the full plan of the cyberattack before its execution, which makes it unnecessary to obtain information from any sensor. Consequently, the only sensor/actuator that needs to be hacked is the CPS. The CPS will be controlled to change the mechanics and/or aerodynamics of the target structure pursuing the increase of the wind-induced excitation as planned from the information available beforehand. The process is conceptually described in Fig. 12, independently of the kind of actuator (CPS). As shown in this figure, all information about the structural system, wind, and CPS is available, and specific models can be built to model the entire system or create a digital twin of the target structure if needed. This includes finite element models (FEM) for the structural behavior, CFD simulations for the aerodynamic analysis, control models of the CPS, and aeroelastic models to anticipate the behavior of the structure under the attack.
- *Uninformed cyberattack.* The opposite case can be defined as uninformed cyberattacks. These attacks are planned without enough previous information about the target structure, so it is required as part of the attack to acquire information from weather stations and the SHM system from the target structure, postprocessing the data, planning the attack based on the extracted data, and hacking the CPS capable of modifying the inertial or aerodynamic characteristics of the structure. Fig. 13 presents a flowchart describing the phases involved in the process. First, wind data must be extracted from weather stations to build a wind model that permits planning the actions of the CPS. Then, the SHM system needs to be hacked to extract the responses of the structure under different wind scenarios. Using the wind data and structural performance, input–output models can be trained to emulate the responses of the target structure. Also, the CPS may need to be hacked to learn about the effects of the actuation on the structure. All this information must be extracted before the cyberattack on the actuator is carried out, which involves developing more complex and longer attacks.
- *Semi-informed (Hybrid) cyberattack.* Halfway between informed and uninformed. Some information is available. Still, some information is required from the sensors of the structure.
- *Blind cyberattack.* The information available is incomplete and insufficient to develop an optimized cyberattack plan properly. However, this kind of attack is planned with limited information available, and no further information is intended to be extracted. The potential damage is more limited, and it is not possible to define an optimal attack due to the lack of information. However, this random attack can still be very disruptive, and its implementation is easier and faster as it does not require learning from the structural system or developing a detailed plan.

Table 5
Summary of different kinds of cyberattack scenarios depending on the attacker's knowledge of the properties of the target structure.

Cyberattack	Information	Knowledge
Informed	Structural dynamics	Available through FEM models
	Wind modeling	Available through accessible weather stations
	Aeroelastic performance	Aeroelastic models with enough information to plan attacks
Uninformed	Structural dynamics	Require hacking SHM system at the target
	Wind modeling	Require hacking weather stations at the target
	Aeroelastic performance	Require hacking SHM system at the target under wind conditions
Hybrid		Combination of informed and uninformed. It requires extracting data.
Blind		Random attack with insufficient information. It does not require extracting data.

Table 5 summarizes the main characteristics of these attacks, which condition the systems that must be hacked to perform the attack. Depending on which scenario we are in, the attack requires hacking different systems, so the design of the defenses must be adapted accordingly to avoid the success of the cyberattacks.

- In an informed scenario, there is no need to extract data from the structure since all the required information is assumed to be available. The attack can be fully designed remotely, and the only system required to be hacked is the cyber–physical system to carry out the actuation. Blind attacks can also be classified into this category, as no further information about the target structure is required.
- In an uninformed scenario, a large set of data is required to plan the attack, which involves hacking a large number of sensors in the structure and then attacking the cyber–physical device. Uninformed attacks must be developed based on the OT/CPS installed in each target, focusing on each SHM system to extract the required information. Details about SHM systems installed in longs-span bridges can be found in the literature, for instance, for the Golden Gate Bridge (Abdel-Ghaffar and Scanlan, 1985; Kim et al., 2007), the Zhanjiang Bay Bridge (Cao et al., 2010), the Sutong Bridge (Wang et al., 2020), Second Jindo Bridge (Jo et al., 2011), or the First Bosphorus Bridge (Bas et al., 2017), among others. In the case of tall buildings, an extensive literature is also available. Some examples are the Burj Khalifa (Abdelrazaq,

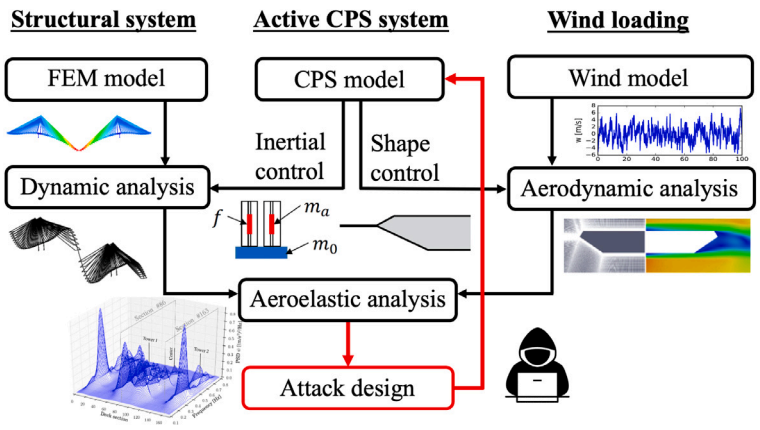

Fig. 12. Conceptual flowchart describing an Informed Cyberattack to a generic long-span bridge equipped with either a mechanical (inertial) or aerodynamic (shape) CPS for mitigating wind-induced loads.

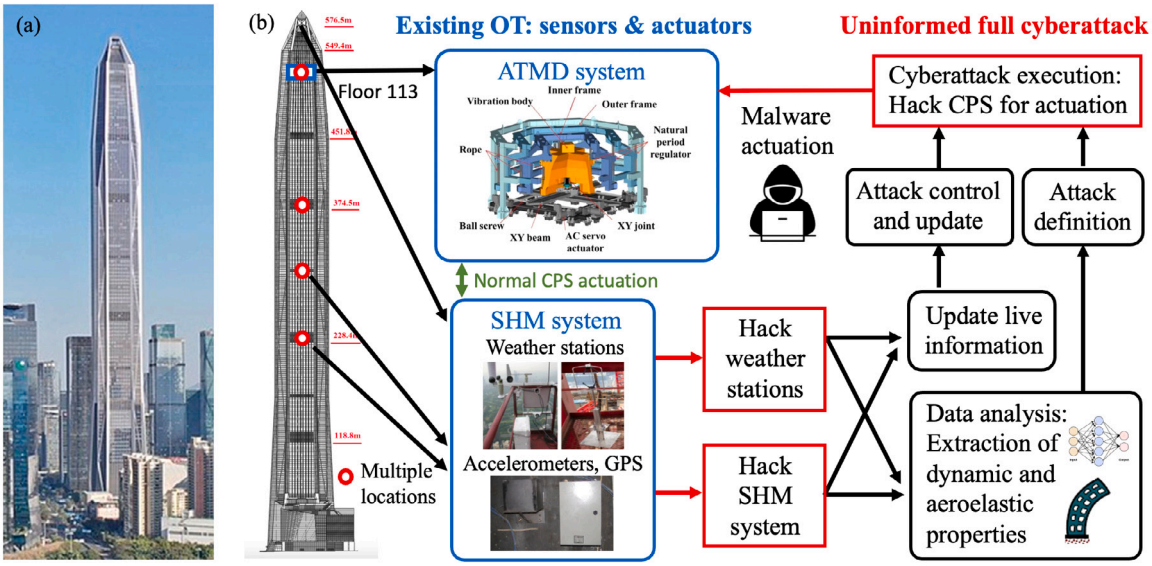

Fig. 13. Conceptual sketch of an Uninformed cyberattack using as an example the OT (SHM & CPS) of the Ping-An Finance Center, China (Zhou et al., 2022; Zhou and Li, 2022). The mechanical CPS is an active mass damper (AMD). (a) General view of the PAFC; (b) Flowchart of the Uninformed Cyberattack, including data extraction. Subfigures reproduced from Ref. Zhou and Li (2022) with permission from Elsevier, ©2022.

2012; Kijewski-Correa et al., 2013; Arul et al., 2020), the Ping-An Finance Center (Zhou et al., 2022; Zhou and Li, 2022), the Canton Tower (Guo et al., 2012b), the Guangzhou New TV Tower (Ni and Zhou, 2010), the Shanghai Tower, (Wu et al., 2021) and several buildings in downtown Chicago (Kijewski-Correa et al., 2006).

4.2. Cyberattacks on wind-sensitive smart structures

The nature of active countermeasures to mitigate wind effects on structures give place to three different kind of attacks: (1) Denial of Service (DoS); (2) False Data Injection (FDI); and (3) Wind-leveraged False Data Injection (WindFDI). The first two kinds of attacks have been applied in other fields (Zambrano et al., 2021), while the third one is described in this study for the first time as a new potential threat that can lead to the collapse of the structure. Table 6 summarizes the main characteristics of these attacks, which will be defined in detail in Sections 4.2.1 to 4.2.2 and 4.2.3. Their descriptions are compared by contrasting three relevant characteristics: (1) Temporality, which describes when this attack can take place; (2) Applicability, which deals with what kind of active systems are subject to this kind of attack and why; and (3) Effectiveness, which quantifies the potential damage that the attack can cause to the wind-sensitive structure.

The potential effect of these attacks is conceptually described in Fig. 14 for a bridge deck equipped with active flaps based on the study by Li et al. (2022). While the right use of the flaps permits the mitigation of the wind-induced response (green line), the misuse of active systems can deny the excitation mitigation (gray line, blocking the use of the flaps, DoS) or even worsen the wind-induced response (red line, misusing the flaps to increase the wind-induced excitation, FDI), potentially leading to instabilities that can cause the collapse of the structure. FDI attacks can be randomly executed to increase the excitation of the structure. However, the impact of FDI can be leveraged by defining the optimal control that maximizes the damage to the structure by harnessing the aerodynamic forces, giving place to the WindFDI.

4.2.1. Denial of Service (DoS)

A Denial of Service attack disables the OT/CPS, leaving the target structure without the benefits of the active control system. The DoS attack can block the operation of only some specific actuators or all of them. This attack does not cause any direct damage to the target structure. The structure is only damaged if the attack is executed during a natural hazard that requires a mitigation action by the blocked

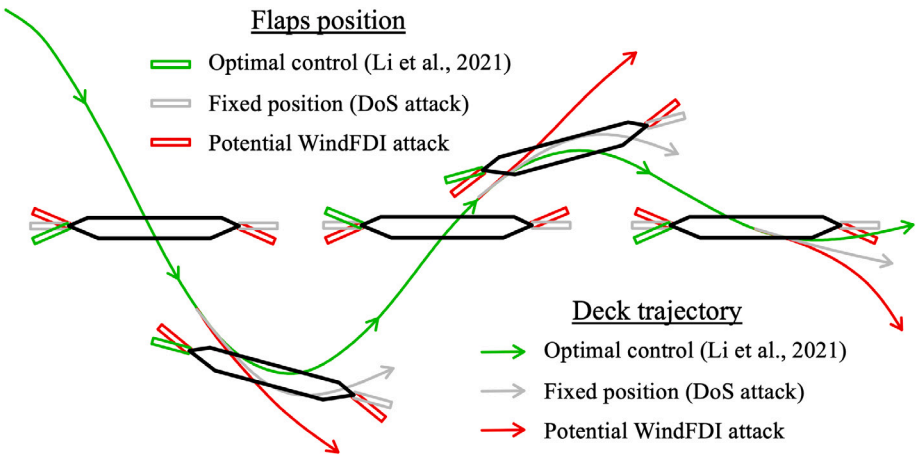

Fig. 14. Graphical explanation of the potential effect of cyberattacks (DoS and WindFDI) on a bridge deck equipped with flaps compared to the optimal control pattern reported in Li et al. (2022).

Table 6
Summary of different kinds of cyberattacks comparing their temporal and physical applicability and potential damage.

Cyberattack	Characteristic	Description
DoS	Temporality	During the action of extreme natural hazards
	Applicability	All active systems
	Effectiveness	Structural response without active system
FDI	Temporality	Always
	Applicability	Only massive CPS whose movement can impact the target structure
	Effectiveness	Structural effect of moving the CPS
WindFDI	Temporality	Under frequent winds capable of amplifying structural excitation
	Applicability	All active systems
	Effectiveness	Extreme amplification of wind effects. Potentially destructive.

actuator. Hence, it is opportunistic since its effect is conditioned to the occurrence of the natural hazard.

From a mathematical perspective, the definition of an optimal DoS attack consists of maximizing the damage ($D\left(\boldsymbol{\pi}_{\mathrm{DoS}}, \boldsymbol{w}\right)$) caused by the natural hazard during the execution of the DoS attack. Hence, the main goal is identifying which actuator should be blocked to cause the highest damage, which can be formulated as follows:

$$\begin{aligned} &\text{find}: \boldsymbol{\pi}_{\mathrm{DoS}} = \left(\pi_i\right),\ i = 1, \ldots, n \\ &\text{maximize}: D\left(\boldsymbol{\pi}_{\mathrm{DoS}}, \boldsymbol{w}\right) \\ &\text{subject to}: \\ &\pi_i \in \{0, 1\}\ \ \forall i = 1, \ldots, n \end{aligned} \tag{1}$$

where $\boldsymbol{\pi}_{\mathrm{DoS}}$ is the vector containing the DoS attack policy of the actuators controlled by the adversary, which is an n-dimensional binary vector that indicates what actuators the adversary will disconnect. $\boldsymbol{w}$ is the weather scenario, which includes the wind speed, direction, turbulence characteristics, etc., and n is the total number of existing actuators. The weather scenario is fundamental for defining the optimum attack, given its influence in the response of any kind of wind-sensitive structures (Doekemeijer and van Wingerden, 2020; Hansen et al., 2011).

This attack can be implemented in several ways, including energy cuts, software service denials, blocking specific actuators, and others. Its effect on the wind-sensitive critical infrastructure discussed in Section 3 is straightforward in several cases. A good example is the problem described in Fig. 14 when the bridge-flap system is under a DoS attack. As the flaps of the deck-flap system are blocked, there is no longer an active mechanism capable of mitigating the wind-induced responses available, which may increase the response or even lead to divergence in some wind scenarios. A similar effect would be caused by denying the activation of active inertial systems in tall buildings and towers. A critical example would be denying the cut-out operational mode in wind turbines when the local wind surpasses the maximum wind velocity (see Section 3.3.3), which could cause serious damage to the wind turbine.

4.2.2. False Data Injection (FDI)

Besides blocking the actuators to deny their capacity to mitigate wind loads, CPS can be maliciously used to damage the target structure using only their own actions. A malicious policy $\boldsymbol{\pi}_{\mathrm{FDI}}$ can be defined seeking the maximization of the damage $D\left(\boldsymbol{\pi}_{\mathrm{FDI}}\right)$ considering not only how many actuators must be controlled but also the specific action in terms of movements they will perform during the execution of the attack. This kind of attack does not depend on the weather; hence, it can be executed at any time, regardless of wind conditions. The FDI attack can be formulated as:

$$\begin{aligned} &\text{find}: \boldsymbol{\pi}_{\mathrm{FDI}} = \left(\pi_i\right),\ i = 1, \ldots, n \\ &\text{maximize}: D\left(\boldsymbol{\pi}_{\mathrm{FDI}}\right) \end{aligned} \tag{2}$$

where $\boldsymbol{\pi}_{\mathrm{FDI}}$ is the vector containing the FDI attack policy of the actuators controlled by the adversary, which contains the actuation pattern for each actuator i, and n is the total number of existing actuators. The damage maximization problem is only a function of the policy π_{FDI}, which is designed and executed independently of the weather scenario $\boldsymbol{w}$. This attack aims to excite the structure by carrying out harmonic motions with the CPS that match the natural frequencies of the target structure, seeking a resonant amplified response. The effectiveness of this attack is conditioned by the kind of CPS, its relative mass with regard to the target structure, and its capacity to excite the target structure with the allowed movements. This attack can be very effective using inertial control systems in tall buildings and towers. However, it may be ineffective for aerodynamic CPS, such as the flaps used in the problem described in Fig. 14 without the action of wind.

4.2.3. Wind-leveraged False Data Injection (WindFDI)

The Wind-leveraged False Data Injection attack seeks to exploit all the potential damage that a CPS can create on the target structure by using the wind as an "external help" to increase the attack's impact. This cyberattack is planned to pursue the opposite goal of control theory (Wilde and Fujino, 1998): maximize the wind-induced responses (damage) $D\left(\boldsymbol{\pi}_{\mathrm{WindFDI}}, \boldsymbol{w}\right)$ instead of mitigating the wind-induced responses. This can be achieved by taking advantage of the positive feedback of the wind loads and the CPS action. The effectiveness of the attack relies on the wind conditions $\boldsymbol{w}$, and can be carried out under frequent

winds or even daily winds as long as they permit the amplification of the structural response. Hence, it can be classified as an opportunistic attack since its performance depends on the weather scenario. The mathematical formulation of the WindFDI attack is an optimization problem seeking to identify the optimum policy that maximizes the structural damage:

$$\begin{aligned} &\text{find} : \boldsymbol{\pi}_{\text{WindFDI}} = \left(\pi_i\right), \ i = 1, \ldots, n \\ &\text{maximize} : \mathcal{D}\left(\boldsymbol{\pi}_{\text{WindFDI}}, \boldsymbol{w}\right) \end{aligned} \tag{3}$$

where $\boldsymbol{\pi}_{\text{WindFDI}}$ is the vector containing the WindFDI attack policy for each actuator controlled by the adversary leveraging the external load of the wind. It is a function of the weather scenario $\boldsymbol{w}$, since for each wind velocity, direction, and turbulence characteristics, the optimum policy $\boldsymbol{\pi}_{\text{WindFDI}}$ may be different.

The WindFDI attack concept is clearly explained in Fig. 14, where it can be seen that the operation of the flaps can be intentionally changed to increase the amplitude of the bridge deck oscillations (red line) instead of decreasing them (green line). The attack plan can be defined by using the analytical expressions for the self-excited forces as a function of the control parameters, such as each flap oscillation phase and amplitude. For instance, taking advantage of the dependency of the flutter derivatives values with the flap phase φ, the control policy can be defined by the flaps phases vector as $\boldsymbol{\pi}_{\text{WindFDI}} = \boldsymbol{\varphi}$. Hence, the optimization problem formulated in Eq. (3) will identify the optimal combination of $\boldsymbol{\varphi}$ that maximizes the bridge response by means of variations in the value of the flutter derivatives. A specific example is reported in Section 5.4 where a WindFDI attack is planned based on the data reported by Cobo del Arco and Aparicio (1999).

5. Proof of concept: Quantifying cyberattacks-induced damage

In Section 3, we identified multiple cases of CI equipped with CPS/OT that can be under the threat of cyberattacks and discussed the potential damage in a qualitative way. In the present section, we provide some results based on data available in the literature that help us to quantitatively analyze the potential damage the aforementioned cyberattacks can cause on smart structures under the action of wind.

5.1. Example #1: Denial of Service (DoS) of aerodynamic control devices in bridges

Denial of service (DoS) attack on active flow modifiers is one of the most straightforward attacks given its similitude with the safety issues due to active systems failure or power outages. The potential damage of these attacks can be found in multiple contributions in the literature studying the effect of uncontrolled active devices. A good example is the study by Sangalli and Braun (2020), where three application cases consisting of bridge decks with active winglets are studied numerically. It is important to bear in mind that the effect of denying the regular service of active countermeasures is not limited to increasing the amplitude of the response but can also eventually lead to flutter instability. That is the conclusion of the example shown in Fig. 15, where it is clear that the rectangular deck cross-section suffers divergence in a no-control scenario.

The same concept can be applied to flexible structures equipped with AMD, such as the bridge deck equipped with AMD reported in Körlin and Starossek (2007) where the uncontrolled configuration of the AMD reduces the critical wind speed by 16.5%. Chang (2020) reported a case where an uncontrolled AMD led to the divergent vertical accelerations of a bridge deck under a constant external force. These examples highlight the high impact of DoS attacks when wind-sensitive structures equipped with active mitigation systems are without control.

5.2. Example #2: Denial of Service (DoS) of multiple aerodynamic control devices in bridges

Another interesting case directly related to planning DoS attacks involving multiple controllers can be found in Kwon and Chang (2000). This study analyzes the effect of the failure of individual controllers along the deck on the flutter velocity of the bridge. This shows the optimal DoS planning process involving multiple controllers formulated in Eq. (1). Fig. 16 compares the performance of the bridge when fully controlled (normal performance without any cyberattack, showing a flutter velocity of about $U_f \approx 52$ m/s), with some controllers not working (not optimal DoS attack on individual controllers, flutter velocity in the range $U_f \approx [46-49]$ m/s), and without any control (full DoS attack blocking all controllers, $U_f \approx 39$ m/s). In this case, it is clear that the optimal DoS consists of blocking all the controllers. However, the optimal DoS attack must be specifically formulated for each target structure.

5.3. Example #3: Denial of Service (DoS) of inertial control devices in buildings

A similar effect can be caused by denying the service of active inertial modification devices. The paper by Yalla et al. (2001) studies the effectiveness of several control algorithms for their implementation in the control of semi-active tuned liquid column dampers (SATLCD) and reports the results of a multi-degree-of-freedom (MDOF) building sketched in Fig. 17(a) and (b). Fig. 17(c) compares the results adopting several control strategies and without control, or, equivalently, under a DoS attack. It can be seen that the amplitude of the response under a DoS attack can be increased up to 5 times compared with the passive control response and much more compared to the controlled response.

5.4. Example #4: WindFDI to a bridge with active winglets seeking the flutter onset anticipation

A clear example of the potential damage of a WindFDI cyberattack can be deduced from the information reported in Cobo del Arco and Aparicio (1999). This reference examines the influence of aerodynamic appendages on the wind stability of box-girder suspension bridges and studies the influence of the out-of-phase angle φ between the movements of the winglets and the girder. Following the assumption and equations summarized in Section 3.1.1, the flutter derivatives of the winglet-deck system can be expressed analytically as a function of their size and movement, and then the flutter instability can be easily assessed. Cobo del Arco and Aparicio (1999) reported several cases where controlling the winglets considerably increases the flutter and aerostatic stability critical wind velocities. For instance, Fig. 18 compares the performance of a deck without any kind of flaps or winglets (black line) and with active winglets adopting different values of the phase angle φ (blue and red lines). The cases shown in blue ($\varphi = 0°, 30°, 60°$, and $90°$) show the benefits of adopting active control of the winglets. By taking a value of frequency ratio $\gamma_\omega = \omega_\alpha/\omega_h = 2.25$, similar to some of the bridges reported (Bartoli and Mannini, 2008), such as the Bosporus ($\gamma_\omega = 2.29$), Akashi ($\gamma_\omega = 2.34$), Tsurumi ($\gamma_\omega = 2.39$), and Normandy ($\gamma_\omega = 2.27$), or the cable-stayed bridge used in Cid Montoya et al. (2018a) ($\gamma_\omega = 2.27$), it can be easily seen the effects on the flutter velocity. For instance, imposing a phase of $\varphi = 0°$ (blue continuous line) increases the value of the non-dimensional flutter velocity $\beta = 2U_f/B\omega_h$ from 5.78 to 9.98; this is, an increase of about 73%.

However, in particular cases, the malicious use of the active winglet can lead to catastrophic scenarios. The bad performance of the winglets under some phase angles was highlighted in Cobo del Arco and Aparicio (1999): "*The importance of the election of the phase angle is stressed when looking to the results obtained with $\varphi = -30°$, $\varphi = -60°$; observe that a wrong election in the phase angle may cause the instability of the structure*

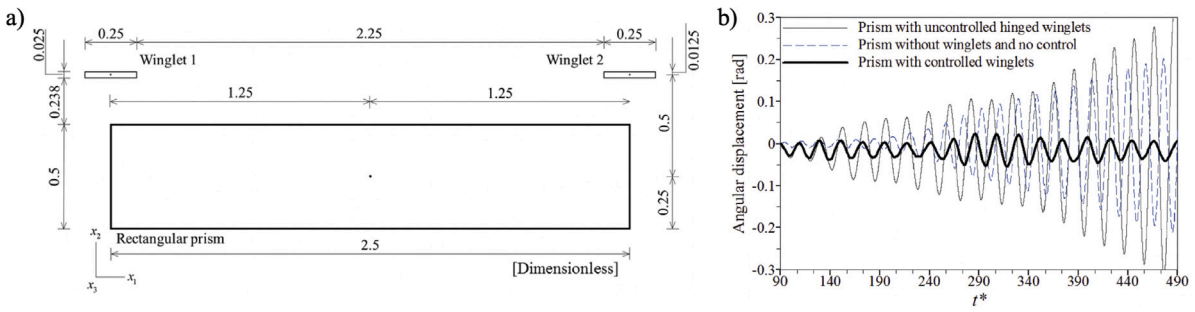

Fig. 15. Potential divergent response on bluff bodies equipped with active winglets due to a DoS cyberattack. Figures reproduced from Ref. Sangalli and Braun (2020) with permission from Elsevier, ©2020.

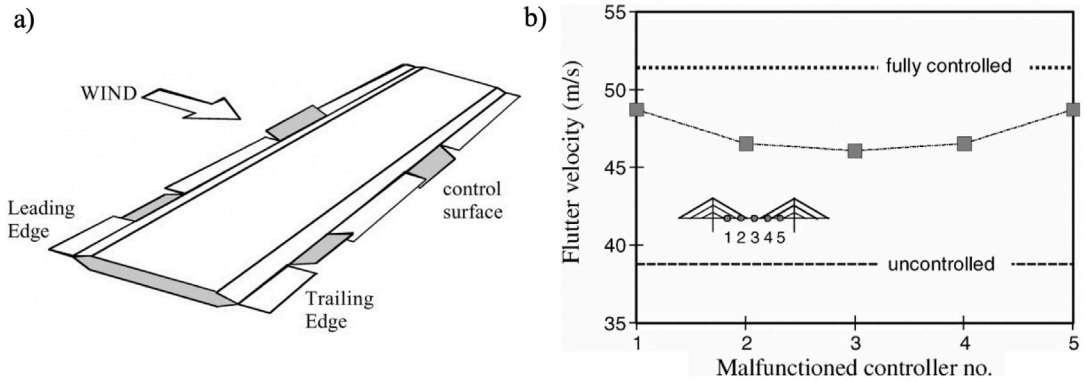

Fig. 16. Potential decrease of the flutter velocity of a cable-stayed bridge equipped with active edges due to a DoS attack on multiple controllers. Figures reproduced from Ref. Kwon and Chang (2000) with permission from Elsevier, ©2000.

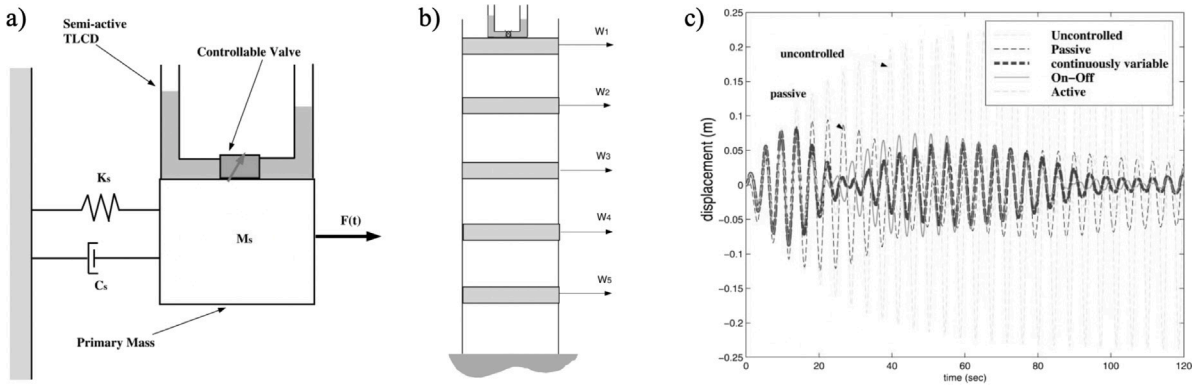

Fig. 17. Potential challenging increase of amplitude in an MDOF building equipped with semi-active tuned liquid column dampers (SATLCD) by a DoS cyberattacks based on the studies reported in Yalla et al. (2001). (a) Schematic representation of the SATLCD-structure combined system; (b) MDOF building equipped with the SATLCD; (c) controlled and uncontrolled responses. Figures reproduced from Ref. Yalla et al. (2001) with permission from Elsevier, ©2001.

at a wind speed lower than in the normal case". Indeed, by adopting a phase lag of $\varphi = 60°$ (red continuous line) involves reducing the index β from 5.78 to 2.87, which means reducing the critical flutter velocity of the structure to half its original value. This reduction in any long-span bridge worldwide may lead to instabilities under winds with very low return periods, demonstrating the effectiveness of WindFDI cyberattacks presented in Section 4.2.3. For instance, the Jiangyin Bridge, China, a single-box suspension bridge with a main span of 1385 m, a frequency ratio of $\gamma_\omega = 2.05$, and a critical wind velocity of 67 m/s (Yang et al., 2011), could have dropped its critical flutter velocity to around 33 m/s if winglets were installed and maliciously used under a WindFDI attack.

Furthermore, it must be highlighted that even lower values of beta could be found by adopting the formulation presented in Eq. (3) (Section 4.2.3), which can be reformulated for this specific application case by seeking the minimization of the value of β by optimizing the phase φ as:

$$\begin{aligned} &\text{find}: \varphi_{\text{WindFDI}} \\ &\text{minimize}: \beta\left(\varphi_{\text{WindFDI}}\right) \end{aligned} \tag{4}$$

Another example of the potential damage that a WindFDI can cause to the flutter stability of a bridge deck can be deduced from the results of the experiments conducted by Hansen et al. (2000), where some specific winglet configurations dropped the critical wind velocity. Also, the case reported by Kwon and Chang (2000) and discussed in Section 5.2 only shows the potential effect of a DoS attack. However, taking control of the winglet controllers and applying a WindFDI attack may further increase the potential damage to the cable-stayed bridge. These examples clearly highlight the potential damage that malicious

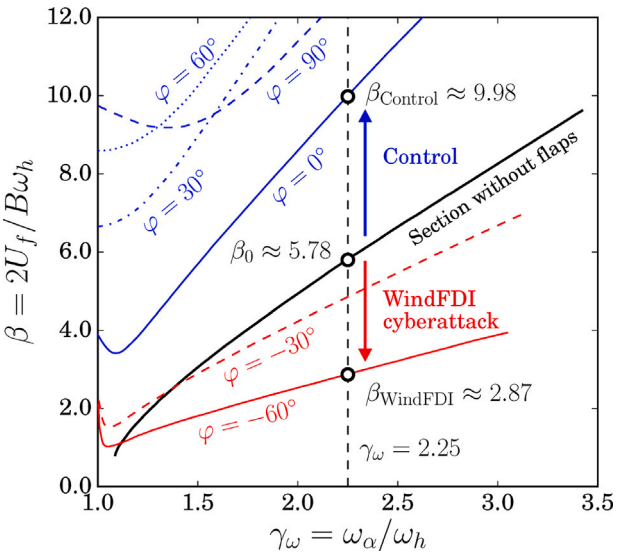

Fig. 18. Potential damage on bridges equipped with winglets caused by a WindFDI cyberattack based on the studies reported in Cobo del Arco and Aparicio (1999).

use of active systems can create on wind-sensitive structures by using the external help of wind loads, as envisioned for WindFDI attacks.

6. Towards attack-resistant smart structures: Development of cyberdefenses

While it is theoretically (and practically) impossible to eliminate the possibility of cyberattacks in structures equipped with OT/CPS, engineers must improve their designs and develop cyberdefenses to try to avoid cyberattacks and reduce their impact on CI. With that in mind, this section starts by describing a risk assessment framework, such that the most impeding risks, e.g., the potential occurrence of a WindFDI attack, can be objectively identified and assessed. Later, a series of mitigation techniques, described in the reminding subsections, can be deployed as a result, in an effort to avoid, mitigate, and limit the capabilities of cyberattacks specifically tailored for CI.

6.1. Risk management framework

So far, one of the main risks considered in active systems was power outages that prevented CPS from carrying out their job of improving the wind-induced responses of the structures. However, the growing number and level of sophistication of cyberattacks demand a more extensive risk management plan, including multiple formats of cyberattacks, such as those described in Section 4. Fig. 19 shows a graphical depiction of a risk management framework adapted from the one provided for Critical Infrastructure by the United States Cybersecurity & Infrastructure Security Agency (CISA, 2020). The framework combines different elements that are relevant to the CI field, e.g., physical, cyber, and human. The initial step (Fig. 19, 1) involves an in-depth analysis of the wind-resistant structures, so the proper defense goals can be identified, e.g., preventing the WindFDI attack described in Section 4.2.3. Next, the second step (Fig. 19, 2) involves the identification of the CPS components that may be the subject of attacks, i.e., the *targets*, such as sensors, actuators, etc. This step may also include the identification of network protocols, interfaces, etc., as well as any relevant human domain-specific positions, a.k.a., *roles*, e.g., operators, engineers, security officers, etc. Next, the third step (Fig. 19, 3) is concerned with analyzing and assessing the potential risks considering the goals and the state of the overall infrastructure as determined in previous steps. As an example, the potential occurrence of a WindFDI attack can be considered a big risk in geographical zones prone to high winds during most of the year, e.g., Corpus Christi, Texas, USA. The next step (Fig. 19, 4) involves the design, deployment, and maintenance of techniques to manage and mitigate the risks just identified. The next Sections 6.2, 6.3, 6.4, and 6.5 provide a series of interesting ideas on how to effectively achieve such a goal. Finally, the last step (Fig. 19, 5) deals with techniques, left for future work, to evaluate the effectiveness of the proposed risk mitigation techniques.

6.2. Redundancy

A redundant system is a secondary system implemented in parallel to the primary system that serves as a backup in case the primary system fails. Hence, redundancy can be defined as a strategy to enhance the reliability of a system by doubling or even tripling some specific critical components. This approach has a long tradition in aerospace engineering to increase aircraft safety against the failure of vital systems (Osder, 1999). Common applications can be found for information processing systems (Lala and Adams, 1989), redundant sensors for fault isolation (Pejsa, 1974), and flight control (Bosch and Kuehl, 1977; Collinson, 1999). This approach is very effective and could be an efficient alternative to address cybersecurity concerns for OT installed in critical infrastructure (Bihary, 2020). However, the nature of some CPS used for wind-sensitive smart structures, sometimes involving large lumped masses, unduplicable actuators, or unreachable implementation costs, can make this approach an unfeasible alternative in some cases.

6.3. Moving target defense

Moving Target Defense (MTD) (Jajodia et al., 2011; Rubio-Medrano et al., 2017) is a well-known cybersecurity defensive technique aimed at protecting cyber-infrastructures by complicating the initial *reconnaissance* phase that is typically carried out before an attack to obtain valuable information, e.g., the *uninformed* attacks described in Section 4.1.2. In such a scenario, an MTD approach would include implementing a series of continuous, pre-scheduled changes in the configuration settings, i.e., *moving*, of sensors and actuators, i.e., the *targets* of a potential attack. This way, any information obtained by attackers, e.g., the IP address of an installed actuator, may be only valid for a limited period of time, before it is renewed as a part of the next *cycle* of MTD-inspired reconfigurations. Referring to Sections 4.2.1, 4.2.2, and 4.2.3, having access to the current IP address of an actuator is crucial for the DoS, FDI, and WindFDI attacks to succeed, as it allows for the target actuator to receive the malicious *payload* sent by an attacker. Therefore, continuously changing such an important configuration parameter may potentially deter the occurrence of a successful attack.

6.4. Intrusion detection systems

Installation of secondary systems to track the structural performance of the critical structure and identify eventual malicious actions. These can be physical or software-based systems:

- **Physical detection**: Installing a secondary, isolated system to monitor the structural performance in parallel to the primary system to identify unintentional or intentional anomalies. Fig. 20 shows a conceptual sketch of a primary system (in black) that is complemented by a secondary system (in blue) with the only goal of tracking the right behavior of the primary system. While similar to redundancy, this secondary tracking system does not perform the same function as the primary system; its only goal is the real-time verification of the primary system's performance. If an attack is detected, counteractions can be activated.

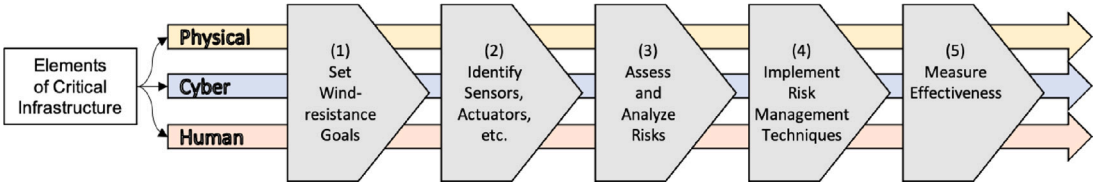

Fig. 19. A CI risk management framework. Adapted from CISA (2020).

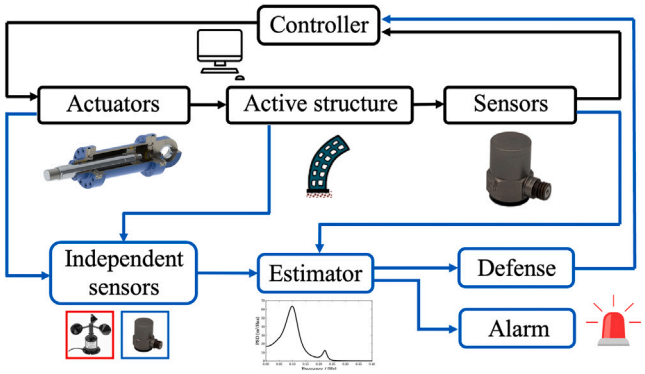

Fig. 20. Conceptual description of a physical intrusion detection system (in blue) for cyberattack detection and counter actuation in structures equipped with active systems (in black).

- **Software-based detection**: Detecting intruders in CPS has been largely studied in the literature (Mitchell and Chen, 2014). Recently, approaches leveraging Deep/Machine Learning (DL/ML) (Li et al., 2021) have been proposed. The idea is to construct a DL/ML model of the CPS cyber-infrastructure part, such that a well-defined, fine-grained description of the *normal* behavior of the system is obtained. As an example, to prevent the WindFDI attack described in Section 4.2.3, a DL/ML model would take into account the effect of the wind under different circumstances based on the geographical location and the time of the year.

6.5. Cyber-secure aero-structural design of CI equipped with OT/CPS

6.5.1. Sensitivity of target's response to control devices properties

The effectiveness of cyberattacks on wind-sensitive CI equipped with OT/CPS can be limited by tailoring the CPS seeking to minimize their damage in scenarios of malicious use. The applicability of this approach is evident by analyzing the data reported by Sangalli and Braun (2020), where it can be seen that the damage caused by the uncontrolled winglets (equivalent to malicious use) is drastically changed depending on the winglet shape-dependent aerodynamic properties. Fig. 21 shows the effect of adding two sets of winglets with different shapes to the deck cross-section of the Great Belt and the consequence of losing their control on the bridge response. It can be seen that the amplitude of the response without control (i.e., under a DoS attack) is drastically different depending on the airfoil section adopted. Hence, a deck equipped with NACA 0012 winglets would be less sensitive to an eventual DoS attack. Consequently, a design including winglets with a NACA 0012 shape is more cyber-secure than one equipped NACA 0021. This fact opens the door to tailoring CPS to minimize the potential damage of cyberattacks.

6.5.2. Cyber-secure aero-structural design

From the design perspective, the existence of a new design scenario (the cyberattack) changes the way active systems for wind-induced load mitigation must be designed. Active systems are currently designed to maximize their effectiveness in mitigating aeroelastic responses or, in other words, in minimizing the aeroelastic responses of the structure since this is their ultimate goal. However, it can be generally stated that the higher their influence on the flow features around the structure (e.g., larger mass in an AMD, larger size of winglets, etc.), the higher their capability to damage the structure under a cyberattack. Hence, to reduce the potential damage that an active system under attack can do to the structure intended to protect, active systems must be designed to improve the aeroelastic response only up to a given threshold, depending on the structure requirements. In other words, the design goal of active systems considering cybersecurity design specifications must pursue the maximization of its mitigating capabilities (minimization of aeroelastic responses of the structure), assuming an optimum control strategy, and minimizing its potential damage to the structure under a cyberattack, assuming an optimum cyberattack plan. These goals are the ones identified in Fig. 19 (1) and (3) as goals and risks. The design problem can be formulated as:

$$\begin{aligned} &\text{find}: \mathbf{x} = \left(x_i\right),\ i = 1, \ldots, G \\ &\text{minimize}: \mathbf{f}\left(\mathbf{x}\right) = \left(f_j\left(\mathbf{x}\right)\right),\ j = 1, \ldots, N \\ &\text{subject to}: \\ &\mathbf{g}\left(\mathbf{x}\right) = \left(g_k\left(\mathbf{x}\right)\right) \leq 0,\ k = 1, \ldots, K \\ &x_i^L \leq x_i \leq x_i^U,\ i = 1, \ldots, G \end{aligned} \tag{5}$$

where $\mathbf{x}$ is the vector containing all design variables that define the mechanical or aerodynamic control device (e.g., the mass of an AMD, size and shape of a winglet, etc.), $\mathbf{f}$ is the vector of objective functions, and $\mathbf{g}$ stand for the list of design constraints that control the performance of the system. G, N, and K stand for the total number of design variables, objective functions, and design constraints, respectively. The lateral constraints or the problem involve lower bounds x_i^L and upper bounds x_i^U to the value that each design variable x_i can adopt. The goal is to minimize all the objective functions included in $\mathbf{f}$, which typically conflict between them and require contradictory modifications on the set of design variables $\mathbf{x}$. Hence, it is required to obtain the set of design variables, known as the Pareto set of design variables $\mathbf{x}^P$, which represent designs that when any design variable is modified to improve any objective function, it worsens, at least, any other objective function. Hence, when minimizing the objective functions, the problem has the mathematical property that there is no design $\mathbf{x}$ that accomplishes:

$$\begin{aligned} &f_i\left(\mathbf{x}\right) \leq f_j\left(\mathbf{x}^P\right),\ j = 1, \ldots, N \\ &\text{and} \\ &\mathbf{g}\left(\mathbf{x}\right) = \left(g_k\left(\mathbf{x}\right)\right),\ j = 1, \ldots, N, \text{ for, at least, an objective function} \end{aligned} \tag{6}$$

where $\mathbf{x}^P$ stand for the Pareto set of design variables, and $\mathbf{f}\left(\mathbf{x}^P\right)$ is the Pareto front. Further details can be found in Arora (2011) and Hernandez (2010). The Pareto front can be obtained using multiple techniques, for instance, the classical weighted sum method (Marler and Arora, 2010) or the weighted min–max method, among others (see Marler and Arora (2004)).

The Pareto front for the two objectives considered in this problem (aeroelastic responses R_a, and aeroelastic response under cyberattack R_{CS}) is graphically shown in Fig. 22, where some particularities of this specific problems can be identified. The structural aeroelastic response in regular service without cyberattacks is represented in the horizontal axis, while the vertical axis shows the potential cyberattack-induced

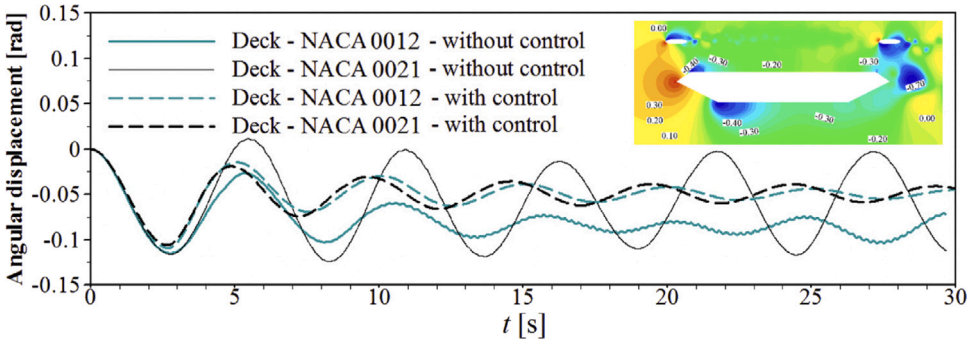

Fig. 21. Sensitivity of the deck-flap system response to the uncontrolled aerodynamic control device shape based on the data reported in Sangalli and Braun (2020). Reproduced from Ref. Sangalli and Braun (2020) with permission from Elsevier, ©2020.

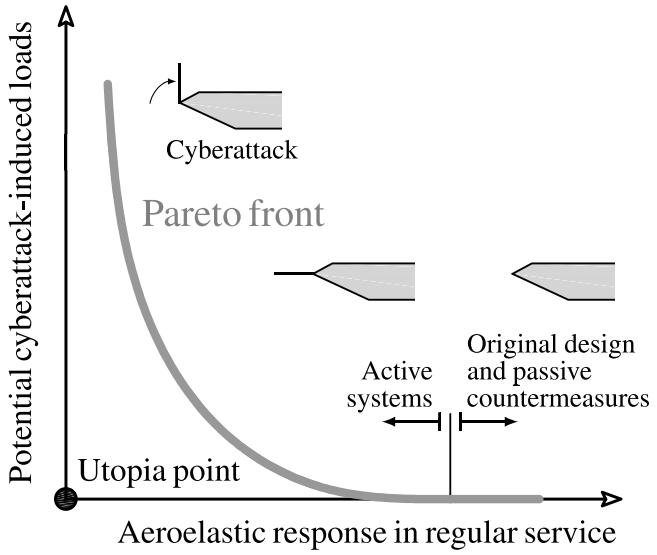

Fig. 22. Conceptual description of the multi-objective design problem of active mitigation and control systems considering cyberattacks..

loads. On the right side of the figure, a vertical line indicates the transition from passive countermeasures, where there is a high aeroelastic response and no potential cyberattacks, to active systems, which permits surpassing the inherent limit of passive countermeasures for further reducing the aeroelastic response in regular service at the cost of creating a margin for potential cyberattacks. As the active systems become more effective, their capacity to mitigate the aeroelastic response in service is higher. However, active systems with high capabilities to change the flow features or the target's mechanical properties are more susceptible to higher damage during an attack. This concept is applicable to any kind of active countermeasures, from flaps that affect the flow features to active dampers that change the structure's mechanical properties. The graph's origin represents a design where there is no aeroelastic response in regular service and no potential damage generated by cyberattacks, which is the utopia point. Hence, the goal of the designer is to define the optimal balance between these two goals that permits the effective mitigation of all aeroelastic responses at the lowest cost under a cyberattack.

7. Concluding remarks and design recommendations

The rapid growth of worldwide populated areas in the last decades has led to a drastic increase in the construction of wind-sensitive civil and architectural structures, such as tall buildings and long-span bridges. Furthermore, higher energy demands and the implementation of green energy policies have led to an unprecedented development of renewable energy sources, such as wind turbines and photovoltaic panels, which are also sensitive to wind loads. Some of these critical infrastructures have active control systems for their operation and/or natural hazard-induced load mitigation. Simultaneously, modern societies that are progressively more dependent on new technology are contemplating an exponential increase in cyberattacks affecting many aspects of citizens' lives, such as personal data privacy, electronic banking security, research, warfare, and many others. This study offers a literature review of the multiple wind-sensitive structures equipped with operational technology (OT) and cyber–physical systems (CPS) categorized as critical infrastructure (CI) due to their fundamental role in society and the drastic impact their failure would cause. Examples include active mechanical and aerodynamic control devices installed in tall buildings, towers, bridges, wind turbines, and solar trackers. These examples cover several critical sectors, such as transportation and energy. This paper discusses recent cyberattacks on OT/CPS technology currently used in wind-sensitive smart structures, such as attacks on cyber–physical systems, programmable logic controllers, and industrial control systems. Then, we take a first look at the potential threat cyberattacks can pose to wind-sensitive structures. By analyzing the mechanism of the well-known Denial-of-Service (DoS) and False-Data-Injection (FDI) cyberattacks and the effect of uncontrolled active CPS installed on wind-sensitive structures for wind load mitigation, the potential damage of cyberattacks on critical infrastructure can be envisioned. In this context, we have conceptually identified a new kind of potential cyberattack based on the fact that the damage created by a classical FDI attack can be drastically amplified by taking advantage of the wind loads and the positive feedback that can be created. This attack, defined as Wind-leveraged False Data Injection (WindFDI), has been qualitatively and quantitatively analyzed based on data available in the literature. Results showed that the misuse of active systems could drastically anticipate the onset of flutter instability in some structures.

It is fundamental for the wind engineering community to actively identify potential cyberattacks, quantify their impact, and develop effective countermeasures to guarantee the cybersecurity of wind-sensitive CI equipped with OT/CPS. Hence, a new design criterion must be considered when designing OT/CPS for the operation and wind load mitigation of wind-sensitive structures: minimizing the damage caused by an eventual cyberattack. The development of new active systems must consider the potential negative effect on the main structural system under eventual malicious actions to fully address all potential scenarios along the structure's life cycle.

CRediT authorship contribution statement

Miguel Cid Montoya: Writing – original draft, Visualization, Methodology, Conceptualization. **Carlos E. Rubio-Medrano:** Writing – original draft, Visualization, Methodology, Conceptualization. **Ahsan Kareem:** Writing – review & editing, Methodology, Conceptualization.

Declaration of competing interest

The authors declare that they have no known competing financial interests or personal relationships that could have appeared to influence the work reported in this paper.

Data availability

No data was used for the research described in the article.

Acknowledgments

Miguel Cid Montoya is supported by the National Science Foundation under grant CMMI #2301824 and the new faculty start-up funds provided by Texas A&M University-Corpus Christi. Carlos E. Rubio-Medrano is supported by the National Science Foundation under grant CNS # 2131263. Ahsan Kareem was supported in part by funding from the Robert M. Moran Professorship.

References

Abdel-Ghaffar, A.M., Scanlan, R.H., 1985. Ambient vibration studies of Golden Gate Bridge: I. Suspended structure. J. Eng. Mech. 111 (4), 463–482. http://dx.doi.org/10.1061/(ASCE)0733-9399(1985)111:4(463).

Abdel-Rohman, M., Leipholz, H.H., 1978. Active control of flexible structures. J. Struct. Div. 104 (8), 1251–1266. http://dx.doi.org/10.1061/JSDEAG.0004968.

Abdelaziz, K.M., Alipour, A., Hobeck, J.D., 2021. A smart façade system controller for optimized wind-induced vibration mitigation in tall buildings. J. Wind Eng. Ind. Aerodyn. 212, 104601. http://dx.doi.org/10.1016/j.jweia.2021.104601.

Abdelrazaq, A., 2012. Validating the structural behavior and response of Burj Khalifa: Synopsis of the full scale structural health monitoring programs. Int. J. High-Rise Build. 1 (1), 37–51.

Abdelwahab, M., Ghazal, T., Nadeem, K., Aboshosha, H., Elshaer, A., 2023. Performance-based wind design for tall buildings: Review and comparative study. J. Build. Eng. 68, 106103. http://dx.doi.org/10.1016/j.jobe.2023.106103.

Abe, M., Fujino, Y., Kimura, S., 1998. Active tuned liquid damper (TLD) with magnetic fluid. In: Proceedings of the SPIE. Vol. 3329, pp. 620–623. http://dx.doi.org/10.1117/12.316931.

Abiola-Ogedengbe, A., Hangan, H., Siddiqui, K., 2015. Experimental investigation of wind effects on a standalone photovoltaic (PV) module. Renew. Energy 78, 657–665. http://dx.doi.org/10.1016/j.renene.2015.01.037.

Adam, B., Smith, I.F., 2008. Reinforcement learning for structural control. J. Comput. Civ. Eng. 22 (2), 133–139. http://dx.doi.org/10.1061/(ASCE)0887-3801(2008)22:2(133).

Al-Mohamad, A., 2004. Efficiency improvements of photo-voltaic panels using a suntracking system. Appl. Energy 79 (3), 345–354. http://dx.doi.org/10.1016/j.apenergy.2003.12.004.

Aldwaik, M., Adeli, H., 2014. Advances in optimization of highrise building structures. Struct. Multidiscip. Opt. 50, 899–919. http://dx.doi.org/10.1007/s00158-014-1148-1.

Aly, A.M., Bitsuamlak, G., 2013. Aerodynamics of ground-mounted solar panels: Test model scale effects. J. Wind Eng. Ind. Aerodyn. 123, 250–260. http://dx.doi.org/10.1016/j.jweia.2013.07.007.

Ammann, O.H., von Kármán, T., Woodruff, G.B., 1941. The Failure of the Tacoma Narrows Bridge. Technical Report, Federal Works Agency, URL https://resolver.caltech.edu/CaltechAUTHORS:20140512-105559175.

Andersson, A., O'Connor, A., Karoumi, R., 2015. Passive and adaptive damping systems for vibration mitigation and increased fatigue service life of a tied arch railway bridge. Comput.-Aided Civ. Infrastruct. Eng. 30 (9), 748–757. http://dx.doi.org/10.1111/mice.12116.

Anguiano, D., 2022. Attacks on Pacific north-west power stations raise fears for US electric grid. Guardian URL https://www.theguardian.com/us-news/2022/dec/09/us-power-grid-pacific-northwest-attacks.

Cobo del Arco, D., Aparicio, A.C., 1999. Improving suspension bridge wind stability with aerodynamic appendages. J. Struct. Eng.-ASCE 125, 1367–1375. http://dx.doi.org/10.1061/(ASCE)0733-9445(1999)125:12(1367).

Argentini, T., Omarini, S., Zasso, A., Petrangeli, M., 2019. Aerodynamic tailoring of a bluff deck section subjected to inclined winds due to the complex orography of the construction site. In: Lect Notes Civil Eng: Proc of the XV Conf of the Italian Assoc for Wind Eng. http://dx.doi.org/10.1007/978-3-030-12815-9_4.

Argentini, A., Rocchi, D., Somaschini, C., Spinelli, U., Larsen, A., 2022. Aeroelastic stability of a twin-box deck: Comparison of different procedures to assess the effect of geometric details. J. Wind Eng. Ind. Aerodyn. 220, 104878. http://dx.doi.org/10.1016/j.jweia.2021.104878.

Arıoğlu, E., 2021. Importance of "Heuristics" in suspension bridge engineering and 1915 Çanakkale Bridge. Springer Tracts Transp. Traffic 17, 19–41. http://dx.doi.org/10.1007/978-3-030-59169-4_2.

Arora, J.S., 2011. Introduction to Optimum Design, third ed. Elsevier/Academic Press, http://dx.doi.org/10.1016/C2013-0-15344-5.

Arul, M., Kareem, A., Kwon, D.K., 2020. Identification of vortex-induced vibrations of tall building pinnacle using cluster analysis for fatigue evaluation: Application to burk khalifa. J. Struct. Eng. 146 (11), 04020234. http://dx.doi.org/10.1061/(ASCE)ST.1943-541X.0002799.

Astiz, M.A., 1996. Wind related behaviour of alternative suspension systems. In: 15th IABSE Congr. Rep.. IABSE, Zurich, pp. 1079–1090.

Astiz, M.A., 1999. Wind-induced vibrations of the Alconétar Bridge, Spain. Struct. Eng. Int. 20 (2), 195–199. http://dx.doi.org/10.2749/101686610791283696.

Ayorinde, E.O., Warburton, G.B., 1980. Minimizing structural vibration with absorbers. Earthq. Eng. Struct. Synam. 8, 219–236, Minimizing structural vibration with absorbers.

Aziz, S., Hassan, S., 2017. On improving the efficiency of a solar panel tracking system. Procedia Manuf. 7, 218–224. http://dx.doi.org/10.1016/j.promfg.2016.12.053.

Bachynski, E.E., Chabaud, V., Sauder, T., 2015. Real-time hybrid model testing of floating wind turbines: Sensitivity to limited actuation. Energy Procedia 80, 2–12. http://dx.doi.org/10.1016/j.egypro.2015.11.400.

Baheti, A.S., Matsagar, V.A., 2022. Wind and seismic response control of dynamically similar adjacent buildings connected using magneto-rheological dampers. Infrastructures 7 (12), 167. http://dx.doi.org/10.3390/infrastructures7120167.

Bai, Hao, Aoues, Y., Cherfils, J.-M., Lemosse, D., 2021a. Design of an active damping system for vibration control of wind turbine towers. Infrastructures 6, 162. http://dx.doi.org/10.3390/infrastructures6110162.

Bai, H., Ji, N., Xu, G., Li, J., 2020. An alternative aerodynamic mitigation measure for improving bridge flutter and vortex induced vibration (VIV) stability: Sealed traffic barrier. J. Wind Eng. Ind. Aerodyn. 206, 104302. http://dx.doi.org/10.1016/j.jweia.2020.104302.

Bai, H., Li, R., Xu, G., Kareem, A., 2021b. Aerodynamic performance of Π-shaped composite deck cable-stayed bridges including VIV mitigation measures. J. Wind Eng. Ind. Aerodyn. 208, 104451. http://dx.doi.org/10.1016/j.jweia.2020.104451.

Balas, M.J., 1978. Feedback control of flexible systems. IEEE Trans. Autom. Control 23, 673–679. http://dx.doi.org/10.1109/TAC.1978.1101798.

Balendra, T., Wang, C.M., Yan, N., 2001. Control of wind-excited towers by active tuned liquid column damper. Eng. Struct. 23 (9), 1054–1067. http://dx.doi.org/10.1016/S0141-0296(01)00015-3.

Bank of America, 2023. Keeping Higher Ed Students Safe from Cyber Attacks. Bank of America Article, URL https://business.bofa.com/content/dam/flagship/gcb/keeping-students-safe/keeping_students_safe.pdf.

Barthelmie, R.J., Jensen, L.E., 2010. Evaluation of wind farm efficiency and wind turbine wakes at the Nysted offshore wind farm. Wind Energy 13, 573–586. http://dx.doi.org/10.1002/we.408.

Bartoli, G., Mannini, C., 2008. A simplified approach to bridge deck flutter. J. Wing Eng. Ind. Aerodyn. 96, 229–256. http://dx.doi.org/10.1016/j.jweia.2007.06.001.

Bas, S., Apaydin, N., Ilki, A., Catbas, N., 2017. Structural health monitoring system of the long-span bridges in Turkey. Struct. Infrastruct. Eng. 14 (4), 425–444. http://dx.doi.org/10.1080/15732479.2017.1360365.

Basaran, S., Bolat, F.C., Sivrioglu, S., 2021. Vibration suppression of wind turbine nacelle with active electromagnetic mass damper systems using adaptive back-stepping control. J. Vib. Control 28 (13–14), 1–14. http://dx.doi.org/10.1177/1077546321998878.

Battista, R.C., Pfeil, M.S., 2000. Reduction of vortex-induced oscillations of Rio–Niterói bridge by dynamic control devices. J. Wing Eng. Ind. Aerodyn. 83 (3), 273–288. http://dx.doi.org/10.1016/S0167-6105(99)00108-7.

Bäumer, R., Starossek, U., 2016. Active vibration control using centrifugal forces created by eccentrically rotating masses. J. Vib. Acoust. 138 (4), 041018. http://dx.doi.org/10.1115/1.4033358.

Bäumer, R., Terrill, R., Wollnack, S., Werner, H., Starossek, U., 2018. Twin rotor damper for the damping of stochastically forced vibrations using a power-efficient control algorithm. J. Sound Vib. 413, 308–331. http://dx.doi.org/10.1016/j.jsv.2017.10.007.

Bayati, I., Belloli, M., Bernini, L., Fiore, E., Giberti, H., Zasso, A., 2016. On the functional design of the DTU10 MW wind turbine scale model of LIFES50+ project. J. Phys. Conf. Ser. 753 (5), 052018. http://dx.doi.org/10.1088/1742-6596/753/5/052018.

Bayati, I., Belloli, M., Bernini, L., Zasso, A., 2017. Wind tunnel wake measurements of floating offshore wind turbines. Eng. Proc. 137, 214–222. http://dx.doi.org/10.1016/j.egypro.2017.10.375.

Belloli, M., Rosa, L., Zasso, A., 2014. Wind loads and vortex shedding analysis on the effects of the porosity on a high slender tower. J. Wind Eng. Ind. Aerodyn. 126, 75–86. http://dx.doi.org/10.1016/j.jweia.2014.01.004.

Bera, K.K., Chandiramani, N.K., 2019. Flutter control of bridge deck using experimental aeroderivatives and LQR-driven winglets. J. Bridge Eng. 24 (11), 04019100. http://dx.doi.org/10.1061/(ASCE)BE.1943-5592.0001467.

Bera, K.K., Chandiramani, N.K., 2020. Aeroelastic flutter control of a bridge using rotating mass dampers and winglets. J. Vib. Control 26 (23–24), 2185–2192. http://dx.doi.org/10.1177/1077546320915341.

Bernardini, E., Spence, S.M.J., Wei, D., Kareem, A., 2015. Aerodynamic shape optimization of civil structures: A CFD-enabled Kriging-based approach. J. Wing Eng. Ind. Aerodyn. 144, 154–164. http://dx.doi.org/10.1016/j.jweia.2015.03.011.

Bihary, C., 2020. Why Cybersecurity Relies on Redundancy to Ensure Network Availability. Technical Report, Garland Technology, URL https://www.garlandtechnology.com/blog/why-cybersecurity-relies-on-redundancy-to-ensure-network-availability.

Boberg, M., Feltrin, G., Martinoli, A., 2015. A novel bridge section model endowed with actively controlled flap arrays mitigating wind impact. In: 2015 IEEE International Conference on Robotics and Automation (ICRA), Pp 1837-1842. IEEE, http://dx.doi.org/10.1109/ICRA.2015.7139437.

Bolton, W., 2015. Programmable Logic Controllers. Newnes, ISBN: 978-0-12-802929-9, http://dx.doi.org/10.1016/C2014-0-03884-1.

Bosch, J.A., Kuehl, W.J., 1977. Reconfigurable redundancy management for aircraft flight control. J. Aircr. 14, 966–971. http://dx.doi.org/10.2514/3.58880.

Bossanyi, E.A., 2003. Individual blade pitch control for load reduction. Wind Energy 6, 119–128. http://dx.doi.org/10.1002/we.76.

Bossanyi, E.A., 2005. Further load reductions with individual pitch control. Wind Energy 8, 481–485. http://dx.doi.org/10.1002/we.166.

Boukhezzar, B., Lupu, L., Siguerdidjane, H., Hand, M., 2007. Multivariable control strategy for variable speed, variable pitch wind turbines. Renew. Energy 32 (8), 1273–1287. http://dx.doi.org/10.1016/j.renene.2006.06.010.

Brodersen, M.L., Bjørke, A.-S., Høgsberg, J., 2016. Active tuned mass damper for damping of offshore wind turbine vibrations. Wind Energy 20 (5), 783. http://dx.doi.org/10.1002/we.2063.

Brown, W.C., 1980. Long span suspensión bridges: A british approach. Ann. N.Y. Acad. Sci. 352 (1), 1–26. http://dx.doi.org/10.1111/j.1749-6632.1980.tb16360.x.

Brown, W.C., 1996. Development of the deck for the 3300 m span Messina Crossing. In: 15th IABSE Congr. Rep.. IABSE, Zurich, pp. 1019–1030.

Bui, H.-L., Tran, N.-A., 2022. Multi-objective optimal design of TMDs for increasing critical flutter wind speed of bridges. J. Wind Eng. Ind. Aerodyn. 225, 104992. http://dx.doi.org/10.1016/j.jweia.2022.104992.

Buljac, A., Kozmar, H., Pospíšil, S., Macháček, M., 2017. Aerodynamic and aeroelastic characteristics of typical bridge decks equipped with wind barriers at the windward bridge-deck edge. Eng. Struct. 137, 310–322. http://dx.doi.org/10.1016/j.engstruct.2017.01.055.

Burton, T., Sharpe, D., Jenkins, N., Bossanyi, E., 2001. Wind Energy Handbook. Wiley, http://dx.doi.org/10.1002/9781119992714.

Cao, Y., Yim, J., Zhao, Y., Wang, M., 2010. Temperature effects on cable stayed bridge using health monitoring system: A case study. Struct. Health Monit. 10, 523–537. http://dx.doi.org/10.1177/1475921710388970.

Carta, G., Jones, I.S., Movchan, N.V., Movchan, A.B., Nieves, M.J., 2017. Gyro-elastic beams for the vibration reduction of long flexural systems. Proc. R. Soc. A 473, 1–17. http://dx.doi.org/10.1098/rspa.2017.0136.

Casciati, F., Giuliano, F., 2009. Performance of multi-TMD in the towers of suspension bridges. J. Sound Vib. 15 (6), 821–847. http://dx.doi.org/10.1177/1077546308091455.

Casciati, F., Rodellar, J., Yildirim, U., 2012. Active and semiactive control of structures - theory and applications: A review of recent advances. J. Intell. Mater. Syst. Struct. 23 (11), 1181–1195. http://dx.doi.org/10.1177/1045389X12445029.

Chang, S., 2020. Active mass damper for reducing wind and earthquake vibrations of a long-period bridge. Actuators 9 (3), 66. http://dx.doi.org/10.3390/act9030066.

Chen, Z., Fu, X., Xu, Y., Li, C.Y., Kim, B., Tse, K.T., 2021. A perspective on the aerodynamics and aeroelasticity of tapering: Partial reattachment. J. Wind Eng. Ind. Aerodyn. 212, 104590. http://dx.doi.org/10.1016/j.jweia.2021.104590.

Chen, W.-L., Gao, D.-L., Yuan, W.-Y., Li, H., Hu, H., 2015. Passive jet control of flow around a circular cylinder. Exp. Fluids 56 (11), 201. http://dx.doi.org/10.1007/s00348-015-2077-5.

Chen, W.-L., Yang, W.-H., Li, H., 2019. Self-issuing jets for suppression of vortex-induced vibration of a single box girder. J. Fluids Struct. 86, 213–235. http://dx.doi.org/10.1016/j.jfluidstructs.2019.02.017.

Cherukupalli, N., Bowman, M., Gilliss, M., Browne, M., Taylor, Z., 2022. Single-Axis Tracker Wind Stability: FTC solar's Differentiated Approach. Technical Report, FTC Solar.

Cid Montoya, M., Bai, H., Ye, M., 2023. Shaping bridge decks for VIV mitigation: A wind tunnel data-driven adaptive surrogate-based optimization method. J. Wing Eng. Ind. Aerodyn. 242, 105568. http://dx.doi.org/10.1016/j.jweia.2023.105568.

Cid Montoya, M., Hernández, S., Kareem, A., 2022. Aero-structural optimization-based tailoring of bridge deck geometry. Eng. Struct. 270, 114067. http://dx.doi.org/10.1016/j.engstruct.2022.114067.

Cid Montoya, M., Hernández, S., Nieto, F., 2018a. Shape optimization of streamlined decks of cable-stayed bridges considering aeroelastic and structural constraints. J. Wing Eng. Ind. Aerodyn. 177, 429–455. http://dx.doi.org/10.1016/j.jweia.2017.12.018.

Cid Montoya, M., Hernández, S., Nieto, F., Kareem, A., 2020. Aero-structural design of bridges focusing on the buffeting response: Formulation, parametric studies and deck shape tailoring. J. Wing Eng. Ind. Aerodyn. 204, 104243. http://dx.doi.org/10.1016/j.jweia.2020.104243.

Cid Montoya, M., Nieto, F., Hernández, S., 2021a. Multi-objective shape optimization of tall buildings considering profitability and multidirectional wind-induced accelerations using CFD, surrogates, and the reduced basis approach. Wind Struct. 32 (4), 355–369. http://dx.doi.org/10.12989/was.2021.32.4.355.

Cid Montoya, M., Nieto, F., Hernández, S., Fontán, A., Jurado, J.A., Kareem, A., 2021b. Optimization of bridges with short gap streamlined twin-box decks considering structural, flutter and buffeting performance. J. Wind Eng. Ind. Aerodyn. 208, 104316. http://dx.doi.org/10.1016/j.jweia.2020.104316.

Cid Montoya, M., Nieto, F., Hernández, S., Kusano, I., Álvarez, A.J., Jurado, J.Á., 2018b. CFD-based aeroelastic characterization of streamlined bridge deck cross-sections subject to shape modifications using surrogate models. J. Wing Eng. Ind. Aerodyn. 177, 405–428. http://dx.doi.org/10.1016/j.jweia.2018.01.014.

CISA, 2020. A Guide to Critical Infrastructure Security and Resilience. December 17th. Cybersecurity & Infrastructure Security Agency, US Department of Homeland Security, URL https://www.cisa.gov/sites/default/files/publications/Guide-Critical-Infrastructure-Security-Resilience-110819-508v2.pdf.

CISA, 2022. APT Cyber Tools Targeting ICS/SCADA Devices. https://www.cisa.gov/uscert/ncas/alerts/aa22-103a.

CISA ICS-CERT, 2019. MAR-17-352-01 HatMan – Safety System Targeted Malware (Update B). URL https://www.cisa.gov/sites/default/files/documents/MAR-17-352-01%20HatMan%20-%20Safety%20System%20Targeted%20Malware%20%28Update%20B%29.pdf.

Clark, A.J., 1988. Multiple passive tuned mass dampers for reducing earthquake induced building motion. In: Proceedings of the Ninth World Conference on Earthquake Engineering. Vol. 5, pp. 779–784.

Coleman, S.A., Baker, C.J., 1992. The reduction of accident risk for high sided road vehicles in cross winds. J. Wind Eng. Ind. Aerodyn. 44, 2685–2695. http://dx.doi.org/10.1016/0167-6105(92)90060-N.

Collinson, R.P.G., 1999. Fly-by-wire flight control. Comput. Control Eng. J. 10 (4), 141–152. http://dx.doi.org/10.1049/cce:19990403.

Coudurier, C., Lepreux, O., Petit, N., 2015. Passive and semi-active control of an offshore floating wind turbine using a tuned liquid column damper. IFAC-Papers Line 28, 241–247. http://dx.doi.org/10.1016/j.ifacol.2015.10.287.

CTBUH, 2023a. CTBUH Skyscraper Database. Technical Report, Council on Tall Buildings and Urban Habitat, URL https://www.skyscrapercenter.com/explore-data.

CTBUH, 2023b. Jeddah Tower – The Skyscraper Center. Counc. Tall Build. Urban Habitat URL https://www.skyscrapercenter.com/building/jeddah-tower/2.

Curadelli, O., Amani, M., 2022. The effectiveness of the gyroscopic effect for controlling structural vibrations. Struct. Eng. Int. 32, 103–111. http://dx.doi.org/10.1080/10168664.2021.1930331.

Datta, T., 2003. A state-of-the-art review on active control of structures. ISET J. Earthq. Technol. 40 (1), 1–17, URL http://home.iitk.ac.in/~vinaykg/Iset430.pdf.

Del Grosso, A., Basso, p., 2010. Adaptive building skin structures. Smart Mater. Struct. 19 (12), 124011. http://dx.doi.org/10.1088/0964-1726/19/12/124011.

Demetriou, D., Nikitas, N., 2016. A novel hybrid semi-active mass damper configuration for structural applications. Appl. Sci. 6, 397. http://dx.doi.org/10.3390/app6120397.

Den Hartog, J.P., 1956. Mechanical Vibrations, fourth ed. McGraw-Hill, New York., ISBN: 9780486647852.

Di Matteo, A., Pirrotta, A., Tumminelli, S., 2017. Combining TMD and TLCD: analytical and experimental studies. J. Wind Eng. Ind. Aerodyn. 167, 101–113. http://dx.doi.org/10.1016/j.jweia.2017.04.010.

Diana, G., Fiammenghi, G., Belloli, M., Rocchi, D., 2013. Wind tunnel test and numerical approach for long span bridges: The Messina bridge. J. Wing Eng. Ind. Aerodyn. 122, 38–49. http://dx.doi.org/10.1016/j.jweia.2013.07.012.

Diana, G., Resta, F., Zasso, A., Belloli, M., Rocchi, D., 2004. Forced motion and free motion aeroelastic tests on a new concept dynamometric section model of the messina suspension bridge. J. Wing Eng. Ind. Aerodyn. 92, 441–462. http://dx.doi.org/10.1016/j.jweia.2004.01.005.

Ding, F., Kareem, A., 2018. A multi-fidelity shape optimization via surrogate modeling for civil structures. J. Wing Eng. Ind. Aerodyn. 178, 49–56. http://dx.doi.org/10.1016/j.jweia.2018.04.022.

Ding, F., Kareem, A., 2020. Tall buildings with dynamic facade under winds. Engineering 6, 1443–1453. http://dx.doi.org/10.1016/j.eng.2020.07.020.

Doekemeijer, B., van Wingerden, J.-W., 2020. Observability of the ambient conditions in model-based estimation for wind farm control: A focus on static models. Wind Energy 23, 1777–1791. http://dx.doi.org/10.1002/we.2495.

Dong, J.K., Wang, X.Z., Sun, H.J., 2011. A new wind vibration control strategy based on active variable stiffness. Adv. Mater. Res. 299–300, 302–305. http://dx.doi.org/10.4028/www.scientific.net/AMR.299-300.302.

Dragos, Inc., 2017a. CRASHOVERRIDE: Analysis of the threat to electric grid operations. [Online]: https://dragos.com/blog/crashoverride/CrashOverride-01.pdf.

Dragos, Inc., 2017b. TRISIS Malware: Analysis of safety system targeted malware. URL https://www.dragos.com/wp-content/uploads/TRISIS-01.pdf.

Edwards, J.W., Breakwell, J.V., Bryson, A.E., 1978. Active flutter control suing generalized unsteady aerodynamic theory. J. Guid. Control 1 (1), 32–40. http://dx.doi.org/10.2514/3.55741.

Elshaer, A., Bitsuamlak, G., 2018. Multiobjective aerodynamic optimization of tall building openings for wind-induced load reduction. J. Struct. Eng. ASCE 144 (10), http://dx.doi.org/10.1061/(ASCE)ST.1943-541X.0002199.

Elshaer, A., Bitsuamlak, G., El Damatty, A., 2016. Aerodynamic shape optimization of tall buildings using twisting and corner modifications. In: BBAA VIII, 8^{Th} International Colloquium on Bluff Body Aerodynamics and Applications.

Elshaer, A., Bitsuamlak, G., El Damatty, A., 2017. Enhancing wind performance of tall buildings using corner aerodynamic optimization. Eng. Struct. 136, 133–148. http://dx.doi.org/10.1016/j.engstruct.2017.01.019.

Enshaei, P., Chowdhury, J., Sauder, H., Banks, D., 2023. Wind tunnel testing of torsional instability of single-axis solar trackers: Summary of methodologies and results. In: AWESW2022: 21^{th} Australasian Wind Engineering Society Workshop.

Enslin, R., 1992. Maximum power point tracking: a cost-saving necessity in solar-energy systems. Renew. Energy 6, 549. http://dx.doi.org/10.1016/0960-1481(92)90017-W.

Eshkevari, S.S., Eshkevari, S.S., Sen, D., Pakzad, S.N., 2023. Active structural control framework using policy-gradient reinforcement learning. Eng. Struct. 274, 115122. http://dx.doi.org/10.1016/j.engstruct.2022.115122.

European Commission, 2023. Delivering on the EU Offshore Renewable Energy Ambitions. Communication from the Commission to the European Parliament, the Council, the European Economic and Social Committee and the Committee of the Regions. Technical Report, European Commission, URL https://eur-lex.europa.eu/legal-content/EN/TXT/?uri=CELEX%3A52023DC0668.

European Wind Energy Association, 2019. EWEA Fact Sheet. Technical Report, https://www.ewea.org/fileadmin/files/library/publications/statistics/Factsheets.pdf.

Falliere, N., Murchu, L.O., Chien, E., 2011. W32. Stuxnet Dossier. White Paper. Symantec Corp. Security Response. URL https://archive.org/details/w32_stuxnet_dossier/mode/2up.

Fan, D., Yang, L., Wang, Z., Triantafyllou, M.S., Karniadakis, G.E., 2020. Reinforcement learning for bluff body active flow control in experiments and simulations. Proc. Natl. Acad. Sci. USA 117 (42), 26091–26098. http://dx.doi.org/10.1073/pnas.2004939117.

Fildes, J., 2010. Stuxnet worm 'targeted high-value Iranian assets'. BBC News URL https://www.bbc.com/news/technology-11388018.

Filipov, E.T., Tachi, T., Paulino, G.H., 2015. Origami tubes assembled into stiff, yet reconfigurable structures and metamaterials. Proc. Natl. Acad. Sci. USA 112 (40), 12321–12326. http://dx.doi.org/10.1073/pnas.1509465112.

Fitzgerald, B., Basu, B., 2013. Active tuned mass damper control of wind turbine nacelle/tower vibrations with damaged foundations. Key Eng. Mater. 569, 660–667. http://dx.doi.org/10.4028/www.scientific.net/KEM.569-570.660.

Fitzgerald, B., Basu, B., 2014. Cable connected active tuned mass dampers for control of in-plane vibrations of wind turbine blades. J. Sound Vib. 333, 5980–6004. http://dx.doi.org/10.1016/j.jsv.2014.05.031.

Fitzgerald, B., Basu, B., Nielsen, S.R.K., 2013. Active tuned mass dampers for control of in-plane vibrations of wind turbine blades. Struct. Control Health Monit. 20, 1377–1396. http://dx.doi.org/10.1002/stc.1524.

Fitzgerald, B., Sarkar, S., Staino, A., 2018. Improved reliability of wind turbine towers with active tuned mass dampers (ATMDs). J. Sound Vib. 419, 103–122. http://dx.doi.org/10.1016/j.jsv.2017.12.026.

Fragoso, S., Garrido, J., Vázquez, F., Morilla, F., 2017. Comparative analysis of decoupling control methodologies and h_∞ multivariable robust control for variable-speed, variable-pitch wind turbines: Application to a lab-scale wind turbine. Sustainability 9, 713. http://dx.doi.org/10.3390/su9050713.

Gambier, A., Nazaruddin, Y., 2018. Collective pitch control with active tower damping of a wind turbine by using a nonlinear PID approach. IFAC PapersOnLine 51, 238–243. http://dx.doi.org/10.1016/j.ifacol.2018.06.072.

Gao, D., Chen, W., Huang, Y., Li, H., 2019. Active control of circular cylinder flow with windward suction and leeward blowing. Exp. Fluids 60 (2), 26. http://dx.doi.org/10.1007/s00348-018-2676-z.

Gao, D., Deng, Z., Yang, W., Chen, W., 2021. Review of the excitation mechanics and aerodynamic flow control of vortex-induced vibration of the main girder for long-span bridges: A vortex-dynamics approach. J. Fluids Struct. 105, 103348. http://dx.doi.org/10.1016/j.jfluidstructs.2021.103348.

Gao, H., Kwok, K.C.S., Samali, B., 1997. Optimization of tuned liquid column dampers. Eng. Struct. 19 (6), 476–486. http://dx.doi.org/10.1016/S0141-0296(96)00099-5.

Gavin, H., 1998. Design method for high-force electrorheological dampers. Smart Mater. Struct. 7, 664–673. http://dx.doi.org/10.1088/0964-1726/7/5/010.

Ge, Y., Xia, J., Zhao, L., Zhao, S., 2011. Full aeroelastic model testing for examining wind-induced vibration of a 5,000 m spanned suspension bridge. Front. Built Environ. 4 (20), 1–12. http://dx.doi.org/10.3389/fbuil.2018.00020.

Ge, Y., Zhao, L., Cao, J., 2022. Case study of vortex-induced vebration and mitication mechanicsm for a long-span suspension bridge. J. Wind Eng. Ind. Aerodyn. 220, 104866. http://dx.doi.org/10.1016/j.jweia.2021.104866.

Gheni, E.Z., Al-Khafaji, H.M.H., Alwan, H.M., 2024. A deep reinforcement learning framework to modify LQR for an active vibration control applied to 2D building models. Open Eng. 14, 20220496. http://dx.doi.org/10.1515/eng-2022-0496.

Ghommema, M., Nayfeh, A.H., Choura, S., Najar, F., Abdel-Rahman, E.M., 2010. Modeling and performance study of a beam micro gyroscope. J. Sound Vib. 329, 4970–4979. http://dx.doi.org/10.1016/j.jsv.2010.06.009.

Giaccu, G.F., Caracoglia, L., 2021. A gyroscopic stabilizer to improve flutter performance of long-span cable-supported bridges. Eng. Struct. 240, 112373. http://dx.doi.org/10.1016/j.engstruct.2021.112373.

Giaccu, G.F., Caracoglia, L., 2023. Multi-unit gyroscopic stabilizer to control flutter of long-span bridges: sensitivity analysis. In: ICWE16: 16^{Th} International Conference on Wind Engineering; Florence, Italy; 27-31 August 2023.

Goff, E., Glantz, C., Massello, R., 2014. Cybersecurity procurement language for energy delivery systems. In: Proceedings of the 9th Annual Cyber and Information Security Research Conference. CISR '14, Association for Computing Machinery, New York, NY, USA, ISBN: 9781450328128, pp. 77–79. http://dx.doi.org/10.1145/2602087.2602097.

Goh, C.J., Caughey, T.K., 1985. On the stability problem caused by finite actuator dynamics in the collocated control of large space structures. Internat. J. Control 41, 787–802. http://dx.doi.org/10.1080/0020718508961163.

Goit, J.P., Mayers, J., 2015. Optimal control of energy extraction in wind-farm boundary layers. J. Fluid Mech. 768, 5–50. http://dx.doi.org/10.1017/jfm.2015.70.

Gu, M., Chen, S.R., Chang, C.C., 2002. Control of wind-induced vibrations of long-span bridges by semi-active lever-type TMD. J. Wind Eng. Ind. Aerodyn. 90 (2), 111–126. http://dx.doi.org/10.1016/S0167-6105(01)00165-9.

Gu, M., Wang, X., Quan, Y., 2020. Wind tunnel test study on effects of chamfered corners on the aerodynamic characteristics of 2D rectangular prisms. J. Wind Eng. Ind. Aerodyn. 204, 104305. http://dx.doi.org/10.1016/j.jweia.2020.104305.

Gu, M., Xiang, H., 1992. Optimization of TMD for suppressing buffeting response of long-span bridges. J. Wind Eng. Ind. Aerodyn. 42 (1–3), 1383–1392. http://dx.doi.org/10.1016/0167-6105(92)90146-2.

Guo, Y.L., Kareem, A., Ni, Y.Q., Liao, W.Y., 2012a. Performance evaluation of canton tower under winds based on full-scale data. J. Wind Eng. Ind. Aerodyn. 104–106, 116–128. http://dx.doi.org/10.1016/j.jweia.2012.04.001.

Guo, Y.L., Kareem, A., Ni, Y.Q., Liao, W.Y., 2012b. Performance evaluation of Canton Tower under winds based on full-scale data. J. Wind Eng. Ind. Aerodyn. 104, 116–128. http://dx.doi.org/10.1016/j.jweia.2012.04.001.

Gutierrez Soto, M., Adeli, H., 2013. Tunned mass dampers. Arch. Comput. Methods Eng. 20 (4), 419–431. http://dx.doi.org/10.1007/s11831-013-9091-7.

Güzel, Ö., 2023. Advanced planning and innovative construction technologies in the challenging bridge projects. In: IABSE Symposium Istanbul 2023: Long Span Bridges; Istanbul, Türkiye; 26-28 April 2023.

Han, B.-Z., Huang, W.-X., Xu, C.-X., 2022. Deep reinforcement learning for active control of flow over a circular cylinder with rotational oscillations. Int. J. Heat Fluid Flow 96, 109008. http://dx.doi.org/10.1016/j.ijheatfluidflow.2022.109008.

Hansen, K.S., Barthelmie, R.J., Jensen, L.E., Sommer, A., 2011. The impact of turbulence intensity and atmospheric stability on power deficits due to wind trubine wakes at Horns Rev wind farm. Wind Energy 15, 183–196. http://dx.doi.org/10.1002/we.512.

Hansen, H.I., Thoft-Christensen, P., 2001. Actice flap control of long suspension bridges. J. Struct. Control 8, 33–82. http://dx.doi.org/10.1002/stc.4300080104.

Hansen, H.I., Thoft-Christensen, P., Mendes, P.A., Branco, F.A., 2000. Wind-tunnel tests of a bridge model with active vibration control. Struct. Eng. Int. 4, 249–253. http://dx.doi.org/10.2749/101686600780481239.

Hao, D., Qi, L., Tairab, A.M., Ahmed, A., Azam, A., Luo, D., Pan, Y., Zhang, Z., Yan, J., 2022. Solar energy harvesting technologies for PV self-powered applications: A comprehensive review. Renew. Energy 188, 678–697. http://dx.doi.org/10.1016/j.renene.2022.02.066.

Hareendran, S.P., Alipour, A., Sarkar, P., 2023. Improving aerodynamic response of tall buildings using smart morphing facades. J. Build. Eng. 80, 107656. http://dx.doi.org/10.1016/j.jobe.2023.107656.

He, H., Xie, X., Wang, W., 2017. Vibration control of tower structure with multiple gardan gyroscopes. Shock Vib. 3548360. http://dx.doi.org/10.1155/2017/3548360.

Hemsley, Kevin E., Fisher, E., et al., 2018. History of Industrial Control System Cyber Incidents. Technical Report, Idaho National Lab.(INL), Idaho Falls, ID (United States), URL https://www.osti.gov/servlets/purl/1505628.

Hernandez, S., 2010. Structural optimization. 1960–2010 and beyond. Comput. Technol. Rev. 2, http://dx.doi.org/10.4203/ctr.2.8.

Hoffmann, F.M., Molz, R.F., Kothe, J.V., Benitez Nara, E.O., Carvalho Tedesco, L.P., 2018. Monthly profile analysis based on a two-axis solar tracker proposal for photovoltaic panels. Renew. Energy 115, 750–759. http://dx.doi.org/10.1016/j.renene.2017.08.079.

Hou, F., Sakar, P.P., Alipour, A., 2023. A novel mechanism - smart morphing façade system - to mitigate wind-induced vibration of tall buildings. Eng. Struct. 275, 115152. http://dx.doi.org/10.1016/j.engstruct.2022.115152.

Housner, G.W., Bergman, L.A., Caughey, T.K., Chassiakos, A.G., Claus, R.O., Masri, S.F., Skelton, R.E., Soong, T.T., Spencer, B.F., Yao, J.T.P., 1997. Structural control: Past, present, and future. J. Eng. Mech. 123 (9), 897–971. http://dx.doi.org/10.1061/(ASCE)0733-9399(1997)123:9(897).

Hrovat, D., Barak, P., Rabins, M., 1983. Semi-active versus passive or active tunned mass dampers for structural control. J. Eng. Mech. 109 (3), 691–705. http://dx.doi.org/10.1061/(ASCE)0733-9399(1983)109:3(691).

Hu, Y., He, E., 2017. Active structural control of a floating wind turbine with a stroke-limited hybrid mass damper. J. Sound Vib. 410, 447–472. http://dx.doi.org/10.1016/j.jsv.2017.08.050.

Hu, C., Zhao, L., Ge, Y., 2019. Mechanism of suppression of vortex-induced vibrations of a streamlined closed-box girder using additional small-scale components. J. Wind Eng. Ind. Aerodyn. 189, 314–331. http://dx.doi.org/10.1016/j.jweia.2019.04.015.

Hur, S.-H., Leithead, W.E., 2016. Adjustment of wind farm power output through flexible turbine operation using wind farm control. Wind Energy 19, 1667–1686. http://dx.doi.org/10.1002/we.1943.

Huynh, T., Thoft-Christensen, P., 2001. Suspension bridge flutter for girders with separate control flaps. J. Bridge Eng. 6 (3), 168–175. http://dx.doi.org/10.1061/(ASCE)1084-0702(2001)6:3(168).

Igusa, T., Xu, K., 1994. Vibration control using multiple tuned mass dampers. J. Sound Vib. 175 (4), 491–503. http://dx.doi.org/10.1006/jsvi.1994.1341.

Irtaza, H., Agarwal, A., 2018. CFD simulation of turbulent wind effect on an array of ground-mounted solar PV panels. J. Inst. Eng.: Ser. A 99 (2), 205–218. http://dx.doi.org/10.1007/s40030-018-0283-x.

Irwin, P., 2008. Bluff body aerodynamics in wind engineering. J. Wind Eng. Ind. Aerodyn. 96 (6–7), 701–712. http://dx.doi.org/10.1016/j.jweia.2007.06.008.

Irwin, P., 2009. Wind engineering challenges of the new generation of super-tall buildings. J. Wind Eng. Ind. Aerodyn. 97, 328–334. http://dx.doi.org/10.1016/j.jweia.2009.05.001.

Jafari, M., Alipour, A., 2021a. Aerodynamic shape optimization of rectangular and elliptical double-skin façades to mitigate wind-induced effects on tall buildings. J. Wind Eng. Ind. Aerodyn. 213, 104586. http://dx.doi.org/10.1016/j.jweia.2021.104586.

Jafari, M., Alipour, A., 2021b. Methodologies to mitigate wind-induced vibrations of tall buildings: A state-of-the-art review. J. Build. Eng. 33, 101582. http://dx.doi.org/10.1016/j.jobe.2020.101582.

Jajodia, S., Ghosh, A.K., Swarup, V., Wang, C., Wang, X.S., 2011. Moving Target Defense: Creating Asymmetric Uncertainty for Cyber Threats, first ed. Springer Publishing Company, Incorporated, ISBN: 1461409764, http://dx.doi.org/10.1007/978-1-4614-0977-9.

Jo, H., Sim, S.-H., Mechitov, K., Kim, R., Li, J., Moinzadeh, P., Spencer, B., Park, J., Cho, S., Jung, H.-J., Yun, C.-B., Bridge, J., 2011. Hybrid wireless smart sensor network for full-scale structural health monitoring of a cable-stayed bridge. In: Proceedings Volume 7981, Sensors and Smart Structures Technologies for Civil, Mechanical, and Aerospace Systems 2011. pp. 45–59. http://dx.doi.org/10.1117/12.880513.

Kagaya, H., Tamaki, T., Nishi, Y., Nagao, Y., Yamaguchi, K., 2011. Vibration control of bridge tower under construction using active mass damper (in Japanese). Trans. Soc. Instrum. Control Eng. 47 (5), 247–252. http://dx.doi.org/10.9746/sicetr.47.247.

Kan, Y., Psinh, Y., Lee, A.-C., 1992. Investigation on the steady-state response of a symmetric rotors. J. Vib. Acoust. 114 (2), 194–208. http://dx.doi.org/10.1115/1.2930249.

Karanouh, A., Kerber, E., 2015. Innovations in dynamic architecture. J. Facade Des. Eng. 3 (2), 185–221. http://dx.doi.org/10.3233/FDE-150040.

Kareem, A., 1995. Methods to control wind induced building motions. In: Structures Congress XII, Atlanta, Georgia, United States, April 24-28, 1994. ASCE.

Kareem, A., Kijewski, T., Tamura, Y., 1999. Mitigation of motions of tall buildings with specific examples of recent applications. Wind Struct. 2 (3), 201–251. http://dx.doi.org/10.12989/was.1999.2.3.201.

Kareem, A., Kline, S., 1995. Performance of multiple mass dampers under random loading. J. Struct. Eng. ASCE 121 (2), 348–361. http://dx.doi.org/10.1061/(ASCE)0733-9445(1995)121:2(348).

Kareem, A., Spence, S., Bernardini, E., Bobby, S., Wei, D., 2013. Using computational fluid dynamics to optimize tall building design. CTBUH J. 3, 38–43, URL https://global.ctbuh.org/resources/papers/download/244-using-computational-fluid-dynamics-to-optimize-tall-building-design.pdf.

Kareem, A., Sun, X.-J., 1987. Stochastic response of structures with fluid-containing appendages. J. Sound Vib. 119 (3), 389–408. http://dx.doi.org/10.1016/0022-460X(87)90405-6.

Karniadakis, G.E., Triantafyllou, G.S., 1992. Three-dimensional dynamics and transition to turbulence in the wake of bluff objects. J. Fluid Mech. 238, 1–30. http://dx.doi.org/10.1017/S0022112092001617.

Karnopp, D., 1990. Design principles for vibration control systems using semi-active dampers. J. Dyn. Syst. Meas. Control 112, 448–455. http://dx.doi.org/10.1115/1.2896163.

Ke, T., Cong, S., ZhiYong, Z., HanXiang, Y., Sungur, P.T, 2014. Numerical investigation on aerodynamic force of streamlined box girder with uniform air suction. J. Eng. Sci. Technol. Rev. 7 (2), 190–196.

Keyser, D., Tegen, S., 2019. The Wind Energy Workforce in the United States: Training, Hiring, and Future Needs. NREL/TP-6A20-73908, National Renewable Energy Laboratory, URL https://www.nrel.gov/docs/fy19osti/73908.pdf.

Khodabandehlou, H., Pekcan, G., Sami Fadali, M., Salem, M.M., 2018. Active neural predictive control of seismically isolated structures. Struct. Control Health Monit. 25 (7), e2201. http://dx.doi.org/10.1002/stc.2061.

Kijewski-Correa, T., Kilpatrick, J., Kareem, A., Kwon, D.-K., Bashor, R., Kochly, B.S., Abdelrazaq, A., Galsworthy, J., Isyumov, N., Morrish, D., Sinn, R.C., Baker, W.F., 2006. Validating wind-induced response of tall buildings: Synopsis of the Chicago full-scale monitoring program. J. Struct. Eng. 132 (10), 1509–1523. http://dx.doi.org/10.1061/(ASCE)0733-9445(2006)132:10(1509).

Kijewski-Correa, T., Kwon, D.K., Kareem, A., Bentz, A., Guo, Y., Bobby, S., Abdelrazaq, A., 2013. SmartSync: An integrated real-time structural health monitoring and structural identification system for tall buildings. J. Struct. Eng. ASCE 139 (10), 1675–1687. http://dx.doi.org/10.1061/(ASCE)ST.1943-541X.0000560.

Kim, S., Pakzad, S., Culler, D., Demmel, J., Fenves, G., Glaser, S., Turon, M., 2007. Health monitoring of civil infrastructures using wireless sensor networks. In: IPSN 2007: Proceedings of the Sixth International Symposium on Information Processing in Sensor Networks. pp. 254–263. http://dx.doi.org/10.1109/IPSN.2007.4379685.

Kim, W., Yi, J.-H., Tamura, Y., Yoshida, A., 2017. Wind-induced responses of super-tall buildings with various complicated cross-sectional shapes. In: Proceedings of the 2017 World Congress on Advances in Structural Engineering and Mechancis (ASEM17), 28 August - 1 September, 2017, Ilsan(Soeul), Korea. URL http://www.i-asem.org/publication_conf/asem17/1.SM/T4A.7.SM1132_4371F1.pdf.

Kim, W., Yoshida, A., Tamura, Y., Yi, J.-H., 2018. Experimental study of aerodynamic damping of a twisted supertall building. J. Wind Eng. Ind. Aerodyn. 176, 1–12. http://dx.doi.org/10.1016/j.jweia.2018.03.005.

Knudsen, T., Bak, T., Svenstrup, M., 2015. Survey of wind farm control - power and fatigue optimization. Wind Energy 18, 1333–1351. http://dx.doi.org/10.1002/we.1760.

Knutson, T.R., McBride, J.L., Chan, J., Emanuel, K., Holland, G., Landsea, C., Held, I., Kossin, J.P., Srivastava, A.K., Sugi, M., 2010. Tropical cyclones and climate change. Nat. Geosci. 3, 157–163. http://dx.doi.org/10.1038/ngeo779.

Kobayashi, H., Nagaoka, H., 1992. Active control of flutter of a suspension bridge. J. Wind Eng. Ind. Aerodyn. 41 (1–3), 143–151. http://dx.doi.org/10.1016/0167-6105(92)90402-V.

Kopp, G.A., Farquhar, S., Morrison, M.J., 2012. Aerodynamic mechanisms for wind loads on tilted, roof-mounted, solar arrays. J. Wind Eng. Ind. Aerodyn. 111, 40–52. http://dx.doi.org/10.1016/j.jweia.2012.08.004.

Korkmaz, S., 2011. Review: A review of active structural control: challenges for engineering informatics. Comput. Struct. 89, 2113–2132. http://dx.doi.org/10.1016/j.compstruc.2011.07.010.

Körlin, R., Starossek, U., 2007. Wind tunnel test of an active mass damper for bridge decks. J. Wind Eng. Ind. Aerodyn. 95, 267–277. http://dx.doi.org/10.1016/j.jweia.2006.06.015.

Koutsoloukas, L., Nikitas, N., Aristidou, P., 2022. Passive, semi-active, active and hybrid mass dampers: A literature review with associated applications on building-like structures. Dev. Built Environ. 12, 100094. http://dx.doi.org/10.1016/j.dibe.2022.100094.

Kozmar, H., Procino, L., Borsani, A., Bartoli, G., 2012. Sheltering efficiency of wind barriers on bridges. J. Wind Eng. Ind. Aerodyn. 107–108, 274–284. http://dx.doi.org/10.1016/j.jweia.2012.04.027.

Krenk, S., Svendsen, M.N., Høgsberg, J., 2012. Resonant vibration control of three-bladed wind turbine rotors. AIAA J. 50 (1), 148–161. http://dx.doi.org/10.2514/1.J051164.

Kubo, Y., 2004. Prospects for the suppression of aerodynamic cibrations of a long-span bridge using boundary-layer control. J. Vib. Control 10, 1359–1373. http://dx.doi.org/10.1177/1077546304042050.

Kubo, Y., Modi, V.J., Kotsubo, C., Hayashida, K., Kato, K., 1996. Suppression of wind-induced vibration of tall structures through moving surface boundary-layer control. J. Wind Eng. Ind. Aerodyn. 61, 181–194. http://dx.doi.org/10.1016/0167-6105(96)00039-6.

Kubo, Y., Modi, V.J., Yasuda, H., Kato, K., 1992. On the suppression of aerodynamic instabilities through the moving surface boundary-layer control. J. Wind Eng. Ind. Aerodyn. 41–44, 205–206. http://dx.doi.org/10.1016/0167-6105(92)90410-C.

Kubo, Y., Yasuda, H., Kotsubo, C., Hirata, K., 1993. Active control of super-tall structure vibrations under wind action by a boundary layer control. J. Wind Eng. Ind. Aerodyn. 50, 361–372. http://dx.doi.org/10.1016/0167-6105(93)90091-2.

Kubo, Y., Yukoku, E., Modi, V.J., Yamaguchi, E., Kato, K., Kawamura, S., 1999. Control of flow separation from leading edge of a shallow rectangular cylinder through momentum injection. J. Wind Eng. Ind. Aerodyn. 83, 503–514. http://dx.doi.org/10.1016/S0167-6105(99)00097-5.

Kumar, D., Chatterjee, K., 2016. A review of conventional and advanced MPPT algorithms for wind energy systems. Renew. Sustain. Energy Rev. 55, 957–970. http://dx.doi.org/10.1016/j.rser.2015.11.013.

Kusano, I., Baldomir, A., Jurado, J.A., Hernández, S., 2015. Probabilistic optimization of the main cable and bridge deck of long-span suspension bridges under flutter constraint. J. Wing Eng. Ind. Aerodyn. 146, 59–70. http://dx.doi.org/10.1016/j.jweia.2015.08.001.

Kwok, K.C.S., 2013. Wind-induced vibrations of structures: With special reference to tall building aerodynamics. Advan. Struct. Wind Eng. 121–155. http://dx.doi.org/10.1007/978-4-431-54337-4_5.

Kwok, K.C.S., Hitchcock, P.A., Burton, M.D., 2009. Perception of vibration and occupant comfort in wind-excited tall buildings. J. Wind Eng. Ind. Aerodyn. 97 (7–8), 368–380. http://dx.doi.org/10.1016/j.jweia.2009.05.006.

Kwok, K.C., Samali, B., 1995. Performance of tuned mass dampers under wind loads. Eng. Struct. 17, 655–667. http://dx.doi.org/10.1016/0141-0296(95)00035-6.

Kwok, K.C.S., Wilhelm, P.A., Wilkie, B.G., 1988. Effect of edge configuration on wind-induced response of tall buildings. Eng. Struct. 10 (2), 135–140. http://dx.doi.org/10.1016/0141-0296(88)90039-9.

Kwon, S.-D., Chang, S.-P., 2000. Suppression of flutter and gust response of bridges using actively controlled edge surfaces. J. Wind Eng. Ind. Aerodyn. 88, 263–281. http://dx.doi.org/10.1016/S0167-6105(00)00053-2.

Kwon, D.K., Kareem, A., 2013. Comparative study of major international wind codes and standards for wind effects on tall buildings. Eng. Struct. 51, 23–35. http://dx.doi.org/10.1016/j.engstruct.2013.01.008.

Kwon, S., Kim, D.H., Lee, S.H., Song, H.S., 2011. Design criteria of wind barriers for traffic. Part 1: wind barrier performance. Wind Struct. 14, 55–70. http://dx.doi.org/10.12989/was.2011.14.1.055.

Lago, A., Trabucco, D., Wood, A., 2018. Damping Technologies for Tall Buildings: Theory, Design Guidance and Case Studies. Elsevier Science and Technology, http://dx.doi.org/10.1016/C2017-0-01327-7.

Lala, J.H., Adams, S.J., 1989. Intercomputer communication architecture for a mixed redundancy distributed system. J. Guid. 12 (4), 539–547. http://dx.doi.org/10.2514/3.20442.

Landers, J., 2023. Can 'Unhackable' Infrastructure be Designed?. Civil Engineering Source, ASCE, URL https://www.asce.org/publications-and-news/civil-engineering-source/civil-engineering-magazine/article/2023/03/can-unhackable-infrastructure-be-designed.

Landers, J., 2024. Message to Congress: Cyberthreats to Infrastructure Surging. Civil Engineering Source, ASCE, URL https://www.asce.org/publications-and-news/civil-engineering-source/civil-engineering-magazine/article/2024/04/message-to-congress-cyberthreats-to-infrastructure-surging.

Langner, R., 2011. Stuxnet: Dissecting a Cyberwarfare Weapon. IEEE Secur. Priv. 9 (3), 49–51. http://dx.doi.org/10.1109/MSP.2011.67.

Larsen, A., Larose, G., 2015. Dynamic wind effects on suspension and cable-stayed bridges. J. Sound Vib. 334, 2–28. http://dx.doi.org/10.1016/j.jsv.2014.06.009.

Larsen, A., Poulin, S., 2005. Vortex-shedding excitation of box-girder bridges and mitigation. Struct. Eng. Int. IABSE 15, 258–263. http://dx.doi.org/10.2749/101686605777962919.

Larsen, A., Wall, A., 2012. Shaping of bridge box girders to avoid vortex shedding response. J. Wind Eng. Ind. Aerodyn. 104–106, 159–165. http://dx.doi.org/10.1016/j.jweia.2012.04.018.

Lee, M., 2023. AI robots capable of carrying our attack on NHS that would case COVID-like disruption, expert warns. Fox News URL https://www.foxnews.com/world/ai-robots-capable-carrying-out-attack-nhs-would-cause-covid-like-disruption-expert-warns.

Lewis, F.L., Vrabie, D., Syrmos, V.L., 2012. Optimal Control. John Wiley & Sons, New York, NY, USA, http://dx.doi.org/10.1002/9781118122631.

Li, K., Ge, Y.J., Guo, Z.W., Zhao, L.L, 2015. Theoretical framework of feedback aerodynamic control of flutter oscillation for long-span suspension bridges by the twin-winglet system. J. Wind Eng. Ind. Aerodyn. 145, 166–177. http://dx.doi.org/10.1016/j.jweia.2015.06.012.

Li, K., Ge, Y.J., Zhao, L.L, Guo, Z.W., 2017. Numerical simulation of feedback flutter control for a single-box-girder suspension bridge by twin-winglet system. J. Wind Eng. Ind. Aerodyn. 169, 77–93. http://dx.doi.org/10.1016/j.jweia.2017.07.013.

Li, Beibei, Wu, Yuhao, Song, Jiarui, Lu, Rongxing, Li, Tao, Zhao, Liang, 2021. DeepFed: Federated deep learning for intrusion detection in industrial cyber–physical systems. IEEE Trans. Ind. Inform. 17 (8), 5615–5624. http://dx.doi.org/10.1109/TII.2020.3023430.

Li, K., Zhao, L., Hui, Y., Yang, Q., Chen, Z., Qian, G., 2022. Active flutter control of a bridge-flap system considering aerodynamic interferences in practical considerations. Smart Mater. Struct. 31, 065006. http://dx.doi.org/10.1088/1361-665X/ac65c5.

Liew, J., Goçmen, T., Lio, W.H., Larsen, G.C., 2015. Model-free closed-loop wind farm control using reinforcement learning with recursive least squares. Wind Energy 1–15. http://dx.doi.org/10.1002/we.2852.

Ma, W., Zhang, W., Zhang, X., Chen, W., Tan, Q., 2023. Experimental investigations on the wind load interference effects of single-axis solar tracker arrays. Renew. Energy 202, 566–580. http://dx.doi.org/10.1016/j.renene.2022.11.112.

Malhotra, A., Roy, T., Matsagar, V., 2020. Effectiveness of friction dampers in seismic and wind response control of connected adjacent steel buildings. Shock Vib. 2020, 8304359. http://dx.doi.org/10.1155/2020/8304359.

Manwell, J.F., McGowan, J.G., Rogers, A.L., 2009. Wind Energy Explained: Theory, Design and Application. Wiley, http://dx.doi.org/10.1002/9781119994367.

Marden, J.R., Ruben, S.D., Pao, L.Y., 2013. A model-free approach to wind farm control using game theoretic methods. IEEE Trans. Control Syst. Technol. 21 (4), 1207–1213. http://dx.doi.org/10.1109/TCST.2013.2257780.

Marivani, M., Hamed, M.S., 2009. Numerical Investigation of Sloshing Motion Inside Tuned Liquid Dampers with and Without Submerged Screens (Ph.D. thesis). Department of Mechanical Engineering - McMaster University, URL http://hdl.handle.net/11375/17557.

Marler, R.T., Arora, J.S., 2004. Survey of multi-objective optimization methods for engineering. Struct. Multidiscip. Optim. 26, 369–395. http://dx.doi.org/10.1007/s00158-003-0368-6.

Marler, R.T., Arora, J.S., 2010. The weighted sum method for multi-objective optimization: New insights. Struct. Multidiscip. Optim. 41, 853–862. http://dx.doi.org/10.1007/s00158-009-0460-7.

Marsland, L., Nguyen, K., Zhang, Y., Huang, Y., Abu-Zidan, Y., Gunawardena, T., Mendis, P., 2022. Improving aerodynamic performance of tall buildings using façade openings at service floors. J. Wind Eng. Ind. Aerodyn. 225, 104997. http://dx.doi.org/10.1016/j.jweia.2022.104997.

Martinez-Garcia, E., Blanco-Marigorta, E., Gayo, J.P., Navarro-Manso, A., 2021. Influence of inertia and aspect ratio on the torsional galloping of single-axis solar trackers. Eng. Struct. 243, 112682. http://dx.doi.org/10.1016/j.engstruct.2021.112682.

Martynowicz, P., 2015. Vibration control of wind turbine tower-nacelle model with magnetorheological tuned vibration absorber. J. Vib. Control 23 (20), 1–22. http://dx.doi.org/10.1177/1077546315591445.

McFadden, 2023. Huge cyberattack disables telescopes in Hawaii and Chile, Aug 26^{th}. URL https://interestingengineering.com/science/hawaii-chile-nsf-telescopes-cyberattack.

Meirovitch, L., 1977. Control of spinning flexible spacecraft by modal synthesis. Acta Astronaut. 4, 985–1010. http://dx.doi.org/10.1016/0094-5765(77)90002-9.

Meng, X., Nguyen, D.T., Xie, Y., Owen, J.S., Psimoulis, P., Ince, S., Chen, Q., Ye, J., Bhatia, P., 2018. Design and implementation of a new system for large bridge monitoring-GeoSHM. Sensors 18, 775. http://dx.doi.org/10.3390/s18030775.

Mitchell, Robert, Chen, Ing-Ray, 2014. A survey of intrusion detection techniques for cyber-physical systems. ACM Comput. Surv. (ISSN: 0360-0300) 46 (4), http://dx.doi.org/10.1145/2542049.

Miyashita, K., Katagiri, J., Nakamura, O., Ohkuma, T., Tamura, Y., Itoh, M., Mimachi, T., 1993. Wind-induced response of high-rise buildings: Effects of corner cuts or openings in square buildings. J. Wind Eng. Ind. Aerodyn. 69, 106135. http://dx.doi.org/10.1016/0167-6105(93)90087-5.

Modi, V.J., Fernando, M.S.U.K., Yokomizo, T., 1991. Moving surface boundary control: studies with bluff bodies and application. AIAA J. 29 (9), 1400–1406. http://dx.doi.org/10.2514/3.10753.

Moon, K.S., 2009. Tall building motion control using double skin façades. J. Archit. Eng. 3, 84–90. http://dx.doi.org/10.1061/(ASCE)1076-0431(2009)15:3(84).

Mooneghi, M.A., Kargarmoakhar, R., 2016. Aerodynamic mitigation and shape optimization of buildings: Review. J. Build. Eng. 6, 225–235. http://dx.doi.org/10.1016/j.jobe.2016.01.009.

Mousazadeh, H., Keyhani, A., Javadi, A., Mobli, H., Abrinia, K., Sharifi, A., 2009. A review of principle and sun-tracking methods for maximizing solar systems output. Renew. Sustain. Energy Rev. 13, 1800–1818. http://dx.doi.org/10.1016/j.rser.2009.01.022.

Muscari, C., Shito, P., Viré, A., Zasso, A., van der Hoek, D., van Wingerden, J.W., 2022. Physics informed DMD for periodic Dynamic Induction Control of Wind Farms. J. Phys. Conf. Ser. 2265, 022057. http://dx.doi.org/10.1088/1742-6596/2265/2/022057.

Nagarajaiah, S., Chen, L., Wang, M., 2022. Adaptive stiffness structures with dampers: Seismic and wind response reduction using passive negative stiffness and inerter systems. J. Struct. Eng. 148 (11), 04022179. http://dx.doi.org/10.1061/(ASCE)ST.1943-541X.0003472.

Naskar, A., 2022. Vatican Virus: The Forbidden Fiction. In: Abi Naskar Adventures Series, Neuro Cookies, ISBN: 9798201685874.

Ni, Y.Q., Zhou, H.F., 2010. Guangzhou new TV tower: Integrated structural health monitoring and vibration control. In: 2010 Structures Congress. ASCE, pp. 3155–3164. http://dx.doi.org/10.1061/41130(369)283.

Nieto, F., Hernández, S., Jurado, J.A., 2009. Optimum design of long-span suspension bridges considering aeroelastic and kinematic constraints. Struct. Multidiscip. Opt. 39, 133–151. http://dx.doi.org/10.1007/s00158-008-0314-8.

Nieto, F., Kusano, I., Hernández, S., Jurado, J.Á., 2010. CFD analysis of the vortex-shedding response of a twin-box deck cable-stayed bridge. In: CWE2010: Fifth International Symposium on Computational Wind Engineering.

Nissen, H.D., Sorensen, P.H., Jannerup, O., 2004. Active aerodynamic stabilisation of long suspension bridges. J. Wind Eng. Ind. Aerodyn. 92, 829–847. http://dx.doi.org/10.1016/j.jweia.2004.03.012.

Njiri, J.G., Söffker, D., 2016. State-of-the-art in wind turbine control: Trends and challenges. Renew. Sustain. Energy Rev. 60, 377–393. http://dx.doi.org/10.1016/j.rser.2016.01.110.

Ogawa, K., Ide, T., Saitou, T., 1997. Application of impact mass damper to a cable-stayed bridge pylon. J. Wind Eng. Ind. Aerodyn. 72, 301–312. http://dx.doi.org/10.1016/S0167-6105(97)00265-1.

Oh, S.J., Burhan, M., Ng, K.C., Kim, Y., Chun, W., 2015. Development and performance analysis of a two-axis solar tracker for concentrated photovoltaics. Int. J. Energy Res. 39, 965–976. http://dx.doi.org/10.1002/er.3306.

Okunyté, P., 2023. Ransomware attack spreads chaos at major hospital in Barcelona. Cybernews URL https://cybernews.com/news/ransomware-attack-hospital-in-barcelona/.

Omenzetter, P., Wilde, K., Fujino, Y., 2000. Suppression of wind-induced instabilities of a long span bridge by a passive deck-flaps control system: Part I: Formulation. J. Wind Eng. Ind. Aerodyn. 87, 61–79. http://dx.doi.org/10.1016/S0167-6105(00)00016-7.

Omenzetter, P., Wilde, K., Fujino, Y., 2002. Study of passive deck-flap flutter control system on full bridge model. I: Theory. J. Eng. Mech. 128 (3), http://dx.doi.org/10.1061/(ASCE)0733-9399(2002)128:3(264).

Orcesi, A., O'Connor, A., Diamantidis, D., Sykora, M., Wu, T., Akiyama, M., Alhamid, A.K., Schmidt, F., Pregnolato, M., Li, Y., Salarieh, B., Salman, A.M., Bastidas-Arteaga, E., Markogiannaki, O., Schoefs, F., 2022. Investigating the effects of climate change on structural actions. Struct. Eng. Int. IABSE 32 (4), 563–576. http://dx.doi.org/10.1080/10168664.2022.2098894.

Osder, S., 1999. Practical view of redundancy management application and theory. J. Guid. Control Dyn. 22 (1), 12–21. http://dx.doi.org/10.2514/2.4363.

Ostenfeld, K.H., Larsen, A., 1992. Bridge engineering and aerodynamics. In: Larsen, A. (Ed.), Aerodynamics of Large Bridges. Balkema, Rotterdam, the Netherlands, ISBN: 9781351468046, pp. 3–22.

Ostenfeld, K.H., Larsen, A., 1997. Elements of active flutter control of bridges. In: New Technologies in Structural Engineering, Laboratorio Nacional de Engenharia Civil, Lisbon, Portugal. pp. 683–694.

Pao, L.Y., Johnson, K.E., 2009. A tutorial on the dynamics and control of wind turbines and wind farms. In: Proceedings of the 2009 American Control Conference. IEEE, pp. 2076–2089. http://dx.doi.org/10.1109/ACC.2009.5160195.

Park, W., Park, K.-S., Koh, H.-M., Ha, D.-H., 2006. Wind-induced response control and serviceability improvement of an air traffic control tower. Eng. Struct. 28, 1060–1070. http://dx.doi.org/10.1016/j.engstruct.2005.11.013.

Pattison-Gordon, J., 2022. What's next for defending critical infrastructure? In: Government Technology, April 1st, 2022. URL https://www.govtech.com/security/whats-next-for-defending-critical-infrastructure.

Pejsa, A.J., 1974. Optimum skewed redundant inertial navigators. AIAA J. 12 (7), 899–902. http://dx.doi.org/10.2514/3.49378.

Petersen, Ø.W., Frøseth, G.T., Øiseth, O., 2021. Design and deployment of a monitoring system on a long-span suspension bridge. Proceedings of the International Conference on Structural Health Monitoring of Intelligent Infrastructure. Porto, Portugal, 30 June -2 July 1813–1817.

Phan, D.-H., 2018. Passive winglet control of flutter and buffeting responses of suspension bridges. Int. J. Struct. Stab. Dyn. 18, 1850072. http://dx.doi.org/10.1142/S0219455418500724.

Pomaranzi, G., Daniotti, N., Schito, P., Rosa, L., Zasso, A., 2020. Experimental assessment of the effects of a porous double skin façade system on cladding loads. J. Wind Eng. Ind. Aerodyn. 196, 104019. http://dx.doi.org/10.1016/j.jweia.2019.104019.

Preidikman, S., Mook, D., 1997. A new method for actively suppressing flutter of suspension bridges. J. Wind Eng. Ind. Aerodyn. 69–71, 955–974. http://dx.doi.org/10.1016/S0167-6105(97)00220-1.

Preumont, A., Seto, K., 2008. Active Control of Structures. Hoboken, NJ, USA, Wiley Online Library, ISBN: 9780470033937, pp. 1–296. http://dx.doi.org/10.1002/9780470715703.

Quintela, J., Jurado, J.Á., Rapela, C., Álvarez, A.J., Roca, M., Hernández, S., Cid Montoya, M., López, J.M., Ruiz, A.J., Moreno, I., Jiménez, S., 2020. Experimental and computational studies on the performance of solar trackers under vortex shedding, torsional divergence, and flutter. Int. J. Comput. Methods Exp. Meas. 8 (4), 387–404. http://dx.doi.org/10.2495/CMEM-V8-N4-387-404.

Racharla, S., Rajan, K., 2017. Solar tracking system - A review. Int. J. Sustain. Eng. 10 (2), 72–81. http://dx.doi.org/10.1080/19397038.2016.1267816.

Raggett, J.D., 1987. Stabilizing winglet pair for slender bridge decks. In: Bridges and Transmission Line Structures. American Association for Civil Engineering.

Rahimi, F., Aghayari, R., Samali, B., 2020. Application of tuned mass dampers for structural vibration control: A State-of-the-art Review. Civ. Eng. J. 6 (8), 1622–1651. http://dx.doi.org/10.28991/cej-2020-03091571.

Reavenlord, 2022. Microsoft: Russian cyberattacks increase against Ukraine, supporters. Jun 27th. Tehcpowerup.com URL https://www.techpowerup.com/296216/microsoft-russian-cyberattacks-increase-against-ukraine-supporters.

Reed, D., Yu, J., Yeh, H., Gardarsson, S., 1998. Investigation of tuned liquid dampers under large amplitude excitation. J. Eng. Mech. 124 (4), 405–413. http://dx.doi.org/10.1061/(ASCE)0733-9399(1998)124:4(405).

Reinhorn, A.M., Manolis, G.D., Wen, C.Y., 1987. Active control of inelastic structures. J. Eng. Mech. ASCE 113 (3), 315–333. http://dx.doi.org/10.1061/(ASCE)0733-9399(1987)113:3(315).

Reis, P.M., López Jiménez, F., Marthelot, J., 2015. Transforming architectures inspired by origami. Proc. Natl. Acad. Sci. USA 112 (40), 12234–12235. http://dx.doi.org/10.1073/pnas.1516974112.

Rezaee, M., Aly, A.M., 2018. Vibration control in wind turbines to achieve desired system-level performance under single and mutiple hazard loadings. Struct. Control Health Monit. 25 (12), e2261. http://dx.doi.org/10.1002/stc.2261.

Ricciardelli, F., Occhiuzzi, A., Clemente, P., 2000. Semi-active tuned mass damper control strategy for wind-excited structures. J. Wind Eng. Ind. Aerodyn. 88, 57–74. http://dx.doi.org/10.1016/S0167-6105(00)00024-6.

Ricciardelli, F., Pizzimenti, A.D., Mattei, M., 2003. Passive and active mass damper control of the response of tall buildings to wind gustiness. Eng. Struct. 25, 1199–1209. http://dx.doi.org/10.1016/S0141-0296(03)00068-3.

Rosenberg, A., Selvaraj, S., Sharma, A., 2014. A novel dual-rotor turbine for increased wind energy capture. J. Phys. Conf. Ser. 524, 012078. http://dx.doi.org/10.1088/1742-6596/524/1/012078.

Rubio-Medrano, Carlos E., Lamp, Josephine, Doupé, Adam, Zhao, Ziming, Ahn, Gail-Joon, 2017. Mutated policies: Towards proactive attribute-based defenses for access control. In: Proceedings of the 2017 Workshop on Moving Target Defense. MTD '17, Association for Computing Machinery, New York, NY, USA, pp. 39–49. http://dx.doi.org/10.1145/3140549.3140553.

Sangalli, L.A., Braun, A.L., 2020. A fluid-structure interaction model for numerical simulation of bridge flutter using sectional models with active control devices. Preliminary results. J. Sound Vib. 477, 115338. http://dx.doi.org/10.1016/j.jsv.2020.115338.

Shi, W., Shan, J., Lu, X., 2012. Modal identification of Shanghai World Financial Center both from free and ambient vibration response. Eng. Struct. 36, 14–26. http://dx.doi.org/10.1016/j.engstruct.2011.11.025.

Silva-Ortega, M., Roque da Silva Assi, G., 2017. Suppression of the vortex-induced vibration of a circular cylinder surrounded by eight rotating wake-control cylinders. J. Fluids Struct. 74, 401–412. http://dx.doi.org/10.1016/j.jfluidstructs.2017.07.002.

Simani, S., 2015. Overview of modelling and advanced control strategies for wind turbine systems. Energies 8, 13395–13418. http://dx.doi.org/10.3390/en81212374.

Siringoringo, D.M., Fujino, Y., 2012. Observed along-wind vibration of a suspension bridge tower. J. Wind Eng. Ind. Aerodyn. 103, 107–121. http://dx.doi.org/10.1016/j.jweia.2012.03.007.

Skvorc, P., Kozmar, H., 2023. The effect of wind characteristics on tall buildings with porous double-skin façades. J. Build. Eng. 69, 106135. http://dx.doi.org/10.1016/j.jobe.2023.106135.

Slowik, J., 2018. Anatomy of an attack: Detecting and defeating CRASHOVERRIDE. URL https://www.dragos.com/resources/whitepaper/anatomy-of-an-attack-detecting-and-defeating-crashoverride/.

Snaiki, R., Wu, T., 2020. Hurricane hazard assessment along the United States Northeastern Coast: Surface wind and rain fields under changing climate. Front. Built Environ. 6, 573054. http://dx.doi.org/10.3389/fbuil.2020.573054.

Soleimanzadeh, M., Wisniewski, R., Kanev, S., 2012. An optimization framework for load and power distribution in wind farms. J. Wind Eng. Ind. Aerodyn. 107–108, 256–262. http://dx.doi.org/10.1016/j.jweia.2012.04.024.

Song, G., Gu, H., 2007. Active vibration suppression of a smart flexible beam using a sliding mode based controller. J. Vib. Control 13 (8), 1095–1107. http://dx.doi.org/10.1177/1077546307078752.

Spence, S.M.J., Kareem, A., 2014. Performance-based design and optimization of uncertain wind-excited dynamic building systems. Eng. Struct. 78 (1), 133–144. http://dx.doi.org/10.1016/j.engstruct.2014.07.026.

Spencer, B.F., Dyke, S.J., Sain, M.K., Carlson, J.D., 1997. Phenomenological model for magnetorheological dampers. J. Eng. Mech. 123, 230–238. http://dx.doi.org/10.1061/(ASCE)0733-9399(1997)123:3(230).

Spencer, B.F., Nagarajaiah, S., 2003. State of the art of structural control. J. Struct. Eng. 129, 845–856. http://dx.doi.org/10.1061/(ASCE)0733-9445(2003)129:7(845).

Spruce, C.J., 1993. Simulation and Control of Windfarms (Ph.D. thesis). Department of Engineering Science, University of Oxford, URL https://ora.ox.ac.uk/objects/uuid:24f51a31-e2f9-422f-9837-3c28cfe12ccc.

Staino, D., Basu, B., 2015. Emerging trends in vibration control of wind turbines: a focus on a dual control strategy. Phil. Trans. R. Soc. A 373, 20140069. http://dx.doi.org/10.1098/rsta.2014.0069.

Starossek, U., Ferenczi, T., Priebe, J., 2018. Eccentric-wing flutter stabilizer for bridges-analysis, tests, design, and costs. Eng. Struct. 172, 1073–1080. http://dx.doi.org/10.1016/j.engstruct.2018.06.056.

Stock, A., Leithead, W., 2022. A generic approach to wind farm control and the power adjusting controller. Wind Energy 25 (10), 1735–1757. http://dx.doi.org/10.1002/we.2765.

Stoll, C., 1989. The Cuckoo's Egg: Tracking a Spy Through the Maze of Computer Spionage. Doubleday, ISBN: 0-385-24946-2.

Strobel, K., Banks, D., 2014. Effects of vortex shedding in arrays of long inclined flat plates and ramifications for ground-mounted photovoltaic arrays. J. Wind Eng. Ind. Aerodyn. 133, 146–149. http://dx.doi.org/10.1016/j.jweia.2014.06.013.

Su, Y., Xiang, H., Fang, C., Wang, L., Li, Y., 2017. Wind tunnel tests on flow fields of full-scale railway wind barries. Wind Struct. 25, 171–184. http://dx.doi.org/10.12989/WAS.2017.24.2.171.

Sun, J.Q., Jolly, M.R., Norris, M.A., 1995. Passive, adaptive and active tuned vibration systems - A survey. Trans. ASME 117 (B), 234–242. http://dx.doi.org/10.1115/1.2836462.

Svendsen, M.N., Krenk, S., Høgsberg, J., 2011. Resonant vibration control of rotating beams. J. Sound Vib. 330, 1877–1890. http://dx.doi.org/10.1016/j.jsv.2010.11.008.

Symantec Inc., 2014. Dragonfly: Cyberespionage Attacks Against Energy Suppliers. Tech. Rep., July, URL https://docs.broadcom.com/doc/dragonfly_threat_against_western_energy_suppliers.

Talib, E., Shin, J.-H., Kwak, M.K., 2019. Designing multi-input multi-output modal-space negative acceleration feedback control for vibration suppression of structures using active mass dampers. J. Sound Vib. 439, 77–98. http://dx.doi.org/10.1016/j.jsv.2018.09.052.

Tamura, Y., Kareem, A., Solari, G., Kwok, K.C.S., Holmes, J.D., Melbourne, W.H., 2005. Aspects of the dynamic wind-induced response of structures and codification. Wind Struct. 8 (4), 251–268. http://dx.doi.org/10.12989/was.2005.8.4.251.

Tamura, Y., Kousaka, R., Modi, V.J., 1992. Practical application of nutation damper for suppressing wind-induced vibrations of airport towers. J. Wing Eng. Ind. Aerodyn. 41–44, 1919–1930. http://dx.doi.org/10.1016/0167-6105(92)90612-E.

Tan, P., Liu, G., Zhou, F.L., Teng, J., 2012. Hybrid mass dampers for Canton Tower. CTBUH Res. Pap. 2012 (1), 24–29, URL https://global.ctbuh.org/resources/papers/download/288-hybrid-mass-dampers-for-canton-tower.pdf.

Tanaka, H., Tamura, Y., Ohtake, K., Nakai, M., Kim, Y.C., 2012. Experimental investigation of aerodynamic forces and wind pressures acting on tall buildings with various unconventional configurations. J. Wind Eng. Ind. Aerodyn. 107–108, 179–191. http://dx.doi.org/10.1016/j.jweia.2012.04.014.

Tao, S.B., Tang, A., Liu, K., 2017. Suppressing the vortex-induced vibration of a bridge deck via suction. Eng. Rev. 37 (2), 155–164, URL https://hrcak.srce.hr/181509.

Terrill, R., Starossek, U., 2022. Active vibration control of a multi-degree-of-freedom system via twin rotor damper. J. Vib. Acoust. 144, 011005. http://dx.doi.org/10.1115/1.4051229.

TESolution, 2020. TESolution's AMD installed for bridge tower under construction. [Online] Youtube video: https://www.youtube.com/watch?v=4V5iM1OPZJY.

The New York Times, 2018. Cyberattacks Put Russian Fingers on the Switch at Power Plants, U.S. Says. https://www.nytimes.com/2018/03/15/us/politics/russia-cyberattacks.html.

Theodorsen, T., 1949. General Theory of Aerodynamic Instability and the Mechanism of Flutter. Technical Report NACA-TR-496, National Aeronautics and Space Administration, URL https://ntrs.nasa.gov/citations/19930090935.

Tian, H., Soltani, M.N., Nielsen, M.E., 2023. Review of floating wind turbine damping technology. Ocean Eng. 278, 114365. http://dx.doi.org/10.1016/j.oceaneng.2023.114365.

Truong, Q.-T., Phan, D.-H., 2021. Numerical study of aeroelastic suppression using active control surfaces on a full-span suspension bridge. Structures 33, 606–614. http://dx.doi.org/10.1016/j.istruc.2021.04.035.

Tse, K.T., Hitchcock, P.A., Kwok, K.C., Thepmongkorn, S., Chan, C.M., 2009. Economic perspectives of aerodynamic treatments of square tall buildings. J. Wind Eng. Ind. Aerodyn. 97 (9–10), 455–467. http://dx.doi.org/10.1016/j.jweia.2009.07.005.

Ueda, T., Nakagaki, R., Koshida, K., 1992. Suppression of wind-induced vibration by dynamic dampers in tower-like structures. J. Wind Eng. Ind. Aerodyn. 41–44, 1907–1918. http://dx.doi.org/10.1016/0167-6105(92)90611-D.

U.S. Congress - A.S. King, 2019. S.174 - Securing Energy Infrastructure Act. https://www.congress.gov/116/bills/s174/BILLS-116s174rs.pdf.

USEIA, 2022. Electrical Power Annual 2022. Technical Report, U.S. Energy Information Administration (USEIA), U.S. Department of Energy, URL https://www.eia.gov/electricity/annual/pdf/epa.pdf.

Valentin, D., Valero, C., Egusquiza, M., Presas, A., 2022. Failure investigation of a solar tracker due to wind-induced torsional galloping. Eng. Fail. Anal. 135, 106–137. http://dx.doi.org/10.1016/j.engfailanal.2022.106137.

Varadarajan, N., Nagarajaiah, S., 2011. Wind response control of building with variable stiffness tuned mass damper using empirical mode decomposition/Hilbert transform. J. Eng. Mech. 130 (4), 451–458. http://dx.doi.org/10.1061/(ASCE)0733-9399(2004)130:4(451).

Vilceanu, V., Kavrakov, I., Morgenthal, G., 2023. Coupled numerical simulation of liquid sloshing dampers and wind-structure simulation model. J. Wind Eng. Ind. Aerodyn. 240, 105505. http://dx.doi.org/10.1016/j.jweia.2023.105505.

Wang, H., Mao, J.-X., Xu, Z.-D., 2020. Investigation of dynamic properties of a long-span cable-stayed bridge during typhoon events based on structural health monitoring. J. Wind Eng. Ind. Aerodyn. 201, 104172. http://dx.doi.org/10.1016/j.jweia.2020.104172.

Wang, D., Tse, T.K.T., Zhou, Y., Li, Q., 2015. Structural performance and cost analysis of wind-induced vibration control schemes for a real super-tall building. Struct. Infrastruct. Eng. 11 (8), 990–1011. http://dx.doi.org/10.1080/15732479.2014.925941.

Wang, Z., Zhao, L., Chen, H., Fang, G., Li, K., Ge, Y., 2023. Flutter control of active aerodynamic flaps mounted on streamlined bridge deck fairing edges: An experimental study. Struct. Control Health Monit. 2023, 9970603. http://dx.doi.org/10.1155/2023/9970603.

Weber, F., Huber, P., Distl, H., Braun, C., 2016. Real-time controlled TMD of Danube City Tower. In: CTBUH Research Papers, CTBUH 2016 Shenzhen - Guangzhou - Hong Kong Conference. Vol. 2016, pp. 1145–1152, URL https://global.ctbuh.org/resources/papers/download/2956-real-time-controlled-tmd-of-danube-city-tower.pdf.

Wei, L., 2023. Design innovation of Zhangjinggao Yangtze River Bridge. In: IABSE Symposium Istanbul 2023: Long Span Bridges; Istanbul, Türkiye; 26-28 April 2023.

Whitehead, David E., Owens, Kevin, Gammel, Dennis, Smith, Jess, 2017. Ukraine cyber-induced power outage: Analysis and practical mitigation strategies. In: 2017 70th Annual Conference for Protective Relay Engineers. CPRE, pp. 1–8. http://dx.doi.org/10.1109/CPRE.2017.8090056.

Whiteman, M.L., Fernández-Cabán, P.L., Phillips, B.M., Masters, F.J., Davis, J.R., Bridge, J.A., 2021. Cyber-physical aerodynamic shape optimization of a tall building in a wind tunnel using an active fin system. J. Wing Eng. Ind. Aerodyn. 220, 104835. http://dx.doi.org/10.1016/j.jweia.2021.104835.

Wikimedia Commons, 2015. Shanghai world financial center. [Online] Wikimedia Commons, the free media repository. URL https://commons.wikimedia.org/wiki/File:Shanghai_World_Financial_Center_5166295-HDR.jpg.

Wikimedia Commons (Glabb), 2012. Xihoumen bridge. [Online] Wikimedia Commons, the free media repository. URL https://en.m.wikipedia.org/wiki/File:Xihoumen_Bridge.JPG.

Wikimedia Commons (Rs1421), 2011. Yokohama landmark tower. [Online] Wikimedia Commons, the free media repository. URL https://commons.wikimedia.org/wiki/File:Yokohama-Landmark-Tower-00.jpg.

Wilde, K., Fujino, Y., 1998. Aerodynamic control of bridge deck flutter by active surfaces. J. Eng. Mech.-ASCE 124 (7), 718–727. http://dx.doi.org/10.1061/(ASCE)0733-9399(1998)124:7(718).

Wilde, K., Omenzetter, P., Fujino, Y., 2001. Suppression of bridge flutter by active deck-flaps control system. J. Eng. Mech.-ASCE 127 (1), 80–89. http://dx.doi.org/10.1061/(ASCE)0733-9399(2001)127:1(80).

WindEurope.org, 2023. Daily Wind Power Numbers. Technical Report, WindEurope, Retrieved on November 23, 2023 from https://windeurope.org/about-wind/daily-wind-archive/2023-11-23/.

Wu, T., He, J., Li, S., 2023. Active flutter control of long-span bridges via deep reinforcement learning: A proof of concept. Wind Struct. 36 (5), 321–331. http://dx.doi.org/10.12989/was.2023.36.5.321.

Wu, J., Hu, N., Dong, Y., Zhang, Q., Yang, B., 2021. Wind characteristics atop Shanghai Tower during typhoon Jongdari using field monitoring data. J. Build. Eng. 33, 101815. http://dx.doi.org/10.1016/j.jobe.2020.101815.

Xie, F., Aly, A.-M., 2020. Structural control and vibration issues in wind turbines: A review. Eng. Struct. 210, 110087. http://dx.doi.org/10.1016/j.engstruct.2019.110087.

Xie, Y.Z., Ebad Sichani, M., Padgett, J.E., DesRoches, R., 2020. The promise of implementing machine learning in earthquake engineering: A state-of-the-art review. Earthq. Spectra 36 (4), 1769–1801. http://dx.doi.org/10.1177/8755293020919419.

Xie, B., Luo, X., Zhang, Q., Ding, J., 2023. Dynamic response evaluation of the shanghai tower in along- and across-wind directions during super typhoon lekima. J. Build. Eng. 65, 105808. http://dx.doi.org/10.1016/j.jobe.2022.105808.

Xu, K., Dai, Q., Bi, K., Fang, G., Zhao, L., 2022. Multi-mode vortex-induced vibration control of long-span bridges by using distributed tuned mass damper inerters (DTMDIs). J. Wind Eng. Ind. Aerodyn. 224, 104970. http://dx.doi.org/10.1016/j.jweia.2022.104970.

Xu, G., Kareem, A., Shen, L., 2020. Surrogate modeling with sequential updating: applications to bridge deck-wave and bridge deck-wind interactions. ASCE J. Comput. Civ. Eng. 34 (4), 04020023. http://dx.doi.org/10.1061/(ASCE)CP.1943-5487.0000904.

Xu, Y.L., Kwok, K.C., Samali, B., 1992a. Control of wind-induced tall building vibration by tuned mass dampers. J. Wind Eng. Ind. Aerodyn. 40, 1–32. http://dx.doi.org/10.1016/0167-6105(92)90518-F.

Xu, Y.L., Qu, W.L., Chen, Z.H., 2001. Control of wind-excited truss tower using semiactive friction damper. J. Struct. Eng. 127, 861–868. http://dx.doi.org/10.1061/(ASCE)0733-9445(2001)127:8(861).

Xu, Y.L., Samali, B., Kwok, K.C.S., 1992. Control of along-wind response of structures by mass and liquid dampers. J. Eng. Mech. 118 (1), 20–39. http://dx.doi.org/10.1061/(ASCE)0733-9399(1992)118:1(20).

Yalla, S.K., Kareem, A., 2000. Optimal absorber parameters for tuned liquid column dampers. J. Struct. Eng. ASCE 126 (8), 906–915. http://dx.doi.org/10.1061/(ASCE)0733-9445(2000)126:8(906).

Yalla, S.K., Kareem, A., Kantor, J.C., 2001. Semi-active tuned liquid column dampers for vibration control of structures. Eng. Struct. 23, 1469–1479. http://dx.doi.org/10.1016/S0141-0296(01)00047-5.

Yamada, M., Higashiyama, H., Namiki, M., Kazao, Y., 1997. Active vibration control system using a gyro-stabilizer. Control Eng. Pract. 5 (9), 1217–1222. http://dx.doi.org/10.1016/S0967-0661(97)84360-2.

Yamazaki, S., Nagata, N., Abiru, H., 1992. Tuned active dampers installed in the Minato Mirai (MM) 21 Landmark Tower in Yokohama. J. Wind Eng. Ind. Aerodyn. 41–44, 1937–1948. http://dx.doi.org/10.1016/0167-6105(92)90618-K.

Yang, J.-N., 1975. Application of optimal control theory to civil engineering structures. J. Eng. Mech. Div. 101 (6), 819–838. http://dx.doi.org/10.1061/JMCEA3.0002075.

Yang, D.-C., Ge, Y.-J., Xiang, H.-F., Ma, Z.J., 2011. 3D flutter analysis of cable supported bridges including aeroelastic effects of cables. Adv. Struct. Eng. 14 (6), 1129–1147. http://dx.doi.org/10.1260/1369-4332.14.6.1129.

Yang, Y., Ge, Y., Zhou, R., Chen, S., Zhang, L., 2020. Aerodynamic countermeasure schemes of super long-span suspension bridges with various aspect ratios. Int. J. Struct. Stab. Dynam. 20 (5), http://dx.doi.org/10.1142/S0219455420500613.

Yang, W.-H., Li, W.-L., 2021. Passive aerodynamic control of a single-box girder using self-issuing jets. J. Wind Eng. Ind. Aerodyn. 208, 104443. http://dx.doi.org/10.1016/j.jweia.2020.104443.

Yang, J.N., Samali, B., 1983. Control of tall buildings in along-wind motion. J. Struct. Eng. ASCE 109 (1), 50–68. http://dx.doi.org/10.1061/(ASCE)0733-9445(1983)109:1(50).

Yang, D.-H., Shin, J.-H., Lee, H.W., Kim, S.-K., Kwak, M.K., 2017. Active vibration control of structure by Active Mass Damper and Multi-Modal Negative Acceleration Feedback control algorithm. J. Sound Vib. 392, 18–30. http://dx.doi.org/10.1016/j.jsv.2016.12.036.

Yang, Y., Zhang, J., Cao, F., Ge, Y., Zhao, L., 2022. Evaluation and improvement of wind environment and vehicle safety on long-span bridge deck under strong crosswind. J. Wind Eng. Ind. Aerodyn. 228, http://dx.doi.org/10.1016/j.jweia.2022.105089.

Yao, Y., Hu, Y., Gao, S., Yang, G., Du, J., 2014. A multipurpose dual-axis solar tracker with two tracking strategies. Renew. Energy 72, 88–89. http://dx.doi.org/10.1016/j.renene.2014.07.002.

Young, E., He, X., King, R., Corbus, D., 2020. A fluid-structure interaction solver for investigating torsional galloping in solar-tracking photovoltaic panel arrays. J. Renew. Sustain. Energy 12, 063503. http://dx.doi.org/10.1063/5.0023757.

Zambrano, A., Palacio-Betancur, A., Burlando, L., Niño, A.F., Giraldo, L.F., Soto, M.G., Giraldo, J., Cardenas, A.A., 2021. You make me tremble: A first look at attacks against structural control systems.. In: CCS 21, November 15'19, 2021, Virtual Event, Korea. http://dx.doi.org/10.1145/3460120.3485386.

Zhang, Y., Schauer, T., Bleicher, A., 2022. Optimized passive/semi-active vibration control using distributed-multiple tuned facade damping system in tall buildings. J. Build. Eng. 52, 104416. http://dx.doi.org/10.1016/j.jobe.2022.104416.

Zhang, H., Xin, D., Ou, J., 2016. Wake control of vortex shedding based on spanwise suction of a bridge section model using Delayed Detached Eddy Simulation. J. Wind Eng. Ind. Aerodyn. 155, 100–114. http://dx.doi.org/10.1016/j.jweia.2016.05.004.

Zhang, Y.-A., Zhu, S., 2023. Novel model-free optimal active vibration control strategy based on deep reinforcement learning. Struct. Control Health Monit. 2023, 6770137. http://dx.doi.org/10.1155/2023/6770137.

Zhao, L., Cui, B., Wu, M., Xu, J., 2023. Design innovation of Shiziyang Bridge. In: IABSE Symposium Istanbul 2023: Long Span Bridges; Istanbul, Türkiye; 26-28 April 2023.

Zhao, J., Fang, Y., He, Y., Fang, J., Wen, L., Liang, Y., Xiao, S., 2021. Active power control strategy of wind farm considering fatigue load of wind turbines. Energy Rep. 7, 1466–1476. http://dx.doi.org/10.1016/j.egyr.2021.09.096.

Zhao, X., Gouder, K., Graham, J.M.R., Limebeer, D.J.N., 2016. Buffet loading, dynamic response and aerodynamic control of a suspension bridge in a turbulent wind. J. Fluids Struct. 62, 384–412. http://dx.doi.org/10.1016/j.jfluidstructs.2016.01.013.

Zheng, C., Xie, Y., Khan, M., Wu, Y., Liu, J., 2018. Wind-induced responses of tall buildings under combined aerodynamic control. Eng. Struct. 175, 86–100. http://dx.doi.org/10.1016/j.engstruct.2018.08.031.

Zheng, C.-R., Zhang, Y.-C., 2012. Computational fluid dynamics study on the performance and mechanism of suction control over a high-rise building. Struct. Des. Tall Spec. Build. 21 (7), 475–491. http://dx.doi.org/10.1002/tal.622.

Zhou, K., Li, Q.-S., 2022. Vibration mitigation performance of active tuned mass damper in a super high-rise building during multiple tropical storms. Eng. Struct. 269, 114840. http://dx.doi.org/10.1016/j.engstruct.2022.114840.

Zhou, K., Zhang, J.-W., Li, Q.-S., 2022. Control performance of active tuned mass damper for mitigating wind-induced vibrations of a 600-m-tall skyscraper. J. Build. Eng. 45, 103646. http://dx.doi.org/10.1016/j.jobe.2021.103646.

Zhuo, L.J., Liao, H.L., Li, M.S., 2020. Flutter control of a streamlined box girder with active flaps. J. Vib. Control 27, 662–674. http://dx.doi.org/10.1177/1077546320932745.

Zhuo, L., Liao, H., Zhou, Q., Li, M., 2022. Identification of aerodynamic derivatives of a box-girder bridge deck with twin active flaps using CFD simulations. J. Bridge Eng. 27 (3), 04022002. http://dx.doi.org/10.1061/(ASCE)BE.1943-5592.0001830.